Stanislav (Stas) Babak.

AstroParticule et Cosmologie, CNRS (Paris)

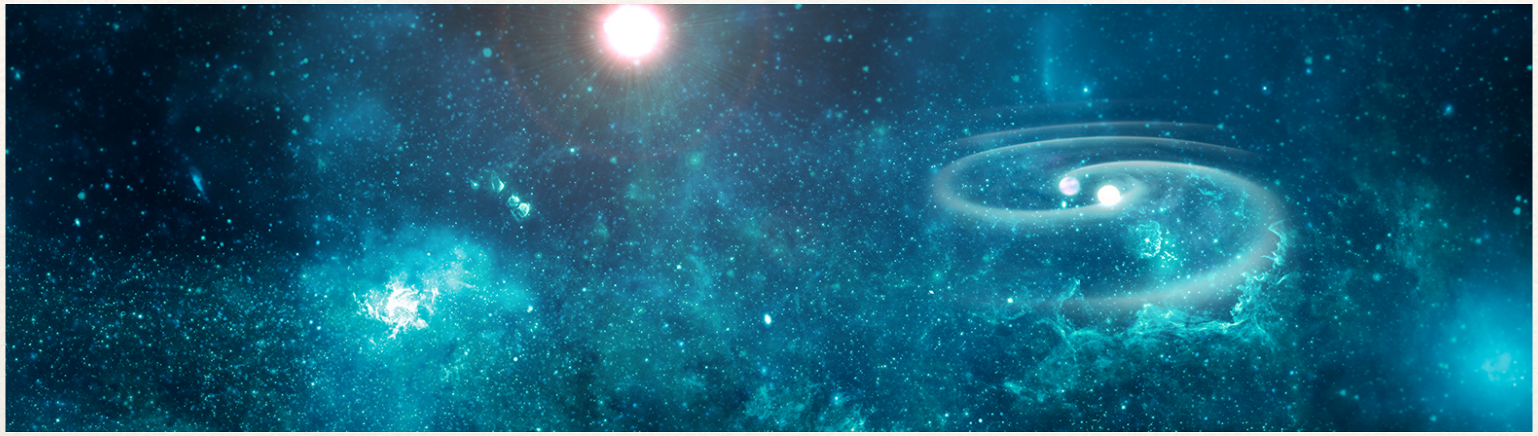

Waveform modelling : Status and challenges

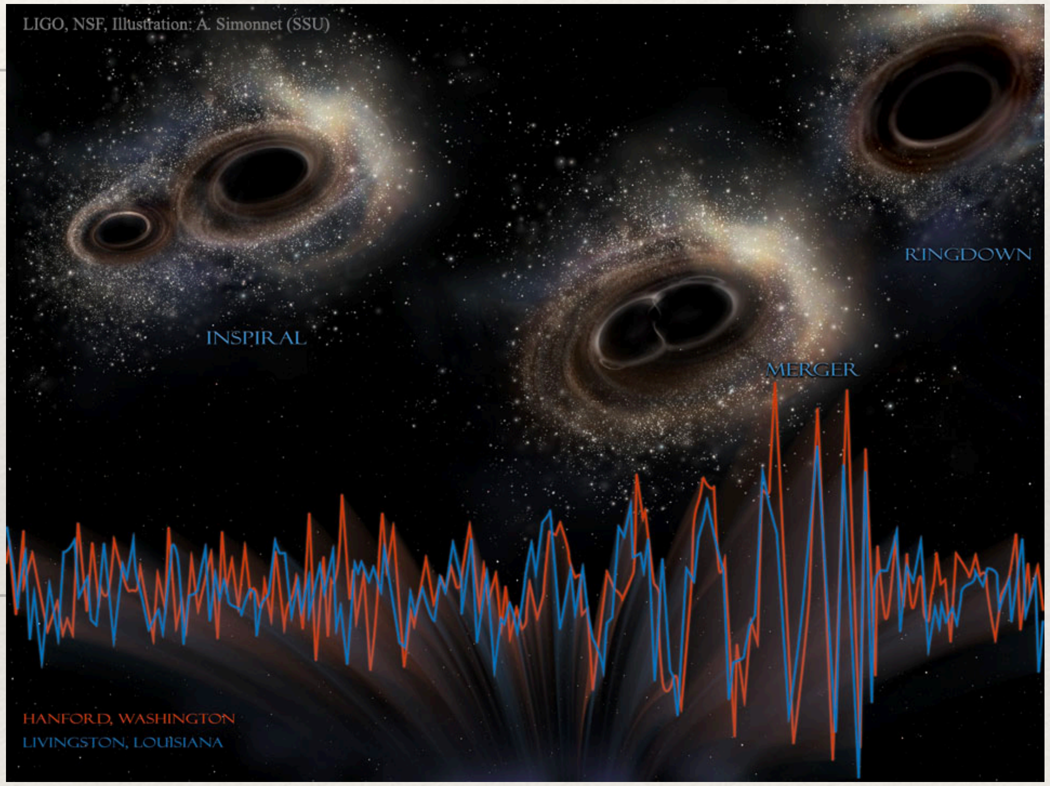

ISAPP, 7-17 June 2021

Literature

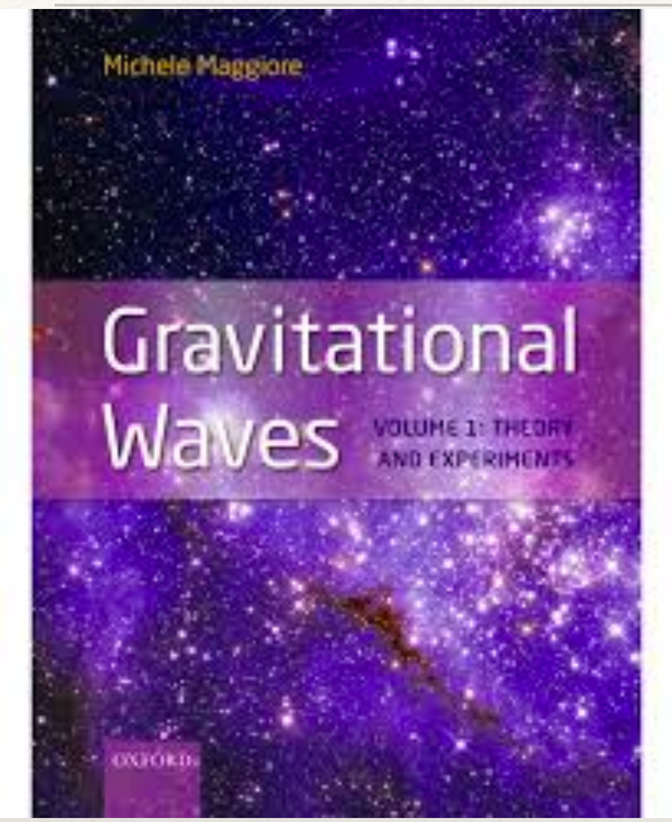

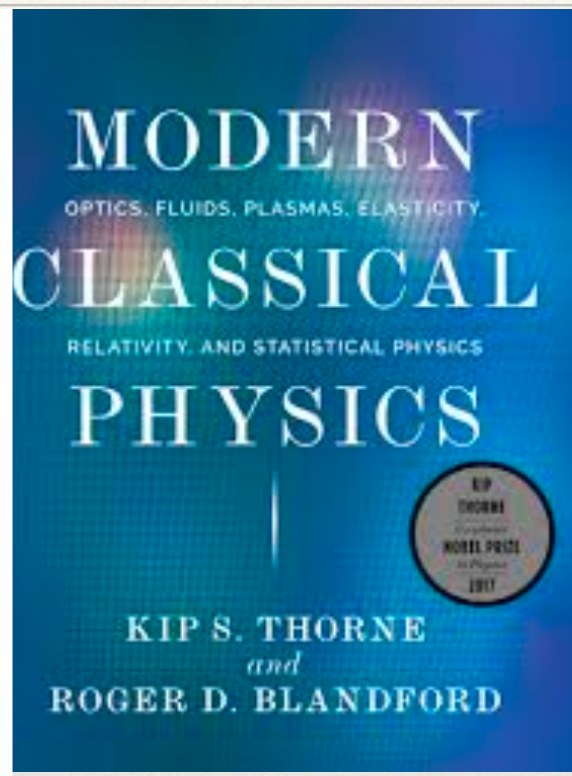

Some figures in these lectures are borrowed from theses books

LSC+Virgo, Phys. Rev. Lett. 116, 221101 (2016), LSC+Virgo, Phys. Rev. X 6, 041015 (2016), LSC+Virgo, Phys.Rev.Lett. 116 241102 (2016), LSC+Virgo, Phys.Rev. X6 041014 (2016), LSC+Virgo, Phys. Rev. Lett. 118, 221101 (2017), Berti et al., Class.Quantum Grav. 32, 243001 (2015), LSC+VIRGO, ArXiV:1805.11579, S. Khan+, Phys.Rev. D93 (2016) 044007, LSC+Virgo arXiv:1805.11579 , LIGO_Virgo, Astrophys.J. 848 (2017) L12, LIGO+Virgo Phys.Rev.Lett. 119 (2017) 161101, Babak+ Phys.Rev. D95 (2017) 103012, LISA consortium arXiv:1702.00786, Klein+ Phys.Rev. D93 (2016) 024003, LISA consortium, arXiv:1305.5720, Amaro-Seoane+ Class.Quant.Grav. 29 (2012) 124016 . https://arxiv.org/pdf/1904.04831.pdf , Phys. Rev. Lett. **111**, 241104, https://arxiv.org/pdf/1812.07865.pdf, https://arxiv.org/pdf/1407.1838.pdf,

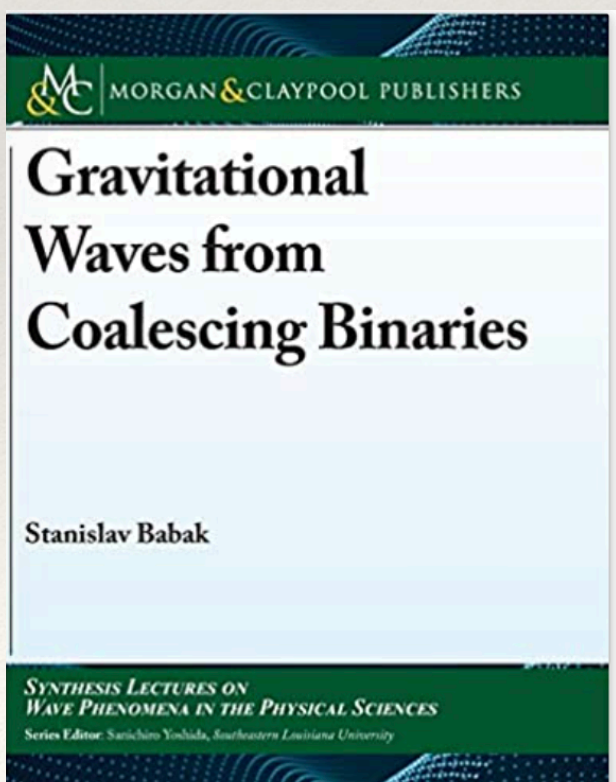

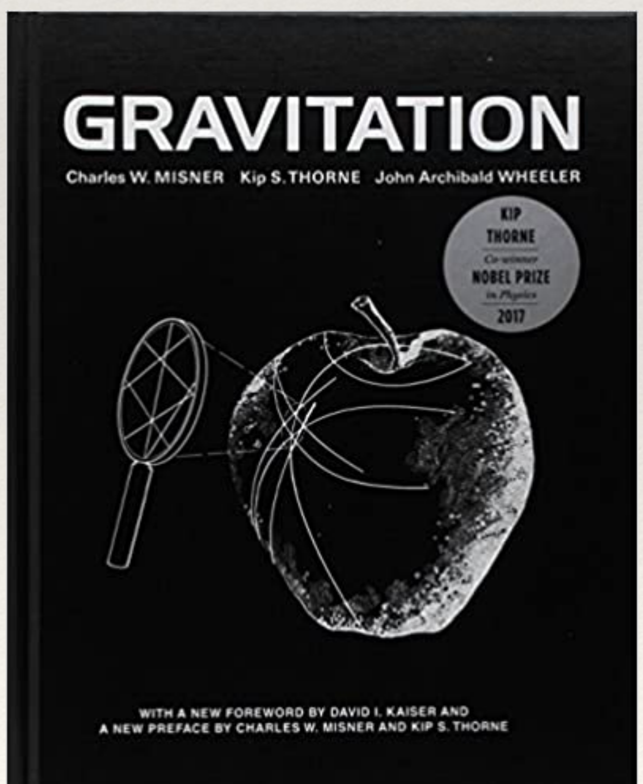

Matched filtering

- The matched filtering is very sensitive to the phase of GW signal: we are tracking phase and amplitude
- Change in the parameters of emitting system -> change in the phase and/or amplitude: basic for the parameter estimation
- Mismatch between real signal and a model signal (used as a template) translates into a drop in ***Overlap*** -> drop in SNR -> drop in detection rate (SNR)^3

$$\mathcal{O} =< \hat{s}|\hat{h} >, \quad < \hat{s}|\hat{s} >=< \hat{h}|\hat{h} >= 1$$

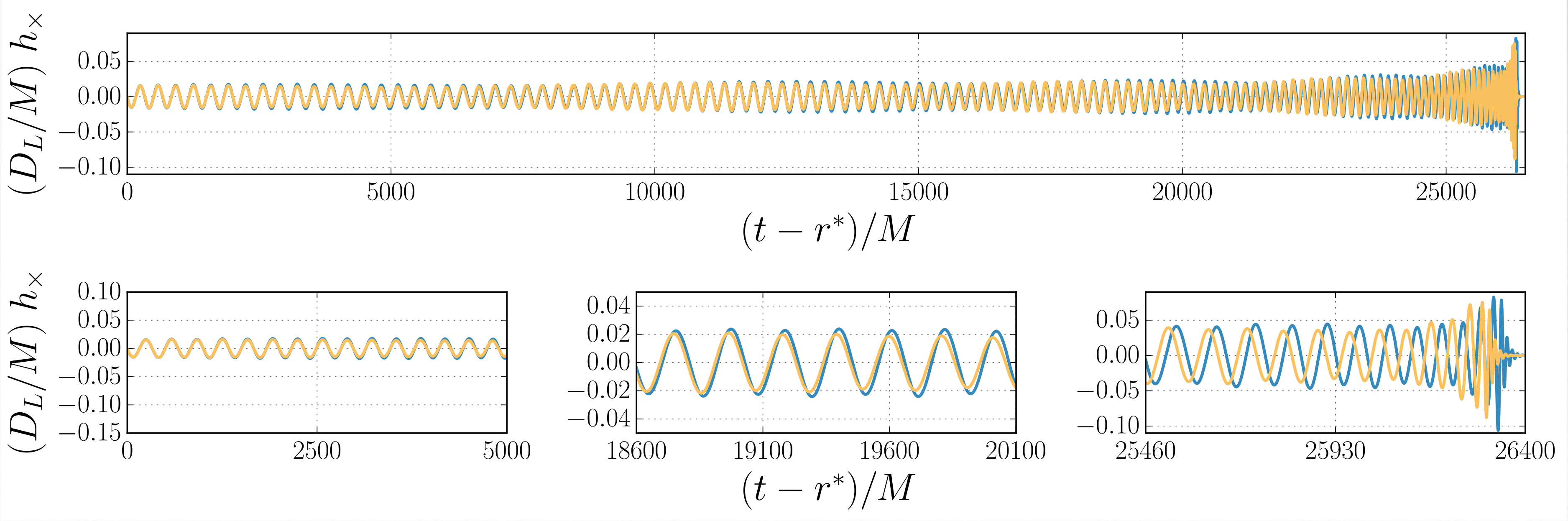

Generation of GWs: short summary

- Assume slow motion (v<<c)
- Take observe far away (far zone) $|\vec{x} - \vec{x}'| \approx R \gg \lambda^{GW}$
- We are interested in the radiative part of gravitational potentials => take "TT" part

$$h_{jk}^{TT} = \left[\frac{4}{R} \int T_{jk}(x', t' = t - R) d^3 x' \right]^{TT}$$

- Use the conservation law $\quad T^{\mu\nu}{}_{,\nu} = 0$

$$\boxed{h_{jk}^{TT} = \left[\frac{2}{R} \frac{d^2}{dt^2} \mathcal{M}_{jk}(t - R) \right]^{TT}}$$

Quadrupole formula (Landau & Lifshitz)

$$\mathcal{M}^{jk} = \int T^{00} \left(x^j x^k - \frac{1}{3} \delta^{jk} r \right) \, d^3 x$$

mass quadrupole moment

Generation of GWs: short summary

- Besides leading order (mass quadrupole) other moments also give contribution. There are two types of moments: mass-moments and current-moments

$I_l \sim ML^l$ mass moments

$S_l \sim MvL^l$ current moments

$$h_{+,\times} \sim \frac{1}{R}\left[\frac{d^2 I_2}{dt^2} \& \frac{d^3 I_3}{dt^3} \& \ldots \& \frac{d^2 S_2}{dt^2} \& \frac{d^3 S_3}{dt^3} \ldots\right] \qquad \frac{1}{R}\frac{d^l I_l}{dt^l} \sim \frac{M}{R} v^l$$

- Einstein equations are non-linear: grav field is its own source (the red term which we have neglected). Post-Newtonian expansion: $\varepsilon = v/c \ll 1$

$$g_{\mu\nu} = \eta_{\mu\nu} + \varepsilon h^{(1)}_{\mu\nu} + \varepsilon^2 h^{(2)}_{\mu\nu} + \ldots$$

Solving Einstein equations iteratively updating the equation of motion at each step

Generation of GWs: short summary

Gravitational waves: can we attach stress energy tensor? Yes, but it is defined as a quantity averaged over several (GW) wavelengths.

$$T^{GW}_{\alpha\beta} = \frac{1}{16}\langle h_{+,\alpha}h_{+,\beta} + h_{\times,\alpha}h_{\times,\beta}\rangle$$

$$\frac{dE}{dt} = -\frac{1}{5}\left\langle \dddot{\mathcal{M}}_{ij}\dddot{\mathcal{M}}_{ij}\right\rangle$$ Energy loss (energy flux): shrinking of binary orbit

$$\frac{dS_j}{dt} = -\frac{2}{5}\epsilon_{jkl}\left\langle \ddot{\mathcal{M}}_{ki}\dddot{\mathcal{M}}_{li}\right\rangle$$ Angular momentum loss: circularization of a binary

Levi-Civita antisymmetric symbol

Generation of GWs: long story
Post-Newtonian approximation (falling into a rabbit hole)

- Post-Newtonian (PN) expansion is valid under assumption of slow motion (v/c << 1): small parameter of expansion, solving Einstein equations iteratively.
  - this expansion is valid in the near zone of the source ($L \leq \lambda_{GW}$, GW wavelength): PN cannot incorporate boundary at infinity (observer)

$$\epsilon \sim \max\left\{\frac{\mathrm{T}^{0\mathrm{i}}}{\mathrm{T}^{00}}, \sqrt{\frac{\mathrm{T}^{\mathrm{ij}}}{\mathrm{T}^{00}}}\right\} \sim \frac{\mathrm{v}}{\mathrm{c}} \qquad 1\mathrm{PN} \rightarrow (\mathrm{v/c})^2,\ 1.5\mathrm{PN} \rightarrow (\mathrm{v/c})^3,\ 2\mathrm{PN} \rightarrow (\mathrm{v/c})^4, \ldots.$$

- Post-Minkowskian (PM) expansion: post-linear expansion in h - perturbation of Minkowsi metric (or effectively expansion in G) is valid in the weak field: valid in the far zone, not valid near source where field is strong
- In addition: we can perform a multipolar expansion of metric (determined at future null infinity) . Two types: mass and current multipoles . The radiative multipoles are those falling as $1/R$ as $R \rightarrow \infty$ with the null coordinates $t - R/c =$ const.

- The idea is to solve Einstein eqns (for 2-body) iteratively splitting spacetime in 3 regions: near zone (PN-formalism), far zone (PM) and some intermediate zone (where we match two solutions). Near zone: PN - solution woth the source, Far zone: PM vacuum solution. Intermediate zone: decompose PN solution in multipoles, decompose PM multipoles in (v/c) and match order by order: matched assymptotic expansion

Generation of GWs: long story
Post-Newtonian approximation (falling into a rabbit hole)

- Einstein eqns can be formulated in $\bar{h}^{\alpha\beta} = \sqrt{-g}\, g^{\alpha\beta} - \eta^{\alpha\beta}$, where $\eta^{\alpha\beta}$ is Minkowski metric and we use harmonic coordinates $\partial_\beta \bar{h}^{\alpha\beta} = 0$, (use G=c=1)

$$\Box \hat{h}^{\alpha\beta} = 16\pi\tau^{\alpha\beta} = 16\pi|g|T^{\alpha\beta} + \Lambda^{\alpha\beta}$$

flat s/t
wave operator

Landau-Lifshitz pseudotensor
(non-linear in metric terms)

- Formal solution

$$\hat{h}^{\alpha\beta} = -4\pi \int_{\text{Volume}} \frac{d^3x'}{|\vec{x} - \vec{x}'|} \tau^{\alpha\beta}(\vec{x}', t - |\vec{x} - \vec{x}'|)$$

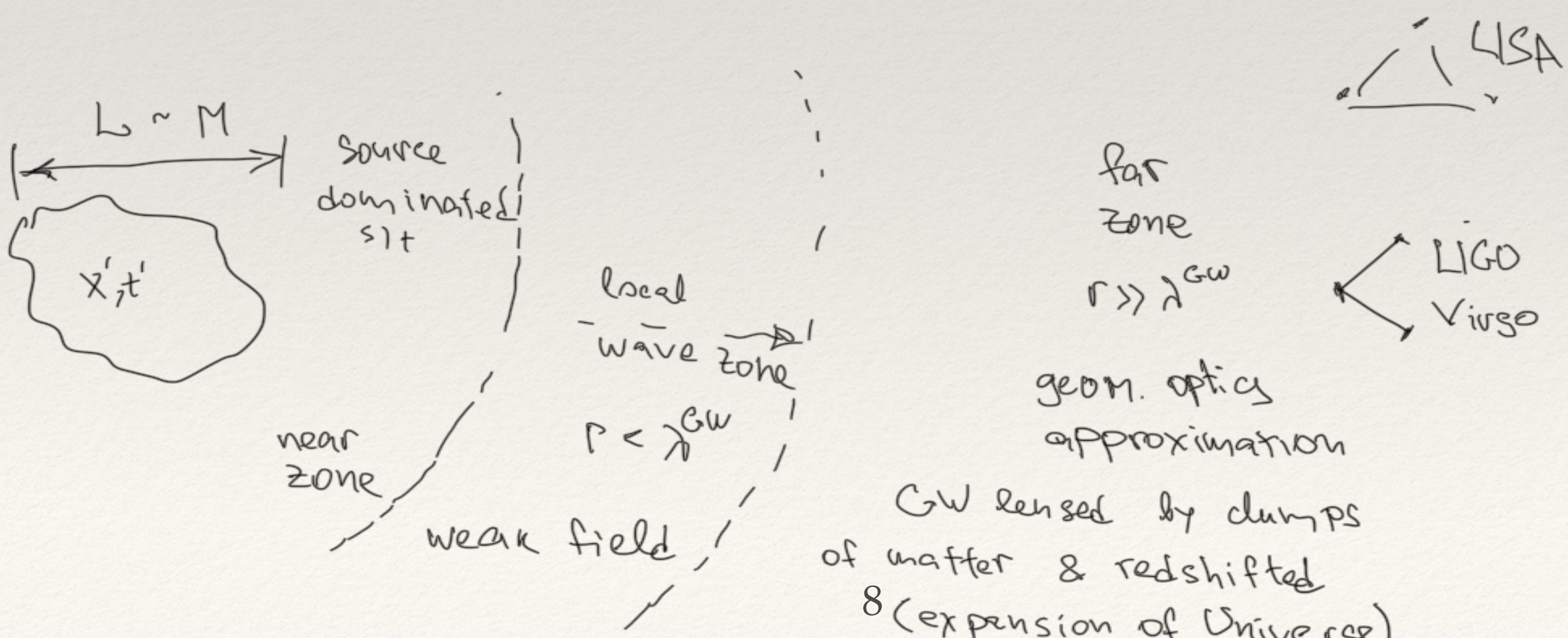

Generation of GWs: long story
Post-Newtonian approximation (falling into a rabbit hole)

- **Far zone solution**: vacuum, retarded multipolar expansion

$$\bar{h}^{\alpha\beta} = \sum_l \partial_L \left(\frac{K_L^{\alpha\beta}(t-R)}{R} \right), \quad L = i_1, i_2, ...i_l$$

and ∂_L is L-th partial derivative

Interested in spacial part (strain)

$$\bar{h}_1^{ij} \to \partial_{L-2}\left(\frac{1}{R}\ddot{I}_{ijL-2}(t-R)\right) \;\&\; \partial_{aL-2}\left(\frac{1}{R}\epsilon_{ab(i}\dot{S}_{j)bL-1}(t-R)\right)$$

mass moments current moments

- In the next iteration: $\Box \bar{h}^{\alpha\beta}_{(2)} = \tau^{\alpha\beta}_{(2)}(\bar{h}_1, \bar{h}_1)$

- Gravitational radiation: $1/R$ terms and also need to take TT (transverse-traceless) part

- We can also expand in v/c

$$I_l \sim ML^l \qquad \frac{1}{R}\frac{d^l I_l}{dt^l} \sim \frac{M}{R} v^l$$

$$S_l \sim MvL^l$$

Generation of GWs: long story
Post-Newtonian approximation (falling into a rabbit hole)

- **Near zone solution**, slow motion

dominant term

$$\Box \bar{h}^{00} = -4\pi\rho, \qquad \Box \to \triangle$$

solution

$$\bar{h}^{00} = 4\int \frac{\rho(\vec{x'})}{|\vec{x}-\vec{x'}|} d^3x'$$

expand in $\frac{r'}{r} \ll 1$: multipole expanstion

$$\bar{h}^{00} = 4\left[\underbrace{\frac{1}{R}\int \rho(\vec{x'}) d^3x'}_{\frac{M}{R}\text{ Newtonian potential}} + \underbrace{\frac{n_j}{R}\int \rho(\vec{x'}) x'^j d^3x'}_{\text{Dipole moment}} + \frac{2n_j n_k}{3R^3}\underbrace{\int \rho(\vec{x'})\left(x'^k x'^j - \frac{1}{3}\delta^{jk} r'^2\right) d^3x'}_{I^{jk}\text{ mass quadrupole moment}}\right]$$

current moments appear in $\bar{h}^{0i}$

Generation of GWs: long story
Post-Newtonian approximation (falling into a rabbit hole)

- **Match solutions in the near wave zone** using near zone solution as boundary

in the near zone we had: $\bar{h}^{00} = 6\frac{I_{jk}n^j n^k}{r^3}$ at $r \ll \lambda_{GW}$, use it as a boundary condition to outgoung wave

- The outgoing wave solution: $\frac{\bar{h}^{ij}(t-R)}{R}$
- Note that: $\bar{h}^{00} \approx 2\left[\frac{1}{R}I_{jk}(t-R)\right]_{,jk}$ because we work in $r \ll \lambda_{GW}$
- Use harmonic condition $\bar{h}^{\alpha\beta}{}_{,\beta} = 0$ to trade spacial derivatives for time derivatives:

$$\left[\bar{h}^{jk}\right]^{TT} = \frac{2}{R}\partial_t^2\left[I_{jk}^{TT}(t-R)\right]$$

- **Non-linear effects:** the non-linear terms on r.h.s — propagation not along null cone of flat spacetime: scattering of GWs on the curvature created by a binary system: back-scattering is continuous procss, it depends on the past history of the system
- **Multipole expansion and spherical harmonics:** in multipole expansion we see $n^i = x^i/r$ — direction of GW propagation, we could use spherical coord. and decompose in spherical (spin-weighted) harmonics:

$$h_+ - ih_\times = \sum_{l\geq 2}\sum_{m=-l}^{l} h_{lm}{}^{(-2)}Y_{lm}(\theta,\phi)$$

Binary system

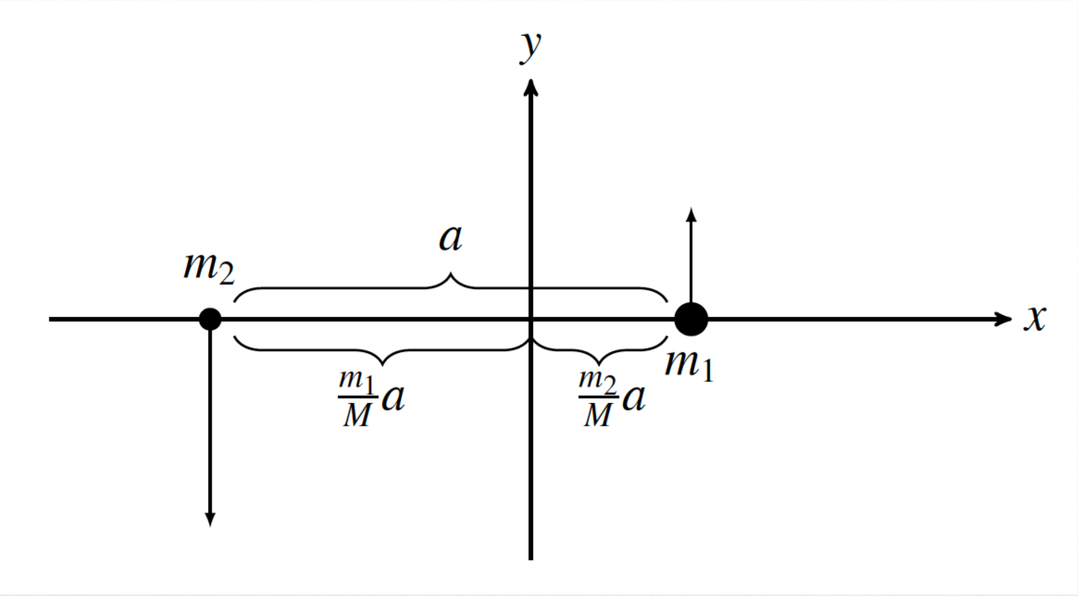

Consider binary system on a circular orbit.

$$m_1 > m_2, \quad M = m_1 + m_2 \quad \mu = m_1 m_2 / M$$

Use Kepler's law $\quad \omega = \sqrt{\frac{M}{a^3}}$

$$x_1 = \frac{m_2}{M} a \cos \omega t, \quad y_1 = \frac{m_2}{M} a \sin \omega t$$
$$x_2 = -\frac{m_1}{M} a \cos \omega t, \quad y_2 = -\frac{m_1}{M} a \sin \omega t$$

$$I_{jk} = \int T^{00} x_j x_k d^3x = \int \left[\delta(\vec{x} - \vec{x}_1) m_1 + \delta(\vec{x} - \vec{x}_2) m_2\right] x_j x_k d^3x = m_1 x_1^j x_1^k + m_2 x_2^j x_2^k$$

$$\ddot{I}_{xx} = -\ddot{I}_{yy} = -2\mu \left(M\omega\right)^{2/3} \cos 2\omega t,$$
$$\ddot{I}_{xy} = \ddot{I}_{yx} = -2\mu \left(M\omega\right)^{2/3} \sin 2\omega t,$$

polarization basis

$$\hat{e}_\theta = \hat{e}_x \cos\theta - \hat{e}_z \sin\theta, \quad \hat{e}_\phi = \hat{e}_y.$$
$$I_{\theta\theta} = I_{xx} \cos^2\theta, \quad I_{\phi\phi} = I_{yy}, \quad I_{\theta\phi} = I_{xy} \cos\theta.$$

$$h_+ = h_{\theta\theta} = -2\left(1 + \cos^2\theta\right) \frac{\mu}{R} (M\omega)^{2/3} \cos\left[2\omega(t - R) - \phi_0\right]$$
$$h_\times = h_{\theta\phi} = -4 \cos\theta \frac{\mu}{R} (M\omega)^{2/3} \sin\left[2\omega(t - R) - \phi_0\right]$$

Binary system

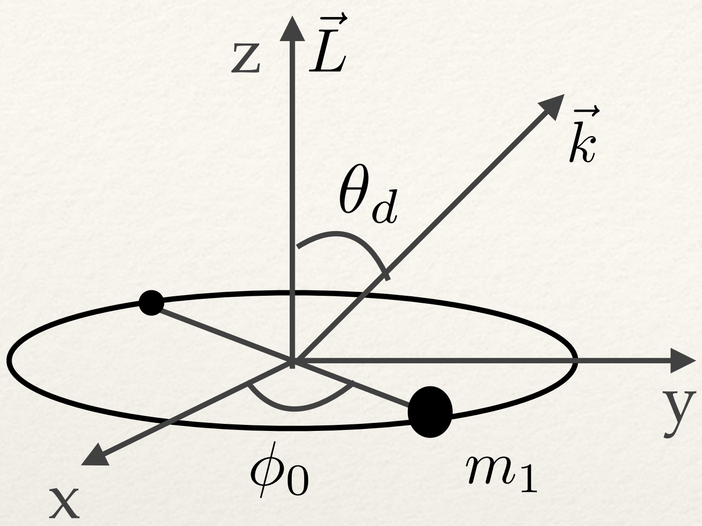

$$\boxed{\begin{aligned} h_+ = h_{\theta\theta} &= -2\left(1+\cos^2\theta_d\right)\frac{\mu}{R}(M\omega)^{2/3}\cos\left[2\omega(t-R)-\phi_0\right] \\ h_\times = h_{\theta\phi} &= -4\cos\theta_d\frac{\mu}{R}(M\omega)^{2/3}\sin\left[2\omega(t-R)-\phi_0\right] \end{aligned}}$$

- Inclination: angle between orb. angular momentum and propagation direction (θ_d), alternatively $\iota = \pi - \theta_d$ angle between L and direction ***to*** the source.

- Distance to the source: luminosity distance $R = D_L$

- GW emission strongest if face on/off, and weakest if the source is edge-on
- If masses are not spinning: the total angular momentum is orbital angular momentum $\vec{L}$
- If masses are spinning, then the total angular momentum: $\vec{J} = \vec{L} + \vec{S}_1 + \vec{S}_2$ if spins have arbitrary orientation (not aligned with the orbital angular momentum) - the orbit precesses (L rotates around J) due to spin-orbital coupling:

$$\dot{\vec{L}} \propto \vec{\Omega} \times \vec{L}$$

- Dominant harmonic: 2 x orbital freq. (circular), there are harminics 1,3,4,…x orbital freq. but lower in amplitude

Binary system

Loss of energy due to GWs

$$Lum = -\frac{dE^{GW}}{dt} = \frac{1}{5}\langle \dddot{\mathcal{M}}_{ij}\dddot{\mathcal{M}}_{ij}\rangle = \frac{32}{5}\eta^2(M\omega)^{10/3}$$

Balance equation

$$\dot{E}^{tot} = \frac{m_1 m_2}{2a^2}\dot{a} = -\frac{32}{5}\eta^2(M\omega)^{10/3}.$$

Total energy of the binary system

$$E^{tot} = \frac{m_1 m_2}{a} + \frac{m_1(\omega r_1)^2}{2} + \frac{m_2(\omega r_2)^2}{2} = -\frac{m_1 m_2}{2a}.$$

This equation can be easily integrated

$$a = \left[\frac{256}{5}\eta M^3(t_c - t)\right]^{1/4},$$

$$\pi f = \left[\frac{256}{5}\eta M^{5/3}(t_c - t)\right]^{-3/8}$$

$$\Delta t = \frac{5}{256 M^{5/3}\eta}(\pi f)^{8/3}$$

$$\phi_{orb}^{(N)} = \int 2\pi f(t)\, dt = -2\left[\frac{1}{5M_c}(t_c - t)\right]^{5/8} + \phi_c$$

$$\eta = \frac{\mu}{M} = \frac{m_1 m_2}{M^2}$$

Binary system

$$a = \left[\frac{256}{5}\eta M^3 (t_c - t)\right]^{1/4}$$

- The orbit shrinks as t —> tc

$$\pi f = \left[\frac{256}{5}\eta M^{5/3} (t_c - t)\right]^{-3/8}$$

- The frequency depend on the "chirp mass" $M_c = M\eta^{3/5}$

- GW (and orbital) frequency grows with time and infinite at tc (approach breaks down)

$$\phi_{orb}^{(N)} = \int 2\pi f(t)\, dt = -2\left[\frac{1}{5M_c}(t_c - t)\right]^{5/8} + \phi_c$$

- The phase depends on the chirp mass: Mc is the best measured parameter

$$\frac{df^{GW}}{dt} = \frac{96}{5\pi} M_c^{5/3} (\pi f)^{11/3}$$

- Very strong dependance on the frequency: very slow evolution for the broad orbits

- If $m_1 \gg m_2, \quad M_c^{5/3} \approx \frac{m_2}{m_1} m_1^{5/3}$

the frequency evolution could be sloweven if the orbit is relativistic (extreme mass ratio inspiral EMRI)

Binary system

$\Delta t = \frac{5}{256 M^{5/3} \eta} (\pi f)^{8/3}$ time to coalescence (merger) starting from freq. f

LIGO/VIRGO: operates on the ground, freq range 30-2000 Hz.
take f=40 Hz, NS-NS system each mass 1.4 solar mass: Δt ~20sec
take f = 30 Hz, BH-BH system each 30 solar mass: Δt ~0.32sec

LISA (space based detector) will operate in freq. range 0.1- 100 mHz
take f=0.1mHz, $M = m_1 + m_2 = 10^6 M_\odot, \quad \Delta t \approx 35\, days/\eta < 1\, year$

- Post-Newtonian iterations: we plug back to Einstein equations the evolving orbit and linear solution for the GW, solve at the next order

$$\Phi = \Phi_0 + \Phi^N + \epsilon^2 \Phi^{1PN} + \epsilon^3 \Phi^{1.5PN} + \epsilon^4 \Phi^{2PN} + \dots$$

Binary system

- Waveform (GW signal) in the frequency domain

GW, leading order in amplitude

$$h_+(t) = A_+ \cos\Phi(t), \quad h_\times = A_\times \sin\Phi(t)$$

Fourier transformation

$$\tilde{h}(f) = \int h(t) e^{-2\pi i f t} dt$$

If amplitude is slowly evolving, monotoneous function of time

$$\tilde{h}_+(f) = (1+\cos^2\iota)\sqrt{\frac{5}{6}}\frac{1}{4\pi^{2/3}}\frac{M_c^{5/6}}{D_L} f^{-7/6} e^{i\Psi(f)},$$

$$\tilde{h}_+(f) = 2i\cos\iota\sqrt{\frac{5}{6}}\frac{1}{4\pi^{2/3}}\frac{M_c^{5/6}}{D_L} f^{-7/6} e^{i\Psi(f)}$$

The phase in freq. domain

$$\Psi(f) = 2\pi f t_c - \phi_0 - \frac{\pi}{4} + \frac{3}{4}(8\pi M_c f)^{-5/3} + ...(Mf)^{-5/3} + ...(Mf)^{-1} + ...(Mf)^{-2/3}$$

- Amplitude and the dominant term in phase depend on M_c only (other terms depend on total mass and mass ratio.
- Amplitude is higher at low frequencies (early inspiral, slow frequency evolution, many cycles.

GW signal

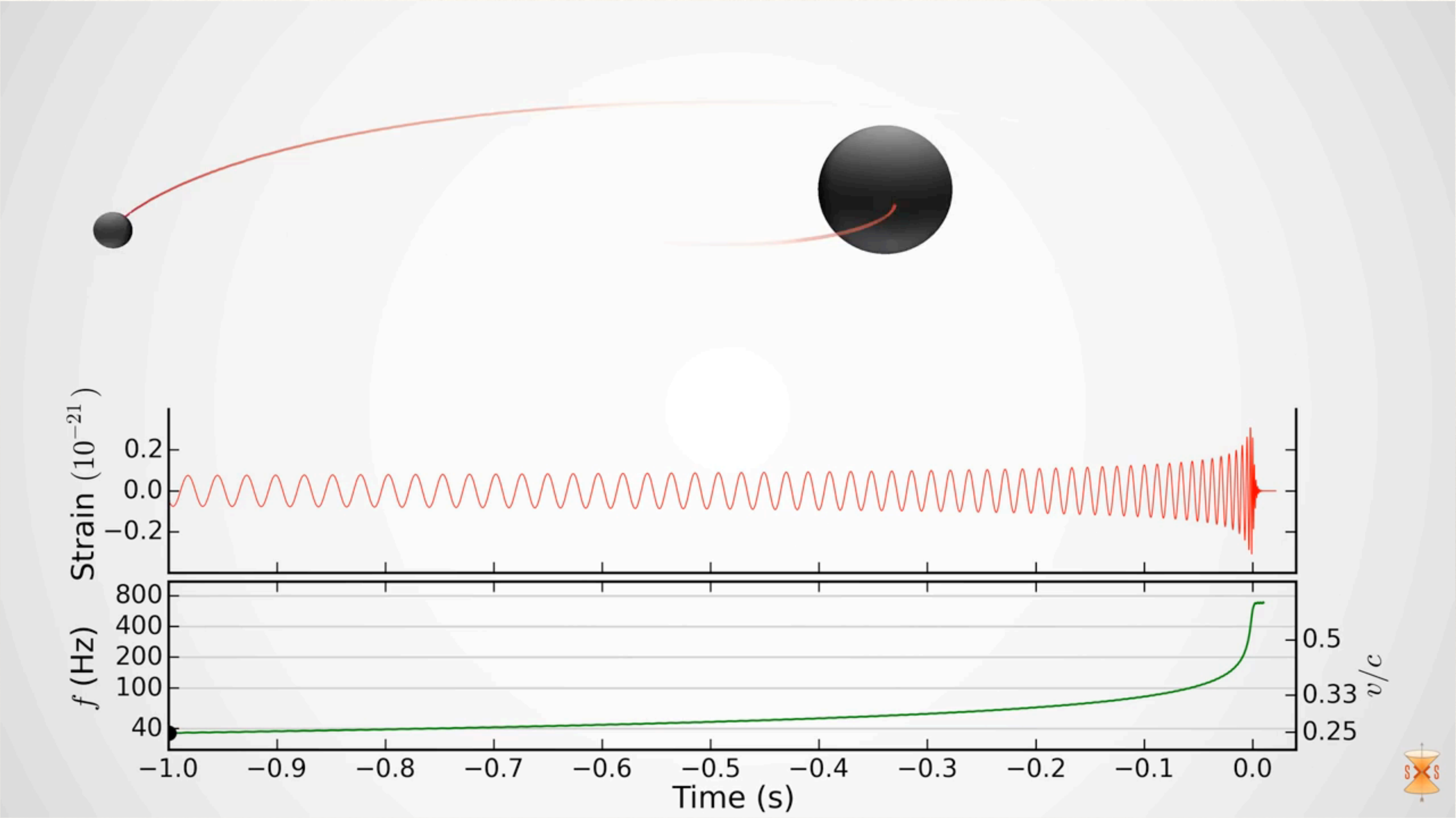

[Credits: SXS collaboration]

Modelling GW signal

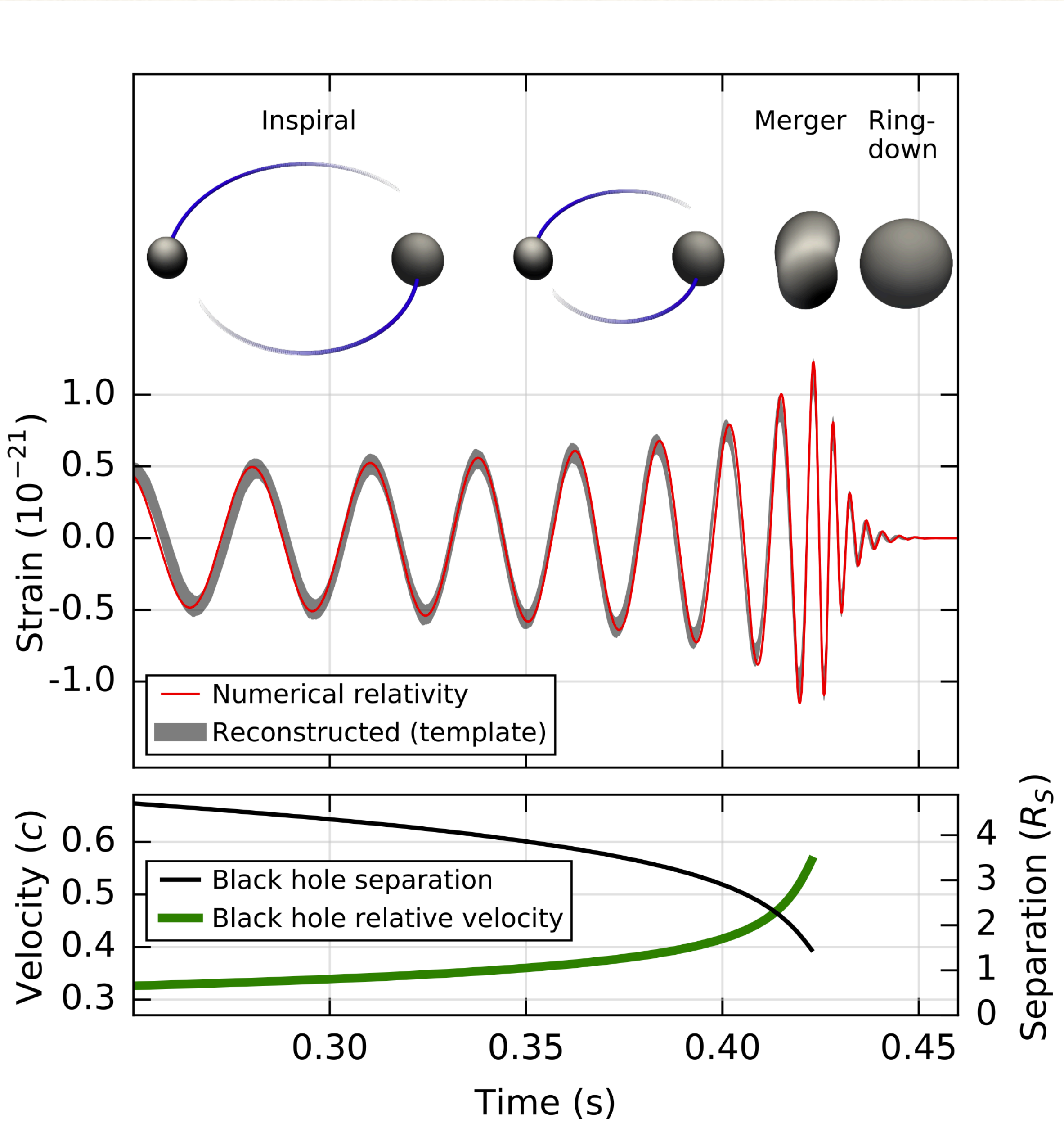

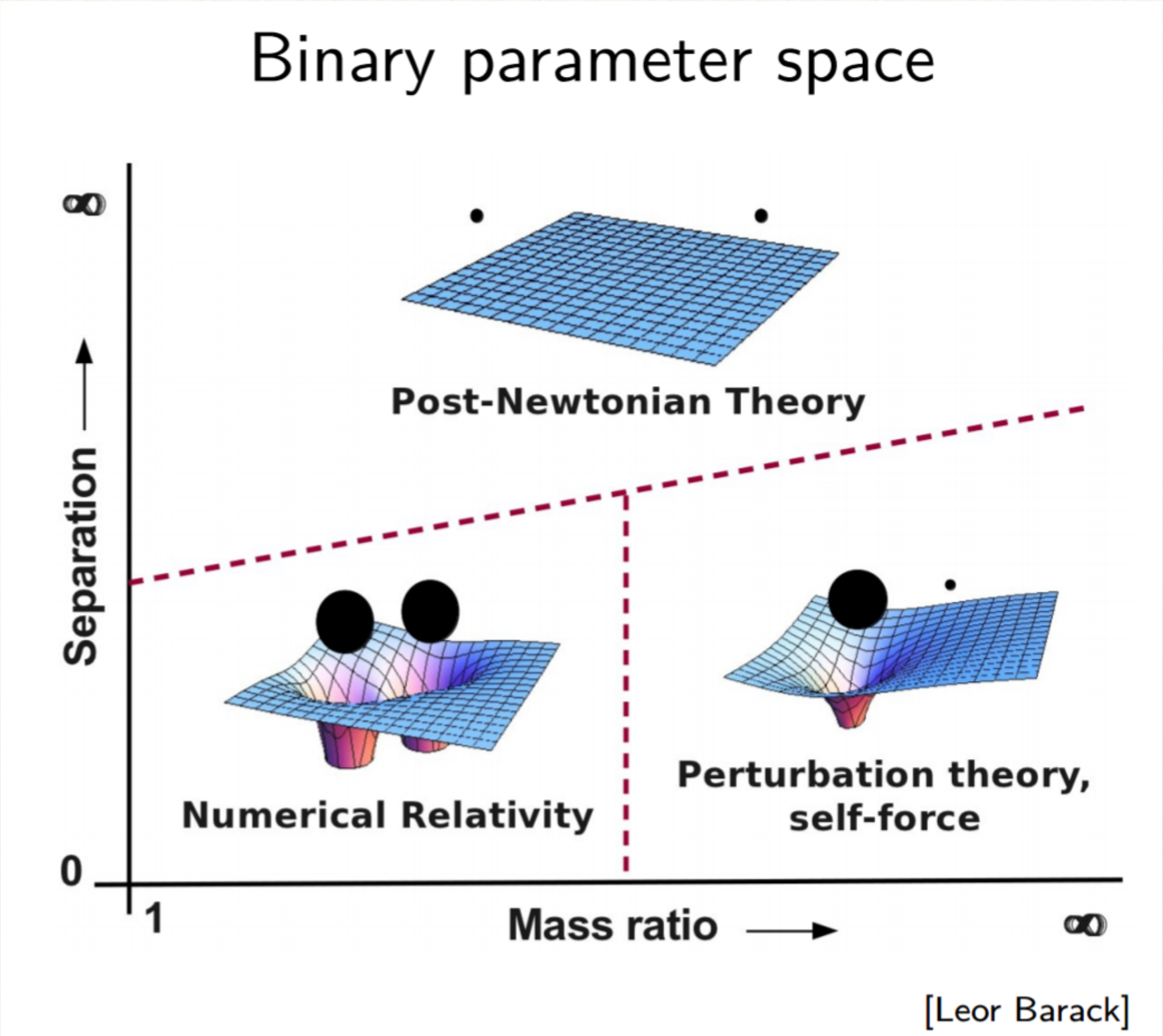

GW signal from binary stsem can be conventionally split into three parts: inspiral (Post-Newtonian decomposiotion, merger (numerical relativity), ringdown (BH perturbation)

NR surrogate waveforms

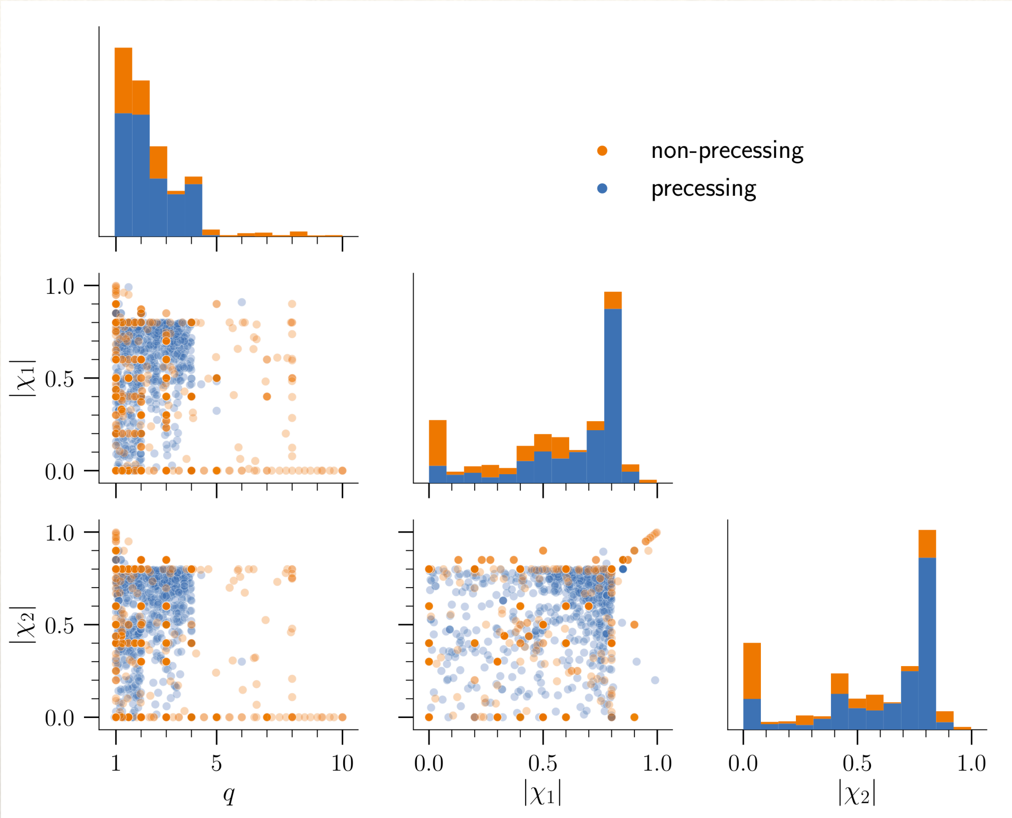

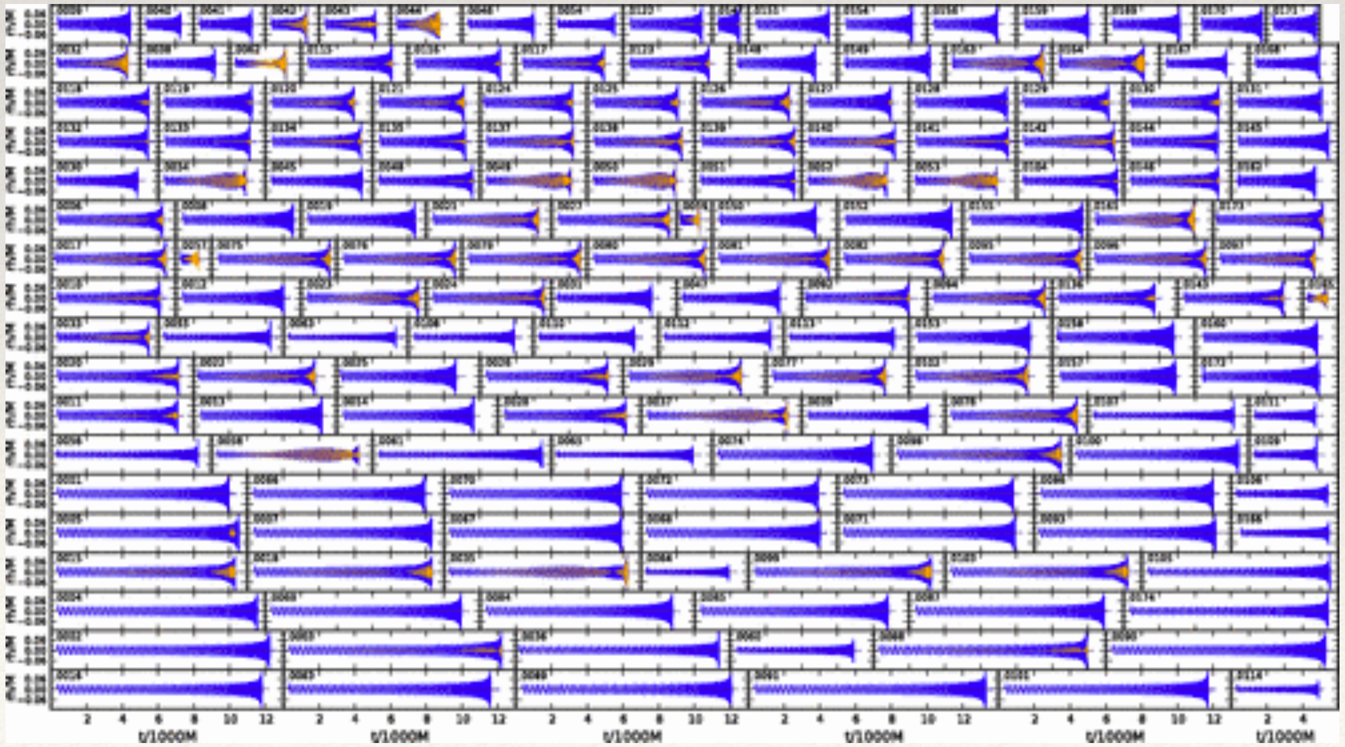

- Using a large number of numerical waveforms (solving Einsten equations numerically: very short - about 20 orbits before the merger.)
- Using them as a basis for waveform decomposition
- Interpolating across parameters space
- The most accurate to-date model, but limited in the parameter space

Phenomenological template family

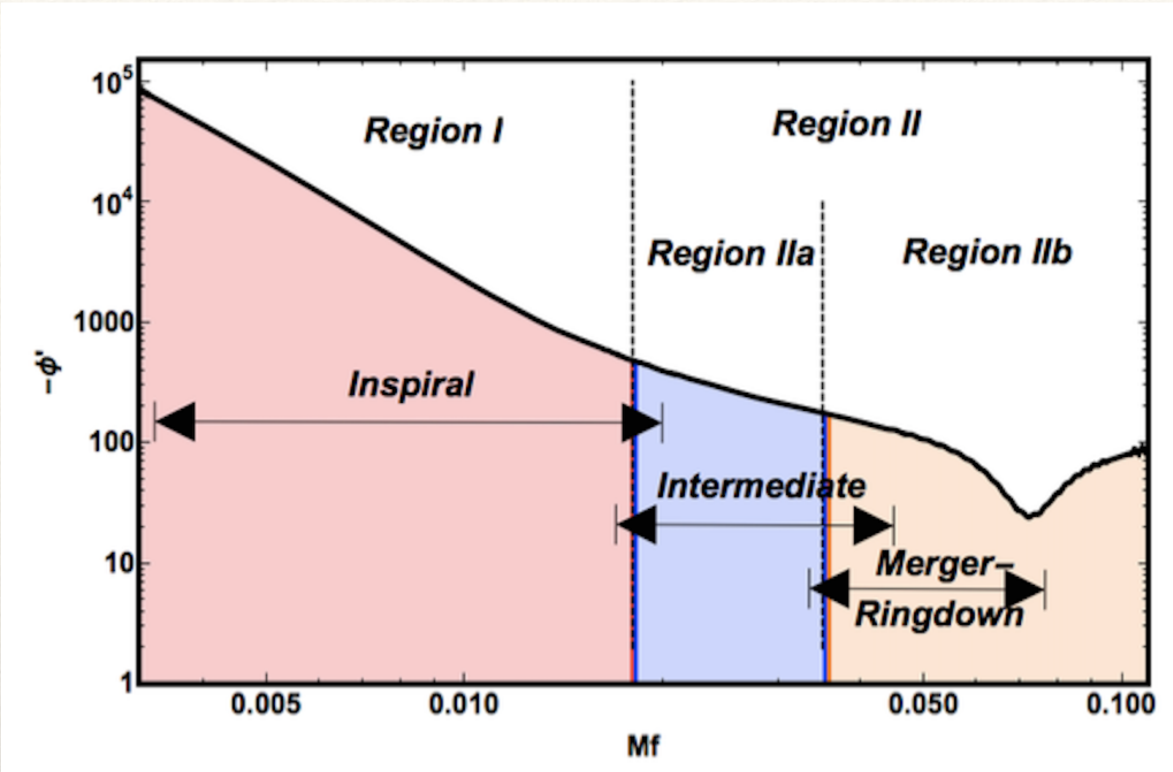

$$\phi_{\rm Ins} = \phi_{\rm TF2}(Mf;\Xi) + \frac{1}{\eta}\left(\sigma_0 + \sigma_1 f + \frac{3}{4}\sigma_2 f^{4/3} + \frac{3}{5}\sigma_3 f^{5/3} + \frac{1}{2}\sigma_4 f^2\right)$$

$$\phi_{\rm Int} = \frac{1}{\eta}\left(\beta_0 + \beta_1 f + \beta_2 \,{\rm Log}(f) - \frac{\beta_3}{3} f^{-3}\right)$$

$$\phi_{\rm MR} = \frac{1}{\eta}\left\{\alpha_0 + \alpha_1 f - \alpha_2 f^{-1} + \frac{4}{3}\alpha_3 f^{3/4} + \alpha_4 \tan^{-1}\left(\frac{f - \alpha_5 f_{\rm RD}}{f_{\rm damp}}\right)\right\}.$$

Comparison of non-precessing waveforms

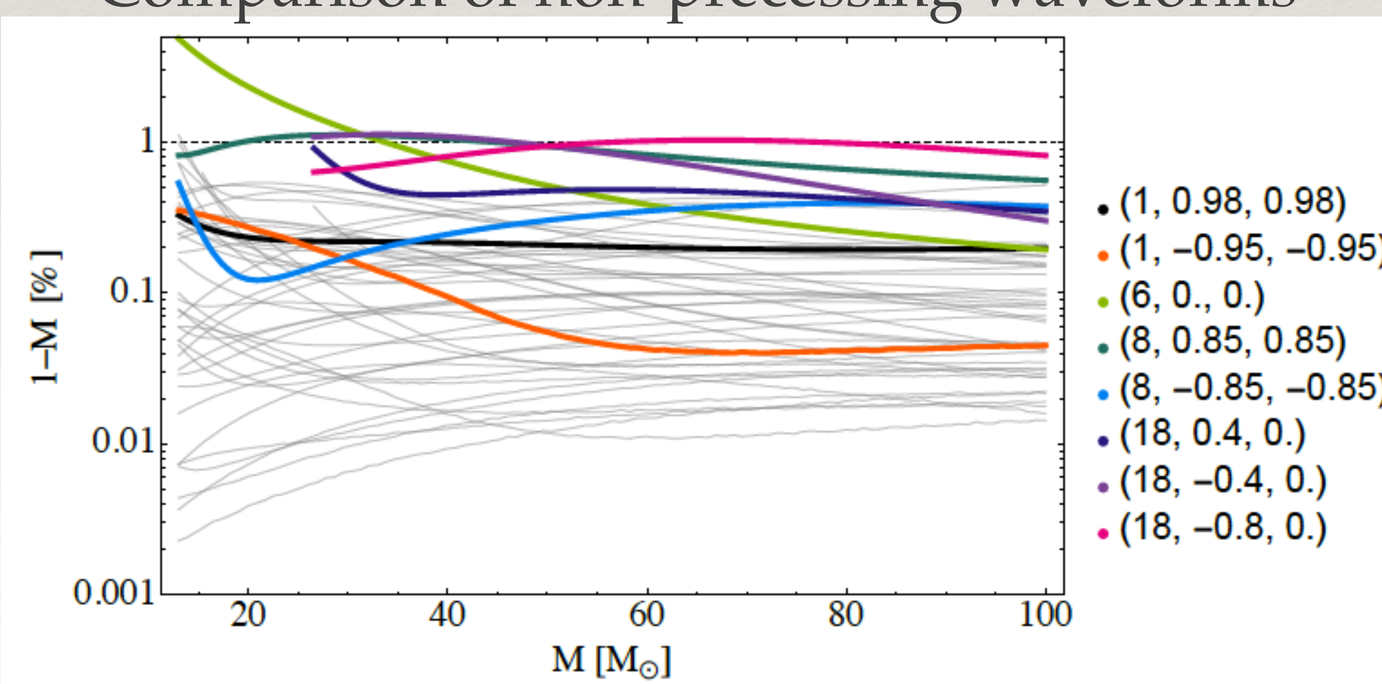

- Waveform constructed in the frequency domain
- Uses Post-Newtonian results for the early evolution (inspiral) of a binary
- For merger-ringdown part: there is an analytical expression with free parameters which are calibrated to fit the NR data
- Precession is added by rotation taken from the Post-Newtonian evolution
- Very fast to generate

Higher order modes

Decomposing the waveform in spherical harmonics $$h_+ - ih_\times = \sum_{l\geq 2}\sum_{m=-l}^{l} h_{lm}\,{}^{(-2)}Y_{lm}(\theta,\phi)$$

For (quasi)circular binaries, the dominant mode is $l = 2, m = \pm 2$ (twice orbital frequency)

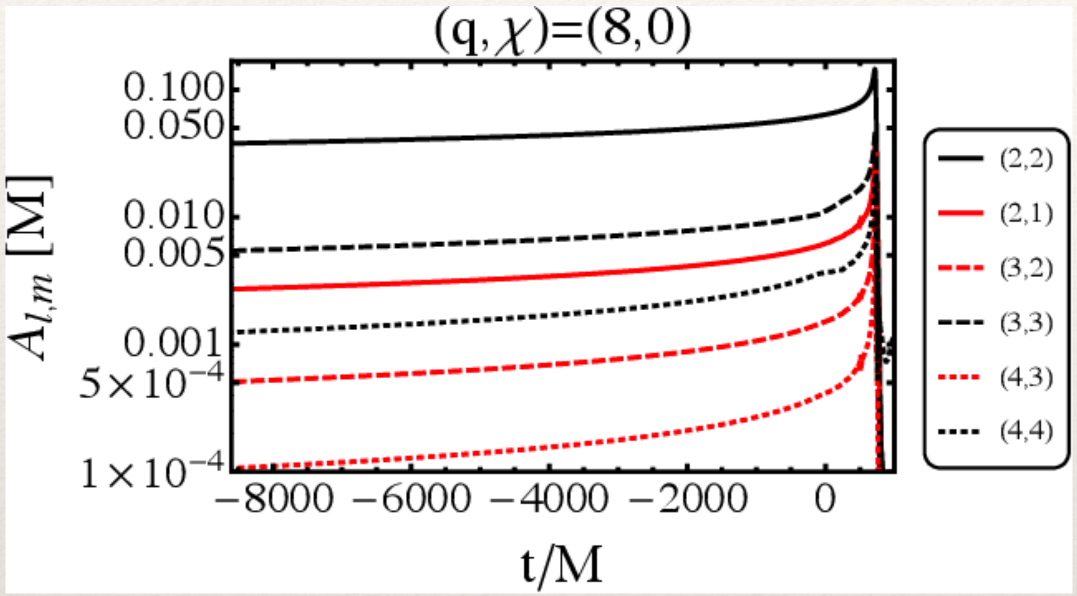

- For inspiral: odd harmonics suppressed by (v/c) and $(m_1 - m_2)/(m_1 + m_2)$)
- Coupled differently to inclination: breaking degeneracy in parameter space

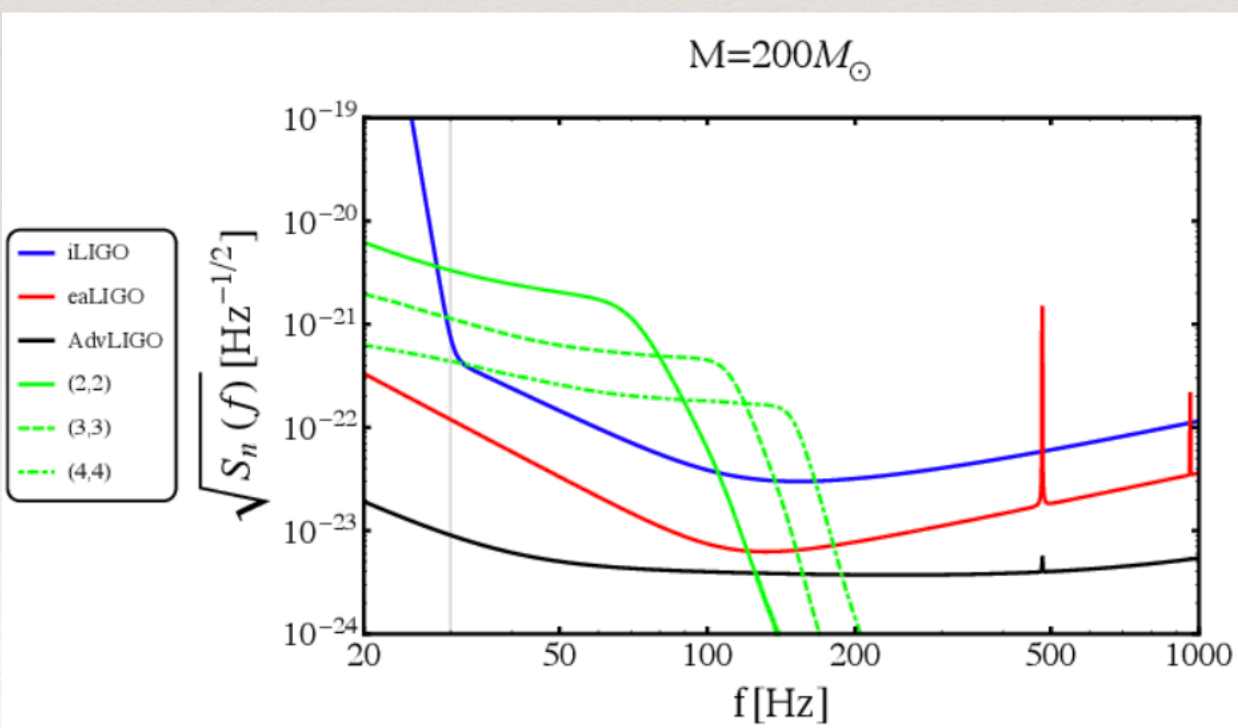

GW190412

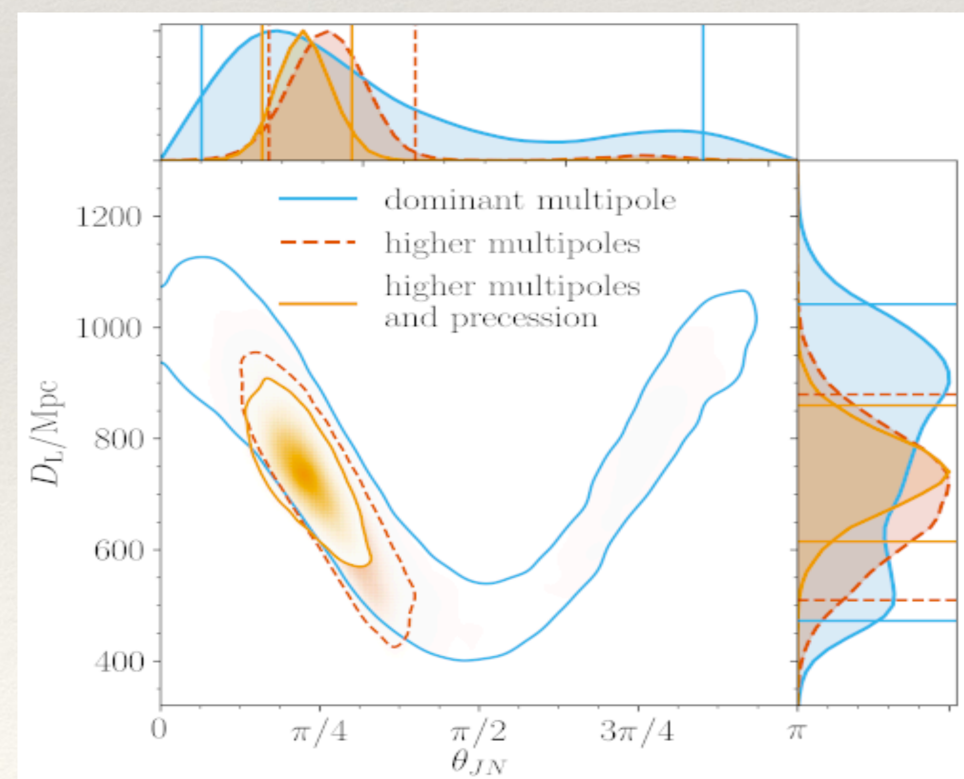

Orbital precession

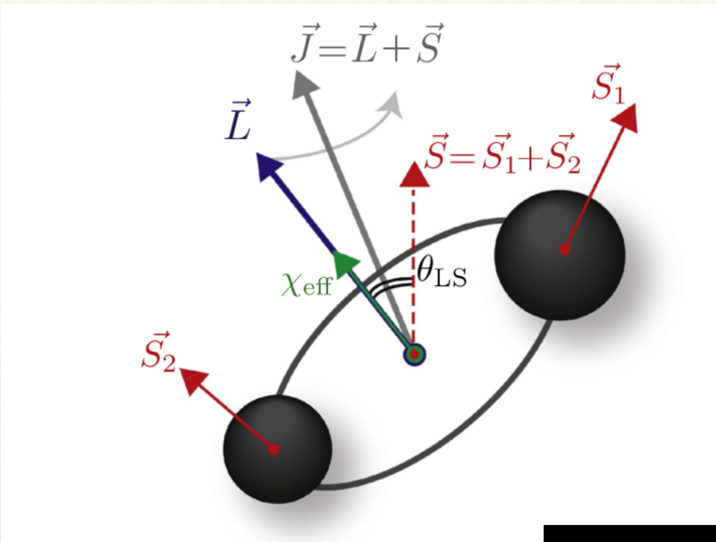

Credit: Carl Rodriguez

- If the spins of BHs are not parallel to the orbital angular momentum: spin and orbital precession around total momentum of the binary

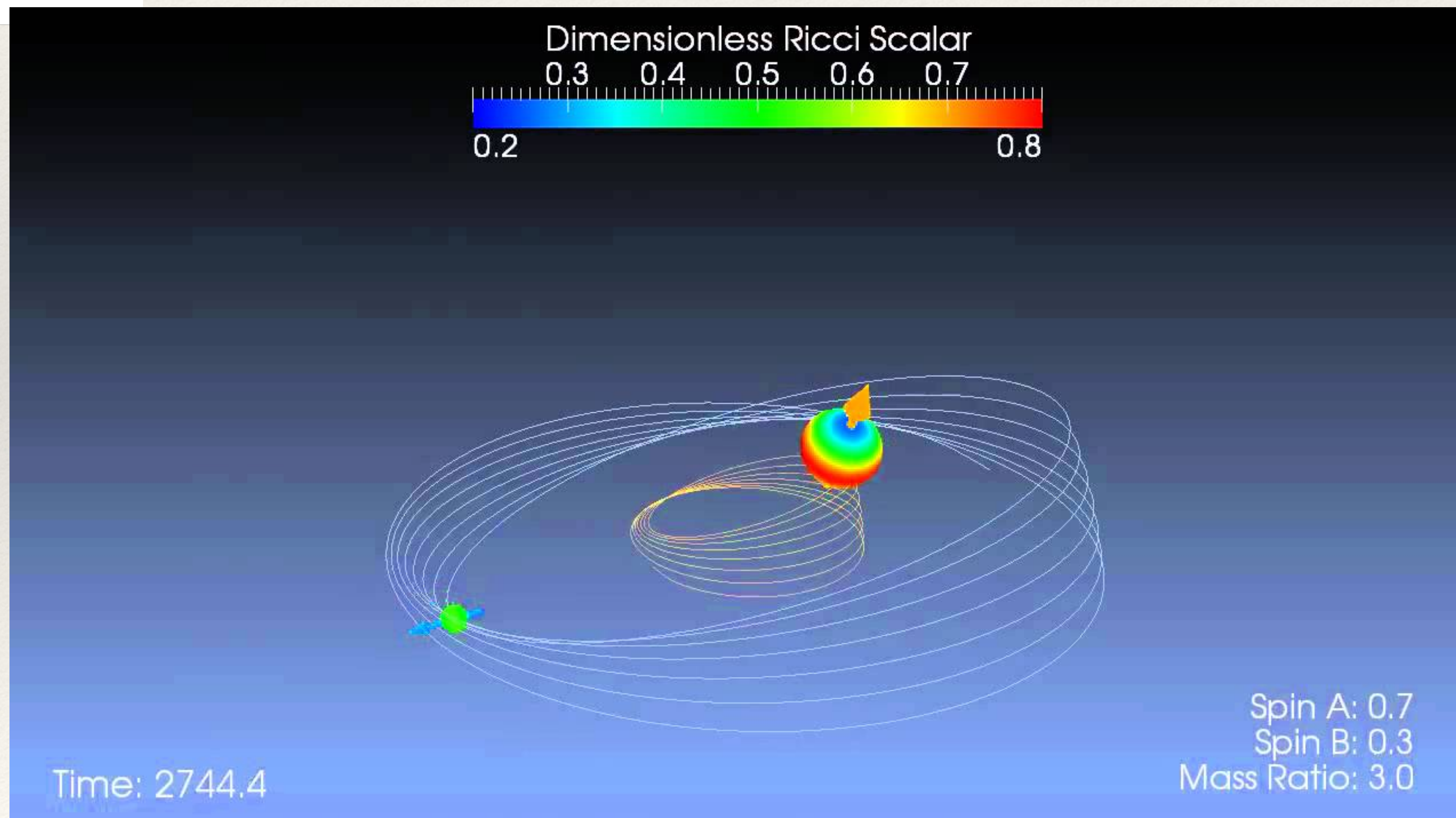

Spins of BHs in detected binaries

Left (right) halves of the circles are shaded in proportion to posterior on spin magnitude and tilt of the more (less) massive component

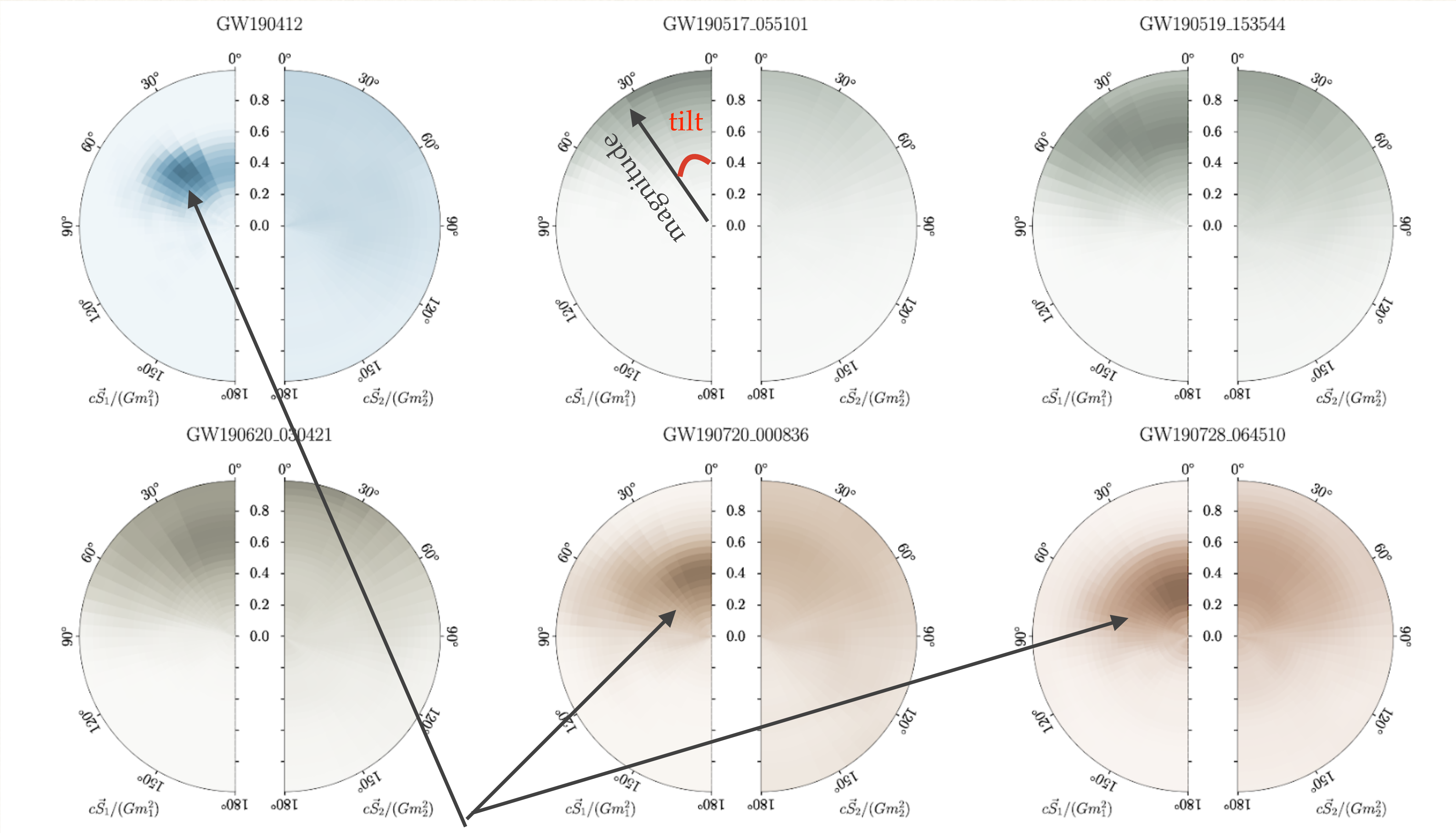

In some cases we find tighter constraints on the spin of the more massive merger component.

In-plane components of the spins: precession?

LVC Catalog paper, arXiv: 2010.14527

- A few systems where posterior on effective precession spin parameter χ_p (measure of spin in orbital plane) differs from the prior.

- More massive component in source of GW190814 has small spin magnitude, and therefore we infer small effective precession spin parameter.

- Mild evidence for spin precession in sources of GW190412 and GW190521.

- No systems with strong evidence of precession

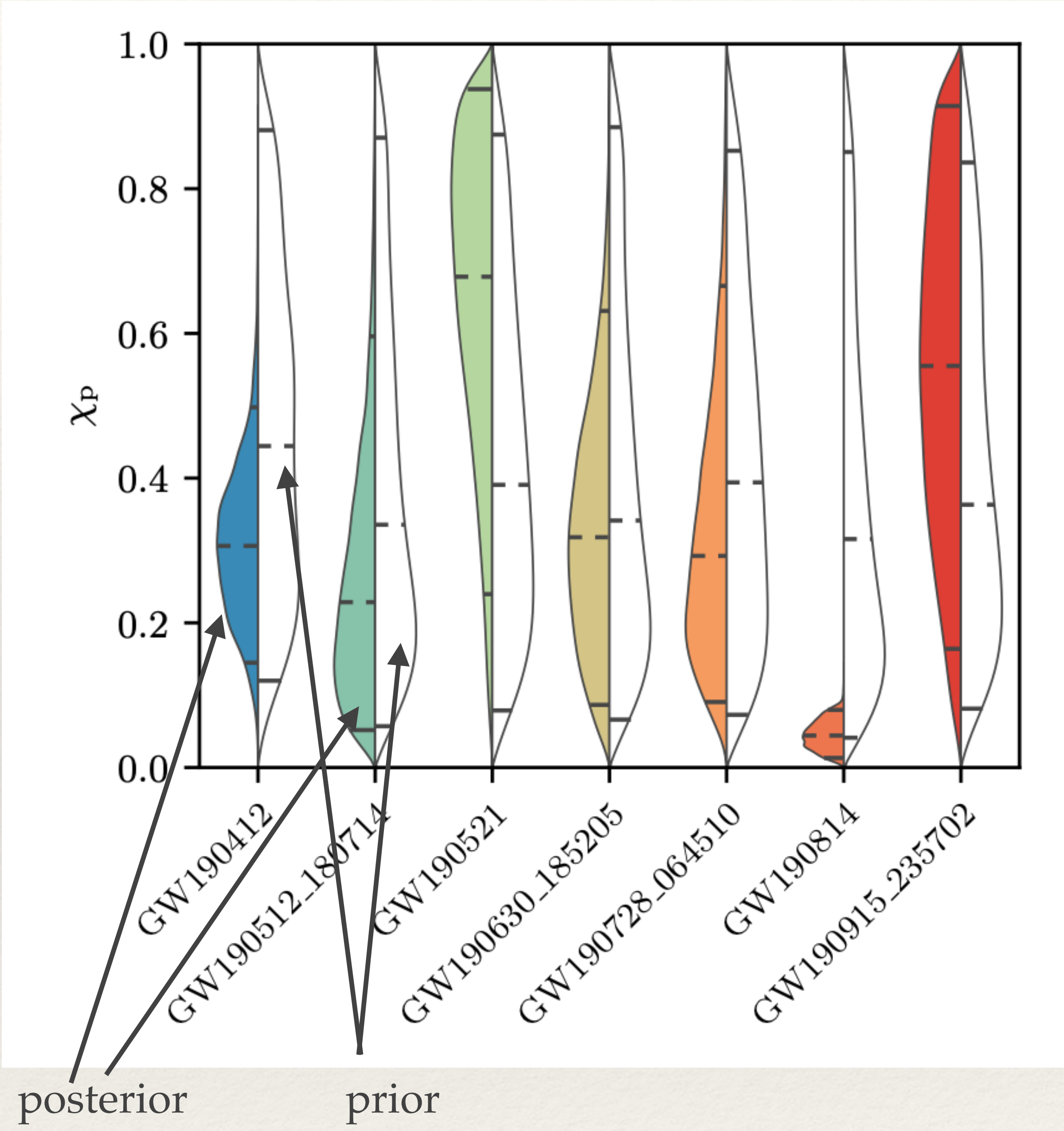

GW190412

Parameter[a]	EOBNR PHM	Phenom PHM	Combined
$m_1/M_\odot$	$31.7^{+3.6}_{-3.5}$	$28.1^{+4.8}_{-4.3}$	$30.1^{+4.6}_{-5.3}$
$m_2/M_\odot$	$8.0^{+0.9}_{-0.7}$	$8.8^{+1.5}_{-1.1}$	$8.3^{+1.6}_{-0.9}$
$M/M_\odot$	$39.7^{+3.0}_{-2.8}$	$36.9^{+3.7}_{-2.9}$	$38.4^{+3.8}_{-3.9}$

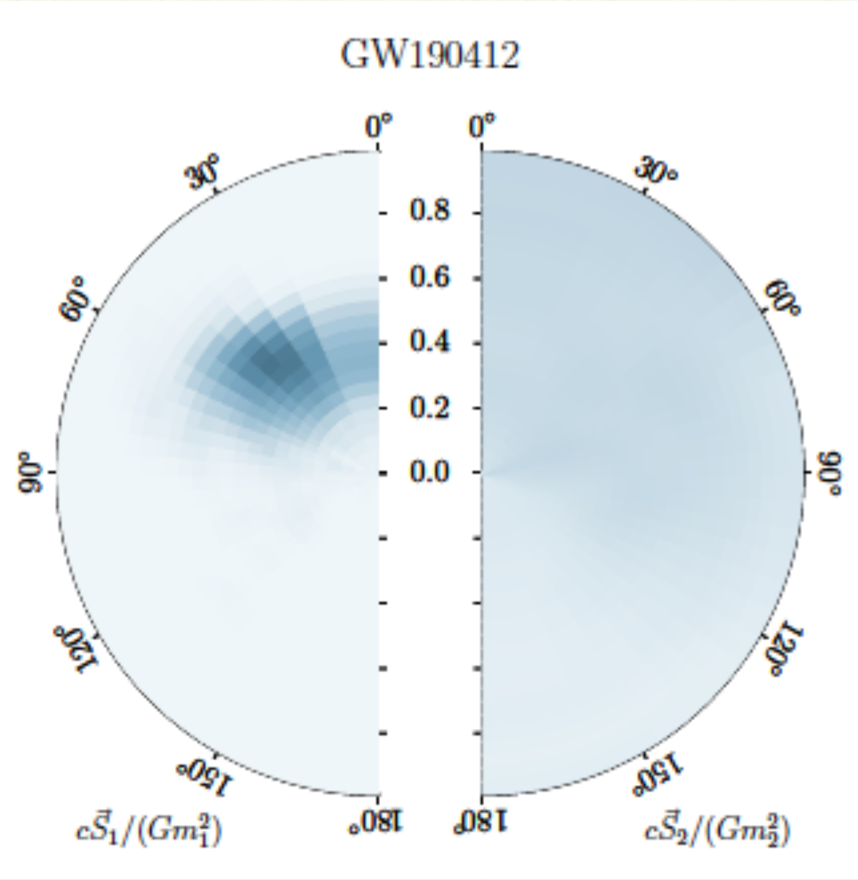

.LVC 2020 GW190412

- Log_{10}(Bayes factor) > 3 in favour of higher order modes (beyond quadrupole)
- Tilt angle ~45.8 deg, χ_1~ 0.44
- Good localization ~21 deg^2, $V_{90\%}$ ~ 0.037Gpc^3
- Questions of formation: densed env., triple or quadruple system, evolution in AGN disk

Extreme mass ratio inspirals

- Capture of a small compact object (CO): stellar mass BH, NS, WD by a massive black hole in the galactic nuclei (LISA sources)
- Extremely larg mass ratio: spend long time in vicinity of MBH before they plunge: (v/c) is not small: PN theory is not accurate. NR — not efficient.
- The mass ratio $(m_2/m_1 \equiv m/M \ll l)$ is now a small parameter
- Geodesic motion in Kerr + adiabatic evolution: osculating elements

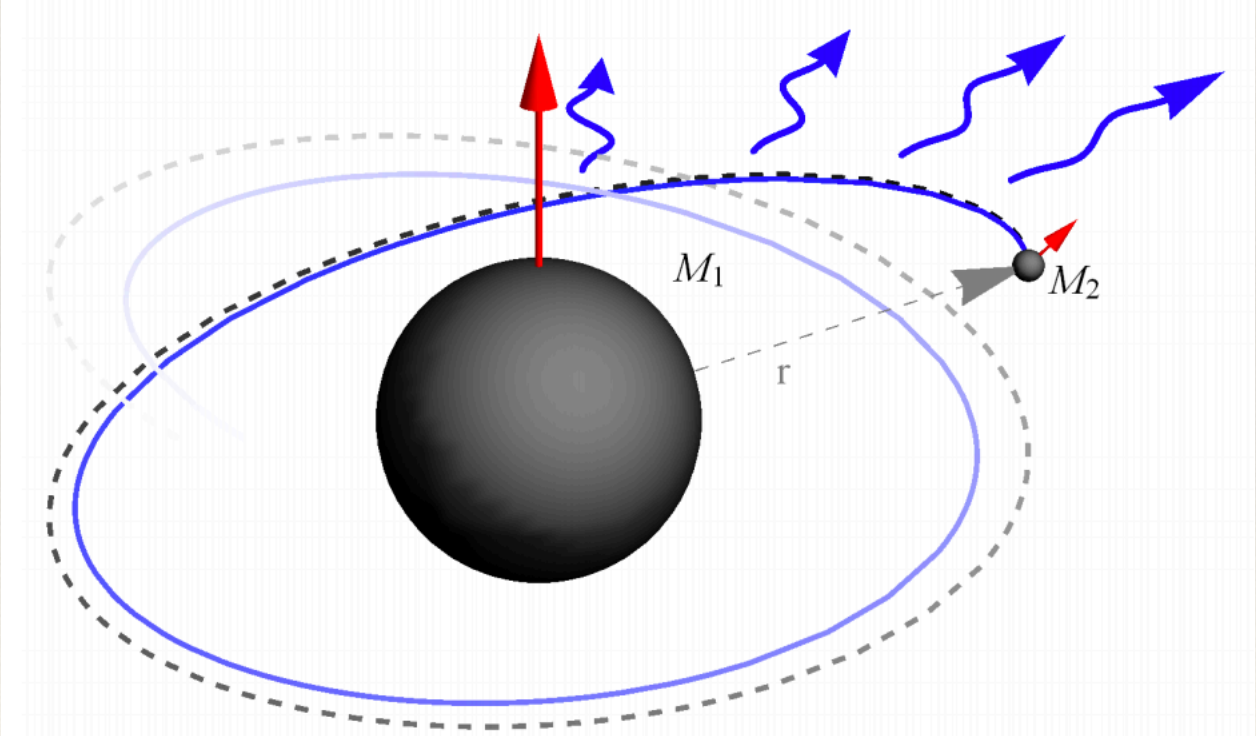

Credits: Maarten van de Meent

Extreme mass ratio inspirals

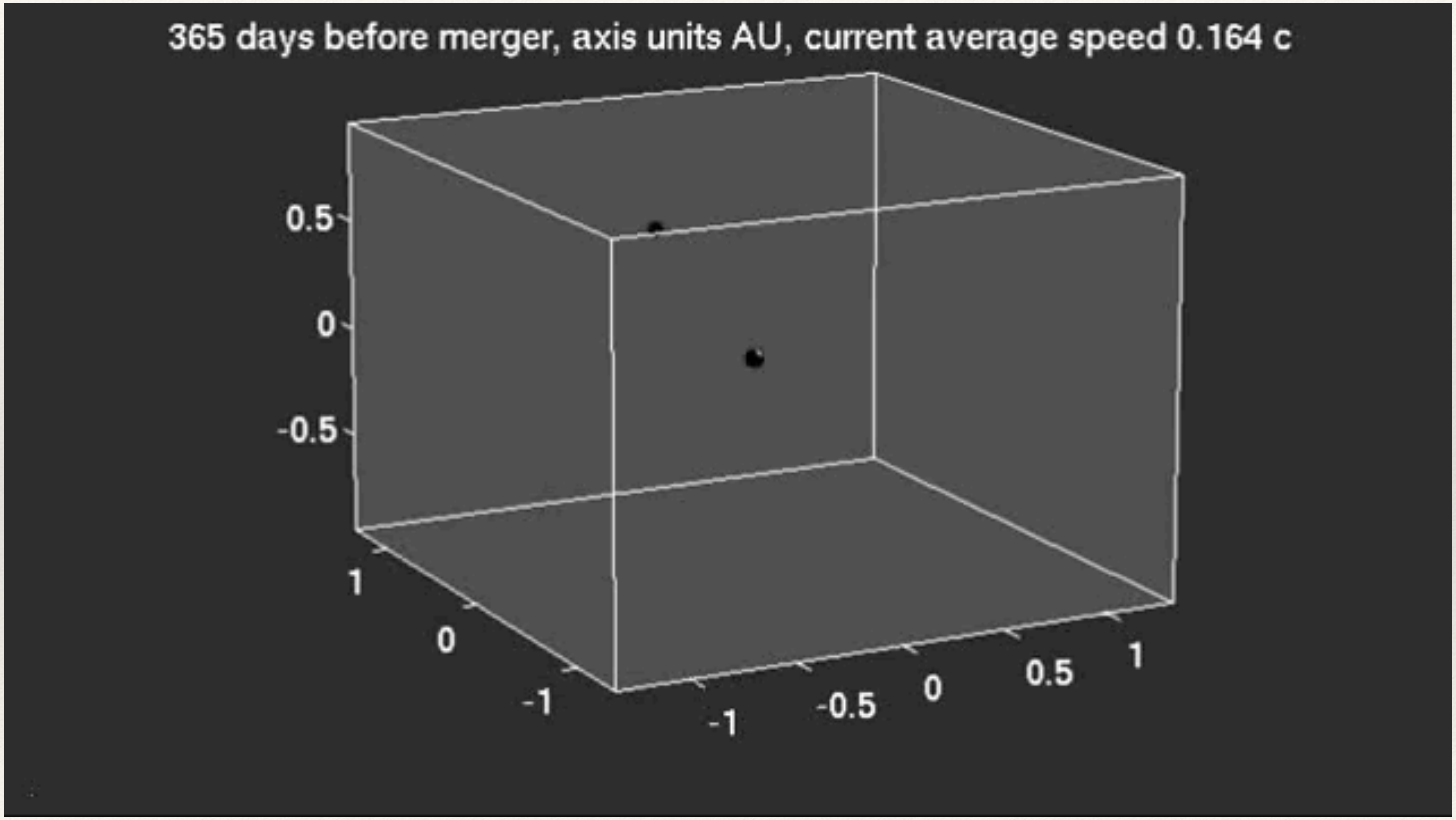

Credits: Steve Drasco

EMRIs: short story

- Orbital motion: (almost) elliptical with a strong relativistic precession + orbital precession due to spin-orbital coupling
- Signal is very rich in structure (hard to detect but gives a lot of information)
- Ultra-precise parameter determination (if detected). Can map spacetime of a heavy object: holiodesy

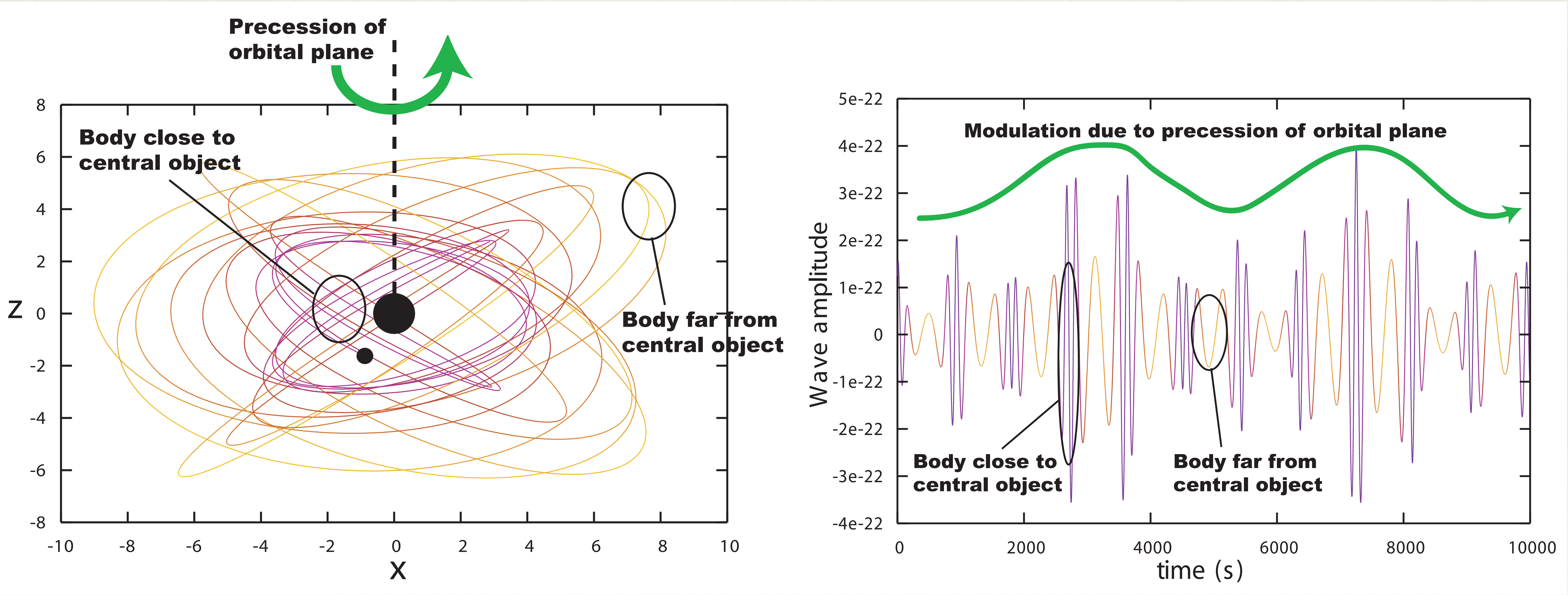

EMRIs: long story

- Geodesic motion of a test mass in Kerr spacetime (Boyer-Lindquist coordinates): derived from super-Hamiltonian: $\mathscr{H} = \frac{1}{2} g_{\mu\nu} p^\mu p^\nu = -\frac{1}{2} m^2$

$$\Sigma \frac{dr}{d\lambda} = \pm\sqrt{R(r, L_z, E, Q)}, \quad \Sigma \frac{d\phi}{d\lambda} = \Phi(r, \theta, L_z, E, Q)$$
$$\Sigma \frac{d\theta}{d\lambda} = \pm\sqrt{\Theta(r, L_z, E, Q)}, \quad \Sigma \frac{dt}{d\lambda} = \mathcal{T}(r, \theta, L_z, E, Q)$$

Turning points

$$\Sigma = r^2 + a^2 \cos^2\theta$$

spin of MBH

- Geodesic is parametrized by affine parameter λ, and there are 8 constants of motion: 4 initial coordinates $(t_0, r_0, \theta_0, \phi_0)$ and 4 1st integrals (E - energy, L_z projection of orbital momentum on the spin of MBH, Q - Carter constant, m)

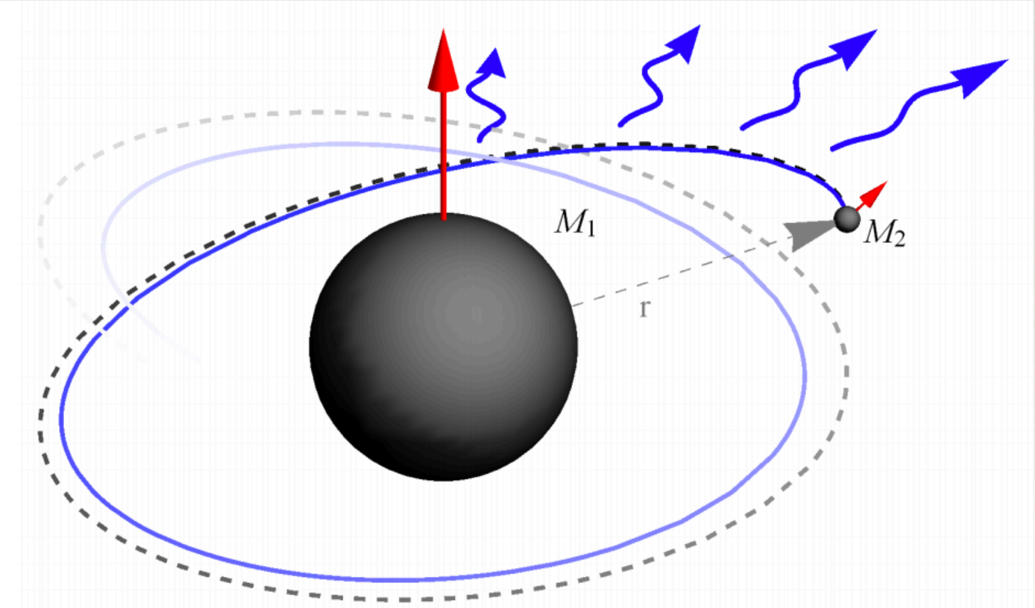

Credits: Maarten van de Meent

- GW carry energy and angular momentum away
- Adiabatic approximation: Orbit evolves slowly
- Osculating approach: at each instance fit a geodesic: slow change from one geodesic to another: $\dot{E}, \dot{L}_z, \dot{Q}$ — slowly changing functions to be plugged into eq. of motion

EMRIs: long story

- More regirously: we need to solve the Einstein equations with the s/e tensor. Approximating small body as delta-function:

$$T^{\mu\nu} = \frac{m u^\mu u^\nu}{\Sigma \sin\theta u^t}\delta(r - r(t))\delta(\theta - \theta(t))\delta(\phi - \phi(t))$$

- The equation we want to solve is of type : $\Box_g \Psi = q\delta(x - z(t))$, and the equation of motion is a forced geodesic motion with a force: *self-force* is defined as $F^\alpha = q\nabla^\alpha \Psi_R$: gradient of the regular part of the retarded field: $\Psi_R = \Psi - \Psi_S$ (full - singular part)

- Computation of regular part is a challenge:
  - Decompose in spherical harmonics $\Psi = \sum_{l.m} \Psi_{lm}(t, r) Y^{lm}(\theta, \phi)$ and regularize each parts in each mode contributing to the singular solution
  - Approximate the singular solution as $\tilde{\Psi}_S$, subtract it from the full and solve eqn for the remaining regular part:

$$\Box_g \tilde{\Psi}_R = q\delta(x^\mu - z^\mu(t)) - \Box_g \tilde{\Psi}_S \equiv S(x^\mu, z^\mu)$$ regular effective source on the r.h.s

coupled to the equation of motion: $m\frac{Du^\mu}{d\tau} = q(g^{\mu\nu} + u^\mu u^\nu)\nabla_\nu \tilde{\Psi}_R$

Modelling GW signal using Effective-one-body (EOB) approach

Effective-one-body approach [Buonanno & Damour 1999]:
The main idea is to map the (real) dynamic of two comparable mass binary to an effective problem of motion of test mass in an effective spacetime

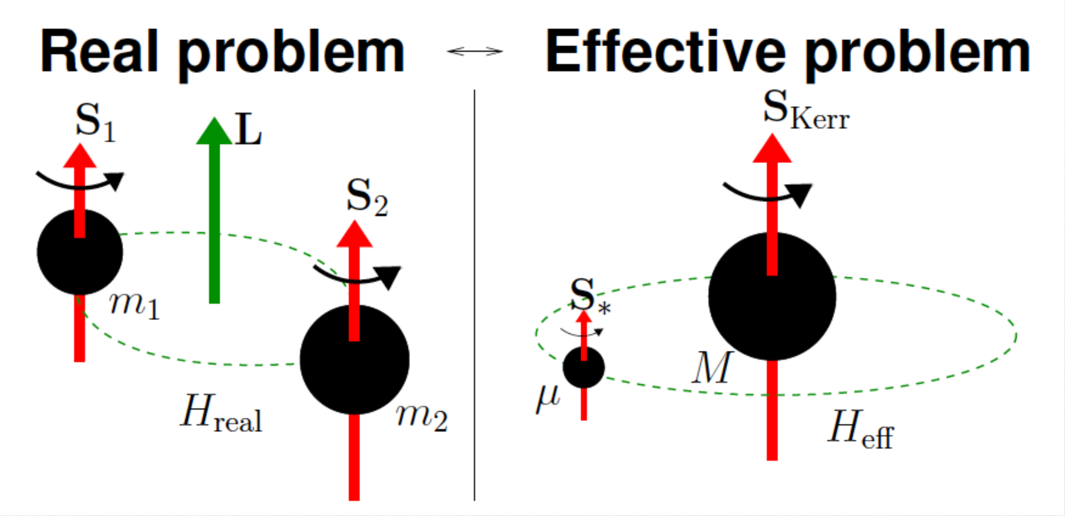

$$M = m_1 + m_2, \quad \mu = \frac{m_1 m_2}{M}$$

EOB has three essential components

- Map conservative two-body dynamics to a motion of a test mass **m** in the field of a central body **M.**
- Add the radiation reaction force
- Construct the waveform based on the computed dynamics with attached the ring-down **RD** part of the signal

See review: [Damour 2012]

Conservative dynamics (non-spinning BHs)

We start with Hamiltonian (in ADM coordinates) for 2-body problem
$\vec{x} = \vec{x}_1 - \vec{x}_2, \;\; \vec{p} = \vec{p}_1 = -\vec{p}_2$

$$H(\vec{x},\vec{p}) = Mc^2 + H_N(\vec{x},\vec{p}) + \sum_k \frac{1}{c^{2k}} H_{kPN}(\vec{x},\vec{p})$$

Known up to 4PN order
[Damour, Jaranowski, Schaefer 2014,15]

$$\boxed{H_N(\vec{x},\vec{p}) = \frac{\vec{p}^2}{2\mu} - \frac{M\mu}{r}}$$

Newtonian part:
test mass **m** in the central field of **M**:
EOB is relativistic generalisation

Conservative dynamics (non-spinning BHs)

The "effective" dynamics is constructed using the "effective" spherically symmetric spacetime

$$\boxed{ds^2_{\rm eff} = -A(r_{\rm eff}, \eta)dt^2 + \frac{D(r_{\rm eff}, \eta)}{A(r_{\rm eff}, \eta)} dr^2_{\rm eff} + r^2_{\rm eff} d\Omega^2,}$$

The Schwarzschild limit requires:

$$\boxed{A(r_{\rm eff}, \eta = 0) = 1 - \frac{2M}{r_{\rm eff}}, \quad D(r_{\rm eff}, \eta = 0) = 1}$$

The (super) Hamiltonian describing geodesic motion:

Geodesic term in effective spacetime

$$\boxed{g^{\mu\nu}_{\rm eff}\, p^{\rm eff}_{\mu}\, p^{\rm eff}_{\nu}} + \boxed{Q(p^{\rm eff}_{\mu})} = -\mu$$

"Post-geodesic" , (at least) quartic in linear momentum

Conservative dynamics: mapping

The Hamiltonian for the effective problem

$$H_{\rm eff}(\vec{r}_{\rm eff},\vec{p}_{\rm eff})/\mu = \sqrt{A(r_{\rm eff})\left[1+\vec{p}^{\,2}_{\rm eff}+\left(\frac{A(r_{\rm eff})}{D(r_{\rm eff})}-1\right)(\vec{n}_{\rm eff}.\vec{p}_{\rm eff})^2+\frac{Q(p_{\rm eff})}{r^2_{\rm eff}}\right]}$$

Both Hamiltonians to be written in terms of action-variables: $J_i = \dfrac{1}{2\pi}\oint p_i dx_i$

Mapping

$$\mathcal{E}_{\rm eff}(N_{\rm eff},J^{\rm eff}_\phi) = f[\mathcal{E}(N,J_\phi)] \quad \Longrightarrow \quad H = M\sqrt{1+2\eta\frac{H_{\rm eff}-\mu}{\mu}}$$

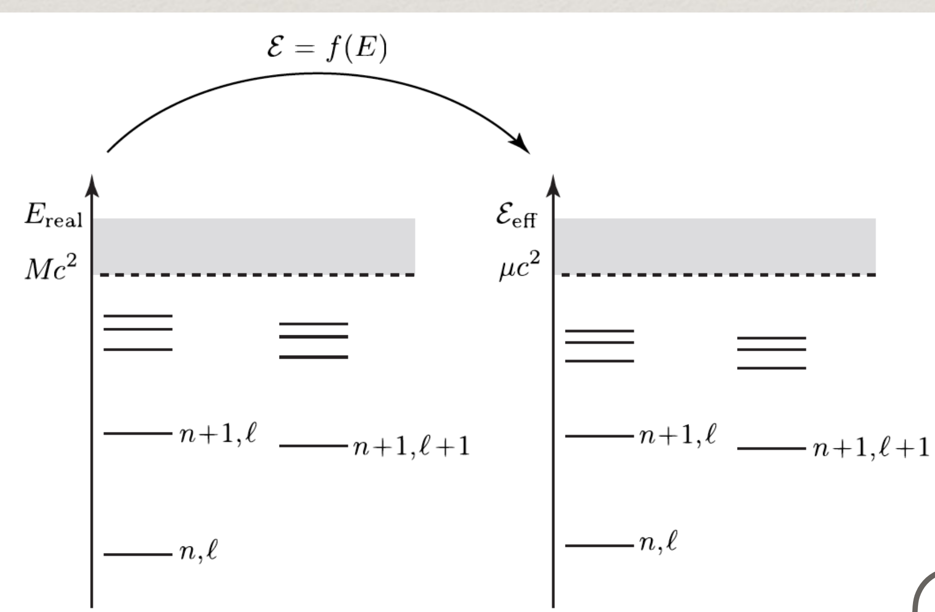

[Damour 2012]

example of tuning parameter

$$A(r) = \boxed{1-\frac{2M}{r}} + 2\eta\left(\frac{M}{r}\right)^3 + \eta\left(\frac{94}{3}-\frac{41}{32}\pi^2\right)\left(\frac{M}{r}\right)^4 \boxed{+\,a_5\left(\frac{M}{r}\right)^4}$$

$$D(r) = 1-6\eta\left(\frac{M}{r}\right)^2 + 2\eta(3\eta-26)\left(\frac{M}{r}\right)^3 + \ldots$$

$$Q = 2\eta(4-3\eta)\left(\frac{M}{r}\right)^2\frac{p_r^4}{\mu^2}$$

$$\boxed{\eta = \frac{m_1 m_2}{M^2}}$$

deformation parameter

EOB: dissipation due to GWs

Equations of motion

$$\frac{d\phi}{dt} = \Omega = \frac{\partial H}{\partial p_\phi}, \quad \frac{dr}{dt} = \frac{\partial H}{\partial p_r},$$

$$\frac{dp_\phi}{dt} = \boxed{F_\phi,} \quad \frac{dp_r}{dt} = -\frac{\partial H}{\partial r}$$

Radiation reaction force
(quasi-circular motion)
[Buonanno, Damour 2000]

$$\left(\frac{dH}{dt}\right) \approx \Omega F_\phi,$$

Dissipation of energy from the system =
flux of energy carried by GWs

$$\boxed{F_\phi = -\frac{1}{\Omega}\left(\frac{2}{16\pi}\sum_\ell \sum_{m=-\ell}^{\ell} (m\Omega)^2 |D_L h_{\ell m}|^2\right)}$$

[Damour, Iyer, Nagar 2009]

Luminosity distance

$$h_+ - i h_\times = \sum_\ell \sum_{m=-\ell}^{\ell} h_{\ell m} Y_{\ell m}^{(-2)}(\theta, \phi)$$

spin weighted (-2) spherical harmonics

EOB: inspiral-merger waveform

We use waveform decomposed in spin(-2) weighted spherical harmonics

$$h_{\ell m} = \boxed{h^{N}_{\ell m}}\,\boxed{\hat{h}^{\mathrm{PN}}_{\ell m}}$$

[Damour, Iyer, Nagar 2009]

"Newtonian" part, where $x = (M\Omega)^{2/3}$

$$\boxed{h^{N}_{\ell m} = \frac{M\eta}{D_L} n^{(\epsilon)}_{lm} c_{\ell+\epsilon}(\eta) x^{(\ell+\epsilon)/2} Y^{\ell-\epsilon,-m}\left(\frac{\pi}{2}, \phi(t)\right)}$$

numerical coefficients (f-ns of $\ell,\ m,\ \eta$)

$$\boxed{\hat{h}^{PN}_{\ell m} = 1 + h_1 x + h_{1.5} x^{3/2} + \ldots = S_{\ell+m} T_{\ell m} (\rho_{\ell m})^{\ell} e^{i\delta}}$$

post-Newtonian resummed / factorized part

EOB: ring-down (RD) signal

- Identify RD attachment time: maximum of orb. freq. ~ light ring
- Generate the RD signal as superposition of damped eigen frequencies of final BH
- Define the amplitude of each QNM by demanding continuity of matching to inspiral-merger part of the signal

$$\left(\frac{D_L}{M}\right) h^{\mathrm{RD}}_{\ell m}(t > t_{\mathrm{match}}) = \sum_{m',n} A_{\ell,m',n} e^{-(i\omega_{\ell m' n} + 1/\tau_{\ell m' n})(t - t_{\mathrm{match}})}$$

EOB dynamics

inspiral-merger

ring-down

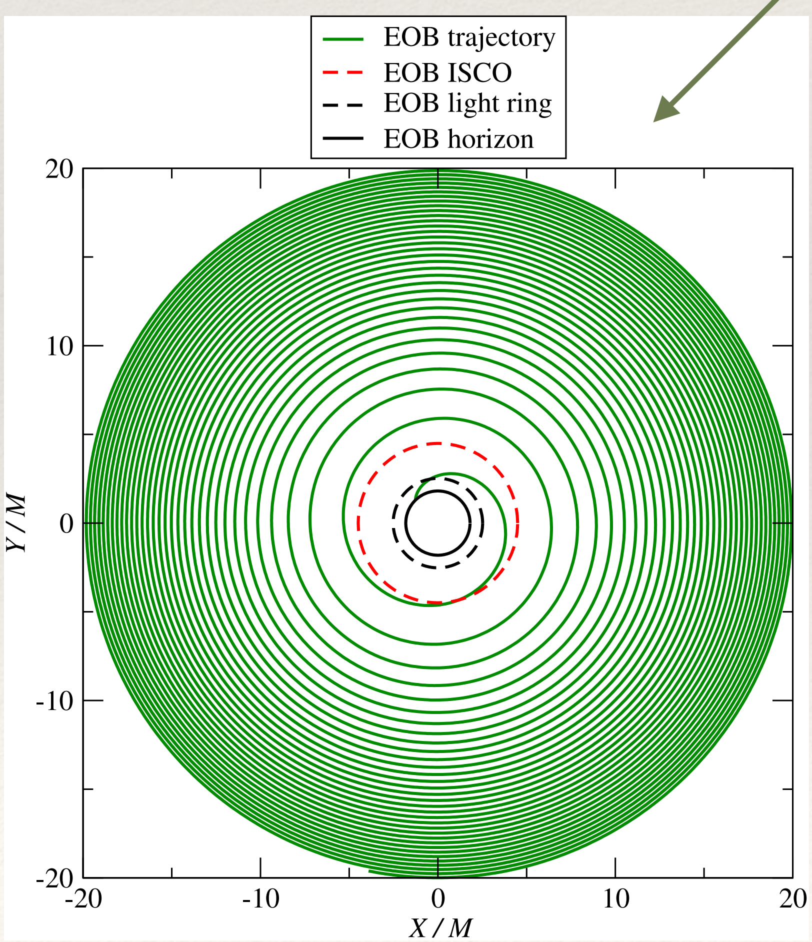

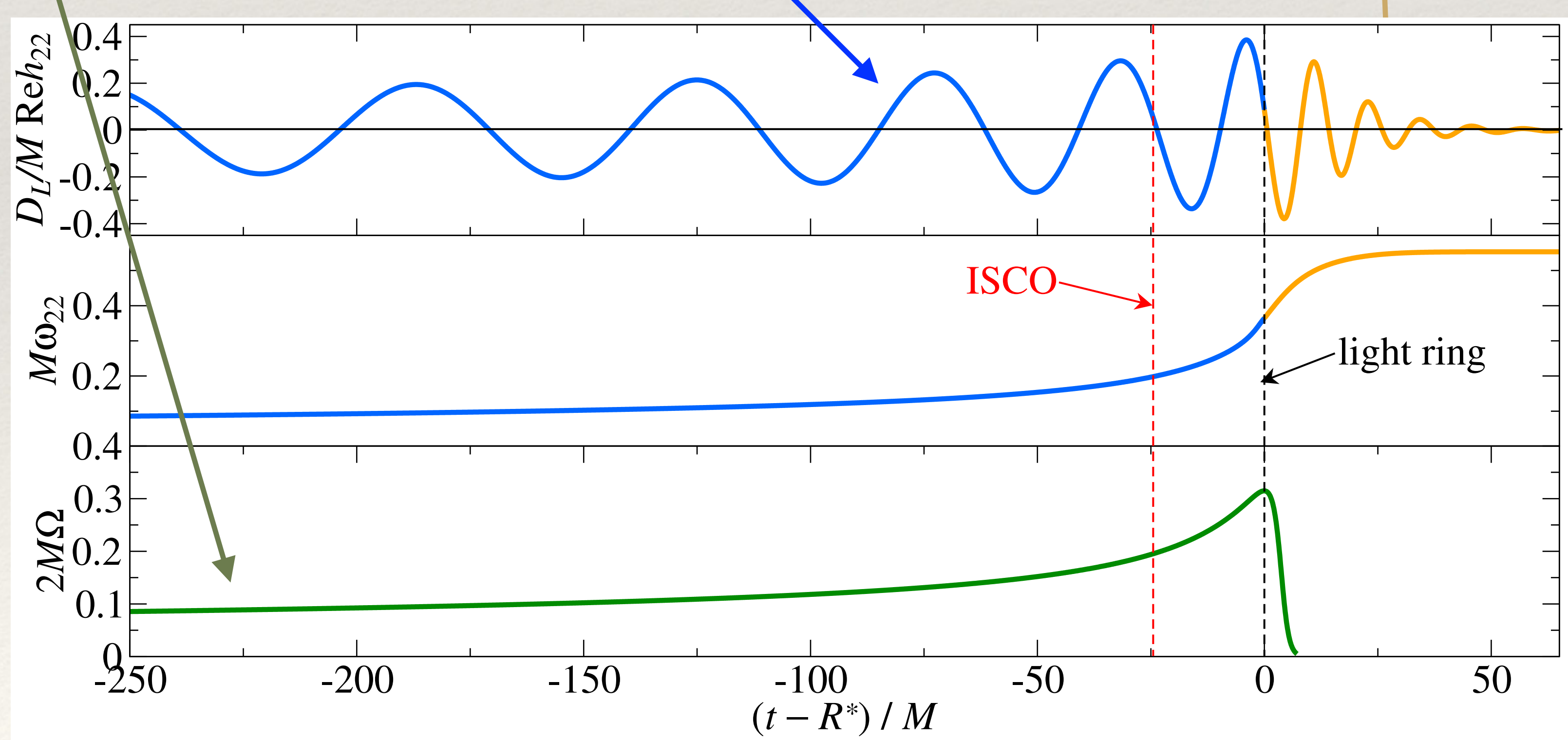

Plot: courtesy of A. Taracchini

EOBNR: calibration

- It was somewhat simplified description of EOB model (reality is a bit ugly)
- Adiabatic transition from circular-to-circular breaks: non-quasi-circular (NQC) corrections
- Missing high PN-terms important close to the merger
- The RD part is taken from the *linear* perturbation of a single BH: two merging BHs pass through a highly non-linear regime: requires extra (pseudo) QNMs or phenomenological RD part [Damour & Nagar 2014].

NR waveforms used to extend and to improve EOB-> EOBNR which also makes them partially phenomenological model

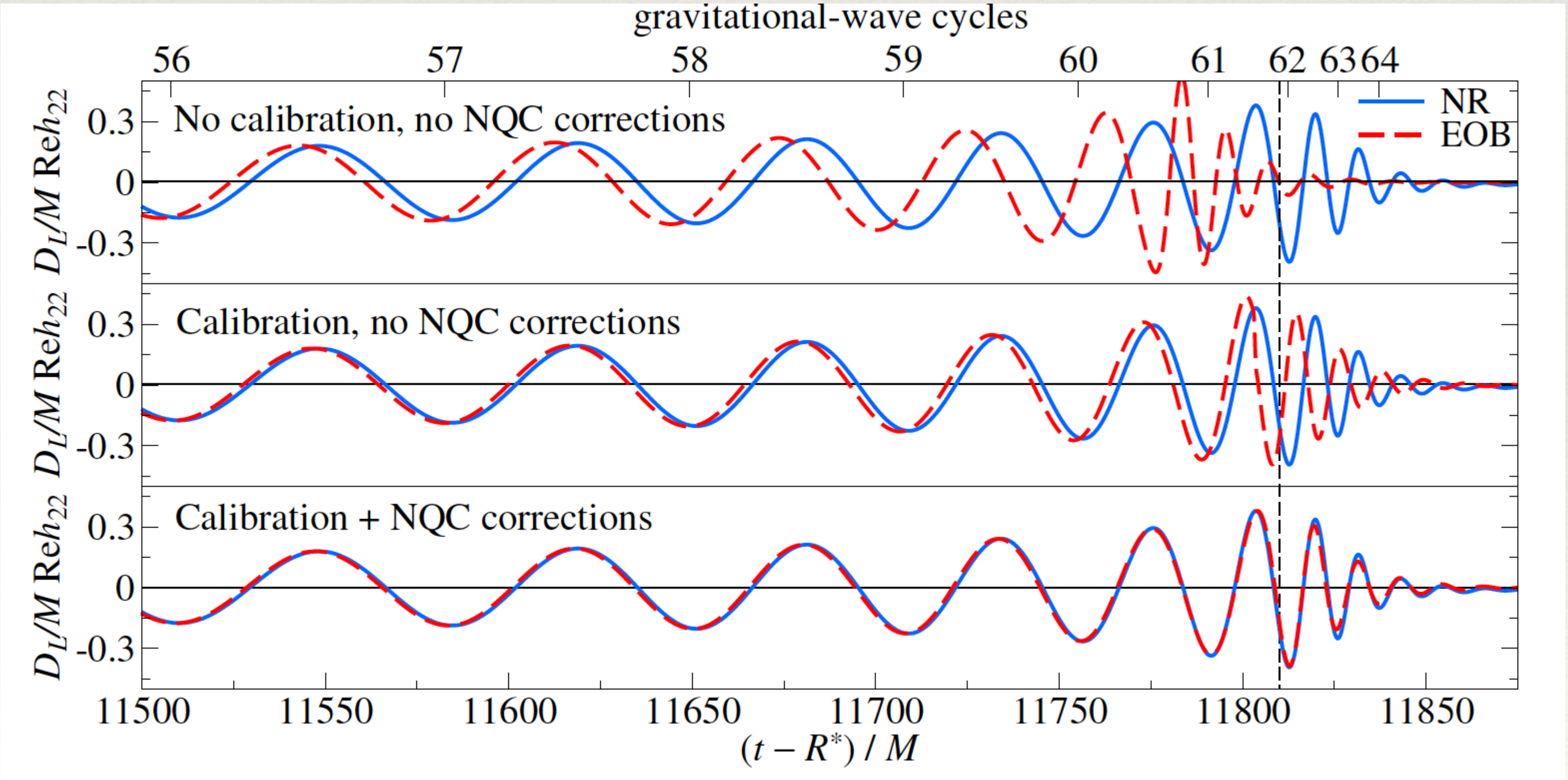

Plot: courtesy of A. Taracchini

Including spins

- Spinning case: spinning particle in deformed Kerr spacetime [Barausse & Buonanno 2010,2011; Nagar+2014, Balmelli & Damour 2015]

- Hamiltonians are more complex and we also need map the spins of two body problem to "effective Kerr".

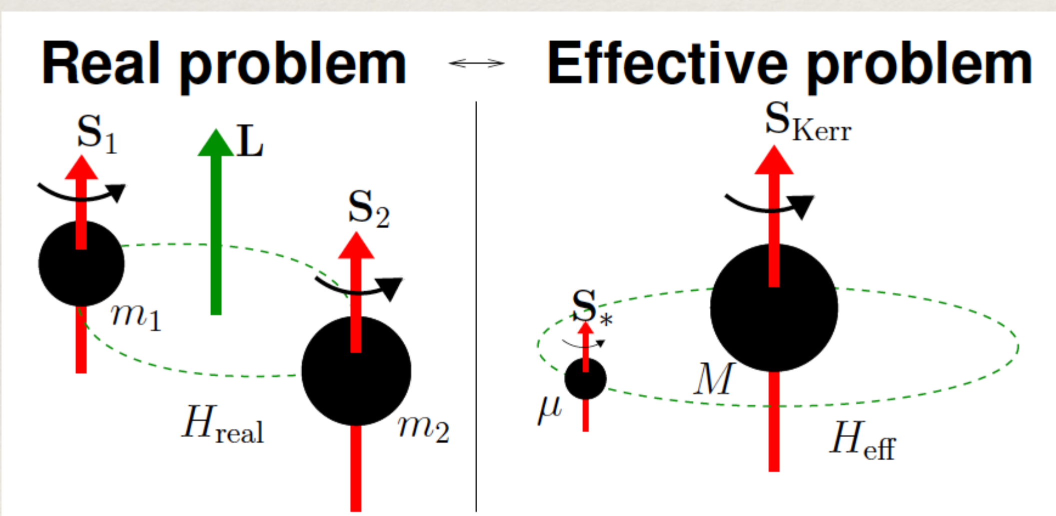

$$\mathbf{S}_{\rm Kerr} = \mathbf{S_1} + \mathbf{S_2}$$

$$\mathbf{S}_* = \mathbf{S}_*(\mathbf{S_1}, \mathbf{S_2})$$

SEOBNR with (anti)aligned spins: [Pan+2013, Taracchini+2014, Nagar+2014, 2015]
SEOBNR: precessing [Pan+2013, Babak+2016]

SEOBNR model for precessing binary BHs

- First we generate the waveform in the precessing frame [Buonanno+ 03, Schmidt+ 11, O'Shaughnessy+ 11, Boyle+ 11]
    - Spins are projected on the orbital angular momentum (but time dependent)
    - Waveform is produced as for (anti)aligned spin configuration, we have generated $\ell = 2,\ m = \pm 1, \pm 2$ modes
    - We use "off the shelf" model of non-precessing SEOBNR [Pan+ 13] **no recalibration is done**
- We rotate the waveforms to the frame aligned with the total momentum of the final BH and attach the RD

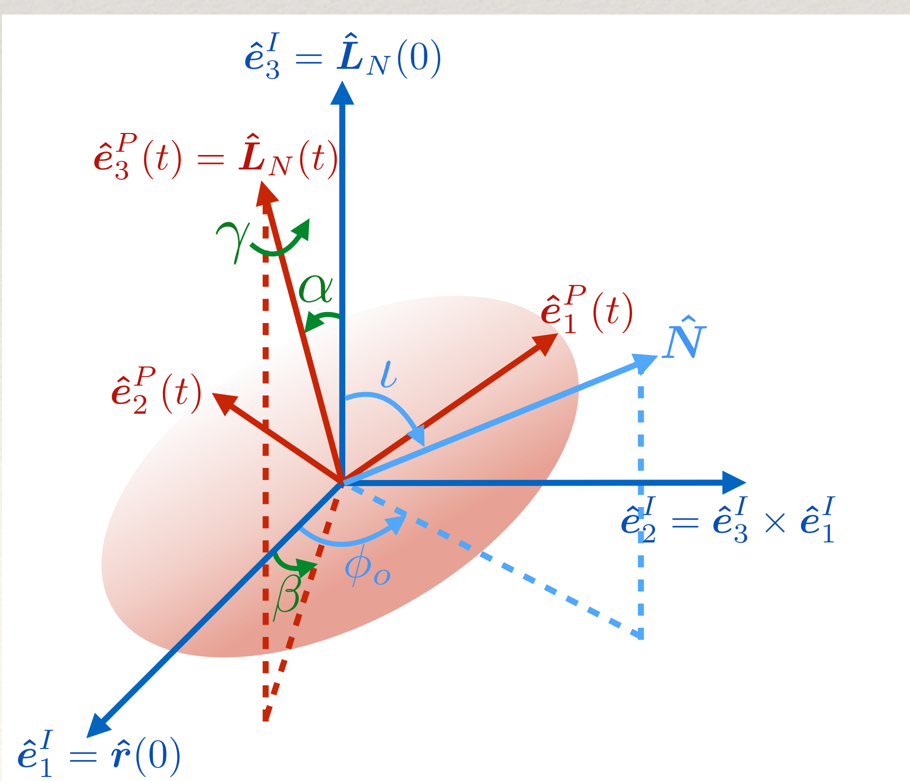

- Finally we rotate waveform to the inertial frame associated with an observer

Comparison precessing SEOBNR and NR waveforms

$$m_1/m_2 = 5, \quad |\mathbf{S_1}/m_1^2| = 0.5, \quad \theta_1 = 90^\circ, \quad \mathbf{S_2} = 0$$

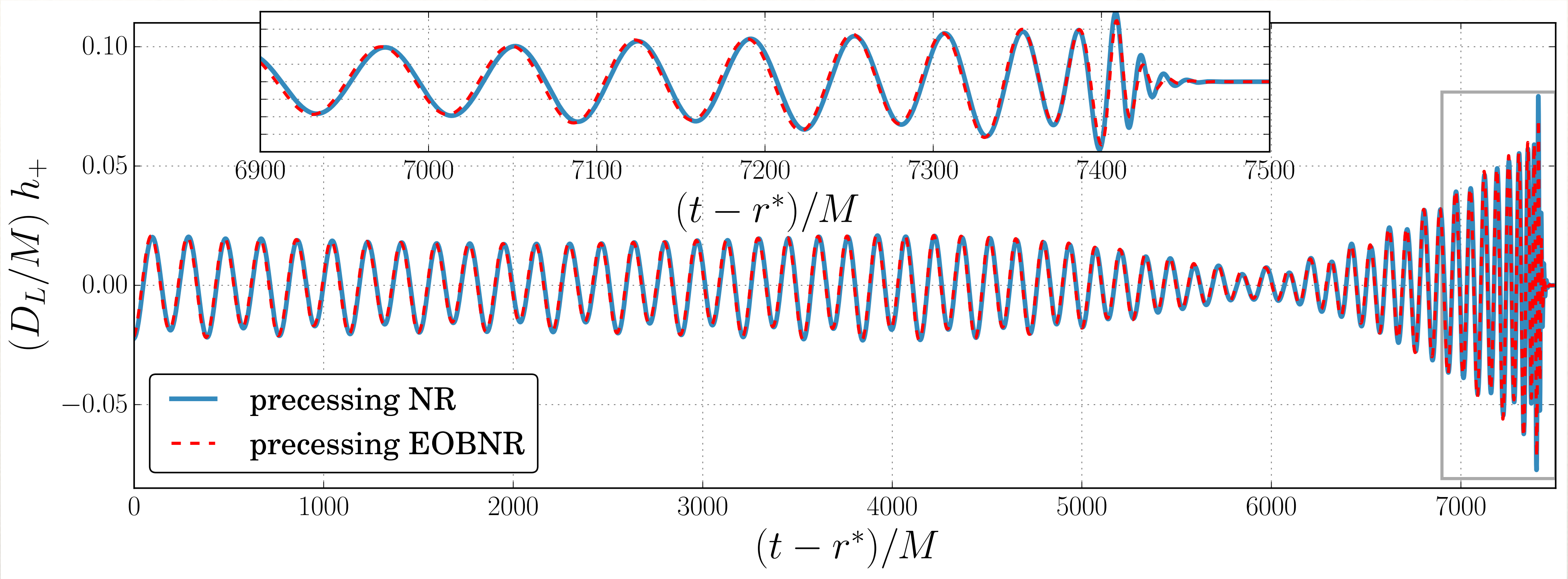

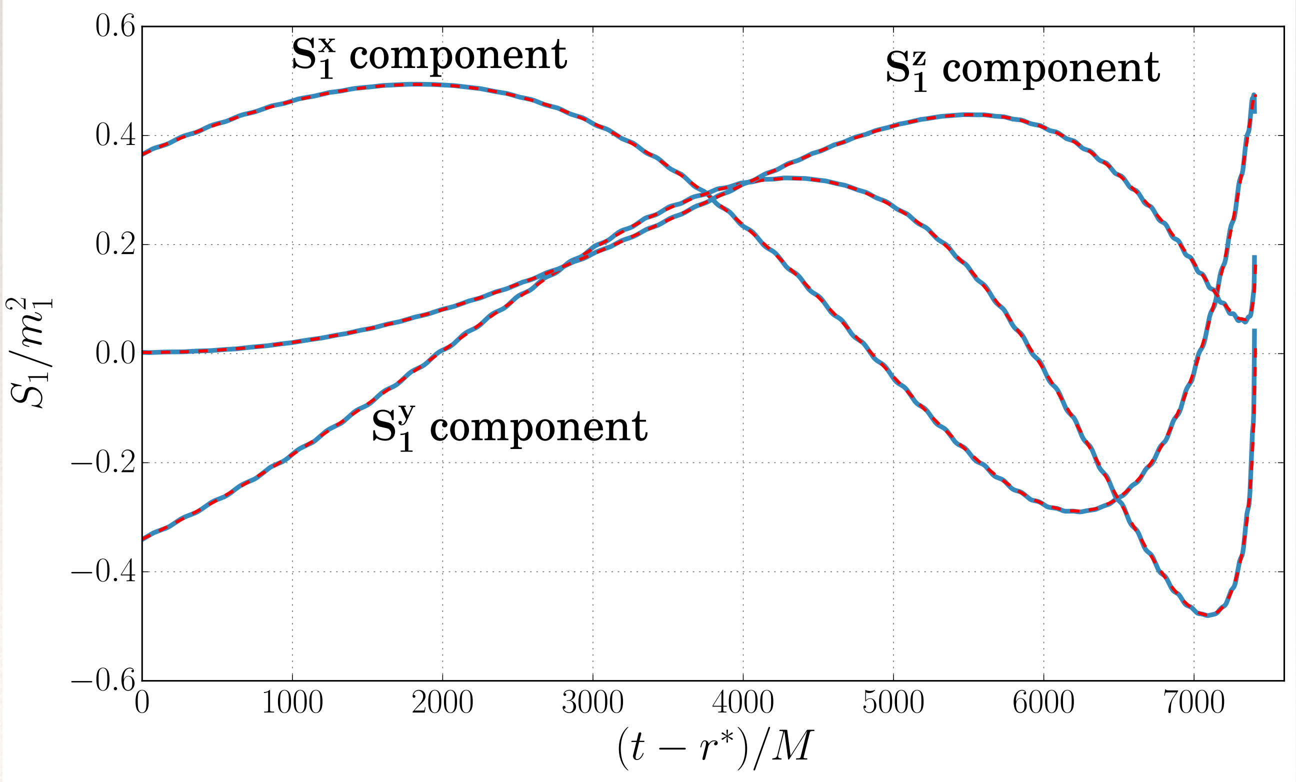

~30 GW cycles

Evolution of spin components: blue is NR

Stanislav (Stas) Babak.
AstroParticule et Cosmologie, CNRS (Paris)

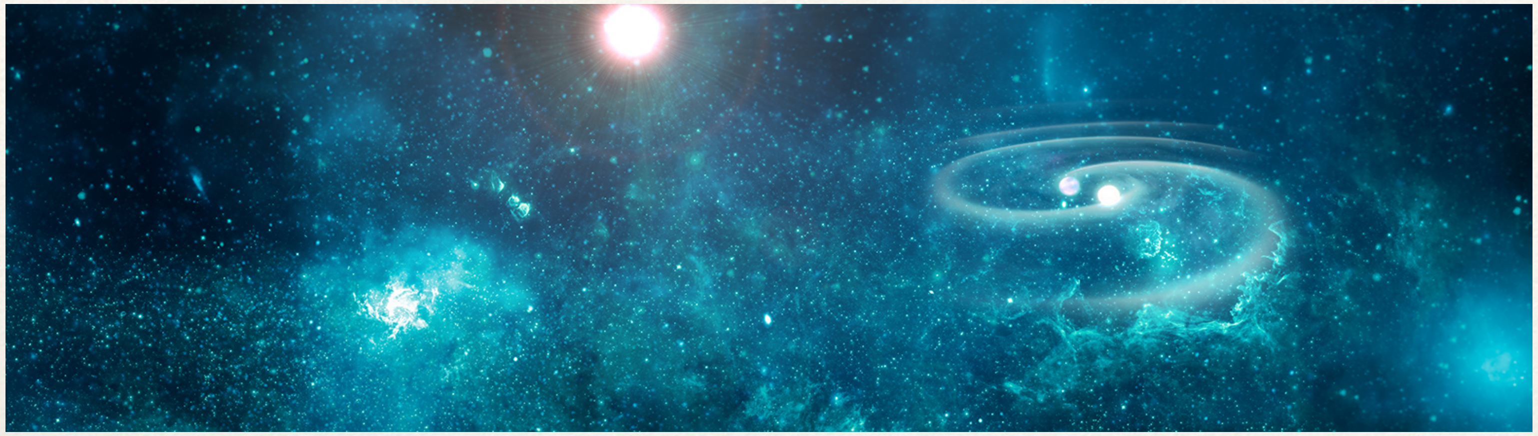

Pulsar Timing Array

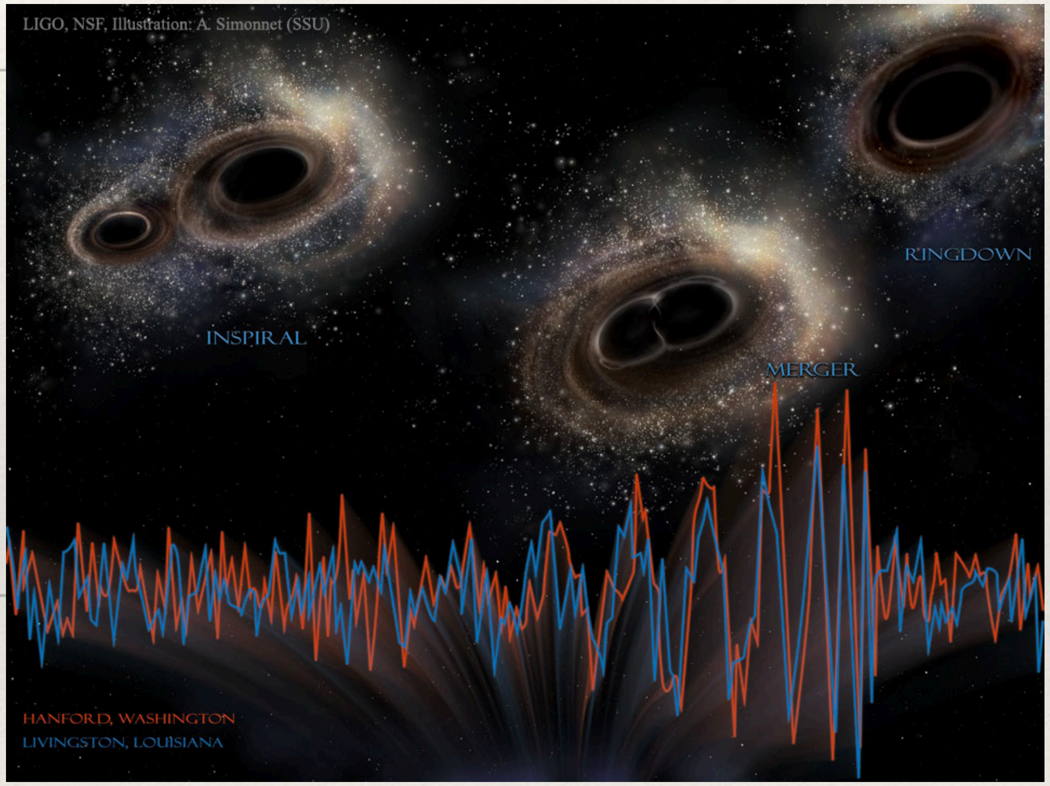

ISAPP, 7-17 June 2021

GW landscape

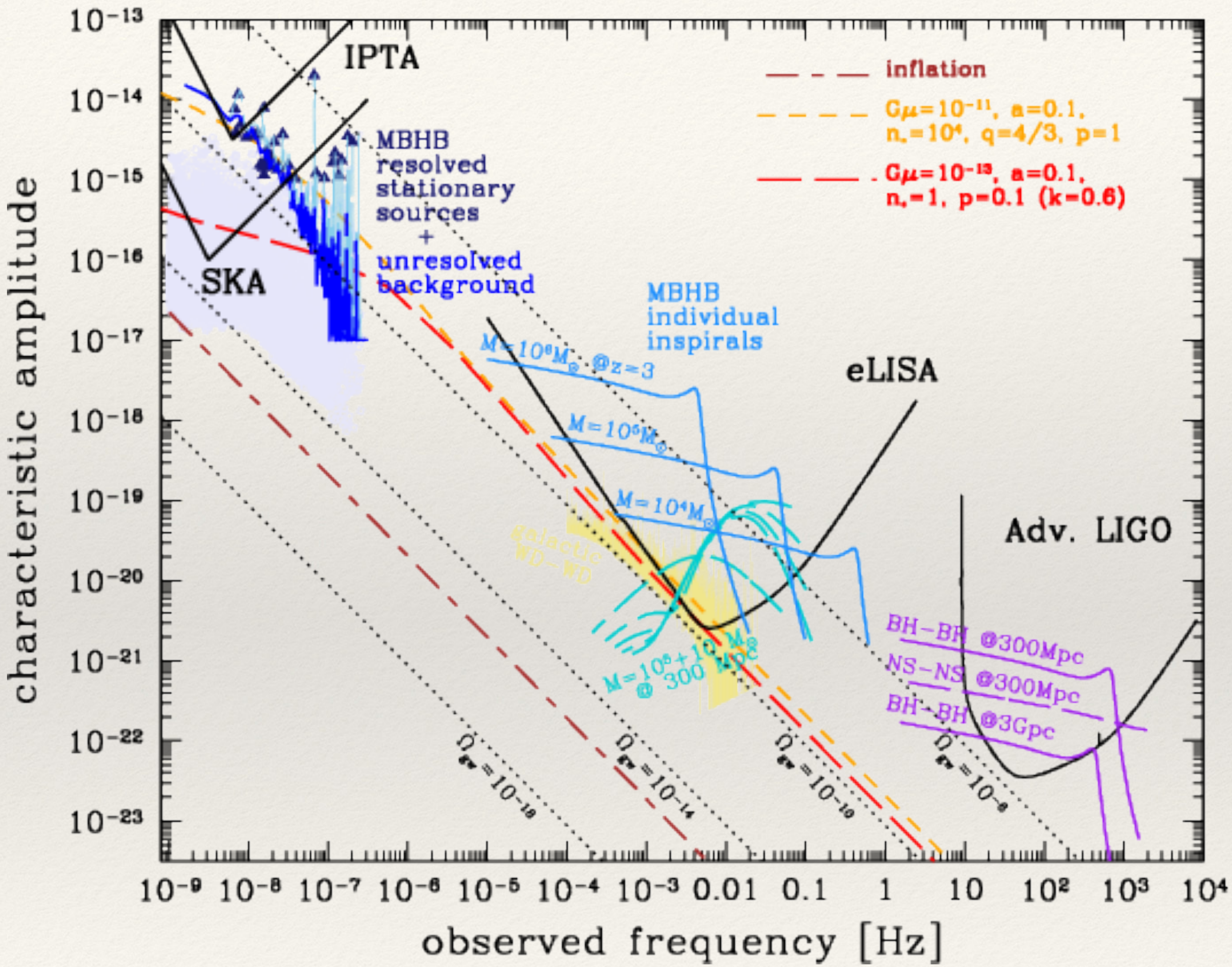

Pulsar Timing Array

The main idea behind pulsar timing array (PTA) is to useultra-stable millisecond pulsars as beacons (clocks sending signals) for detecting GW inthe nano-Hz range (10^{-9} - 10^{-7} Hz).

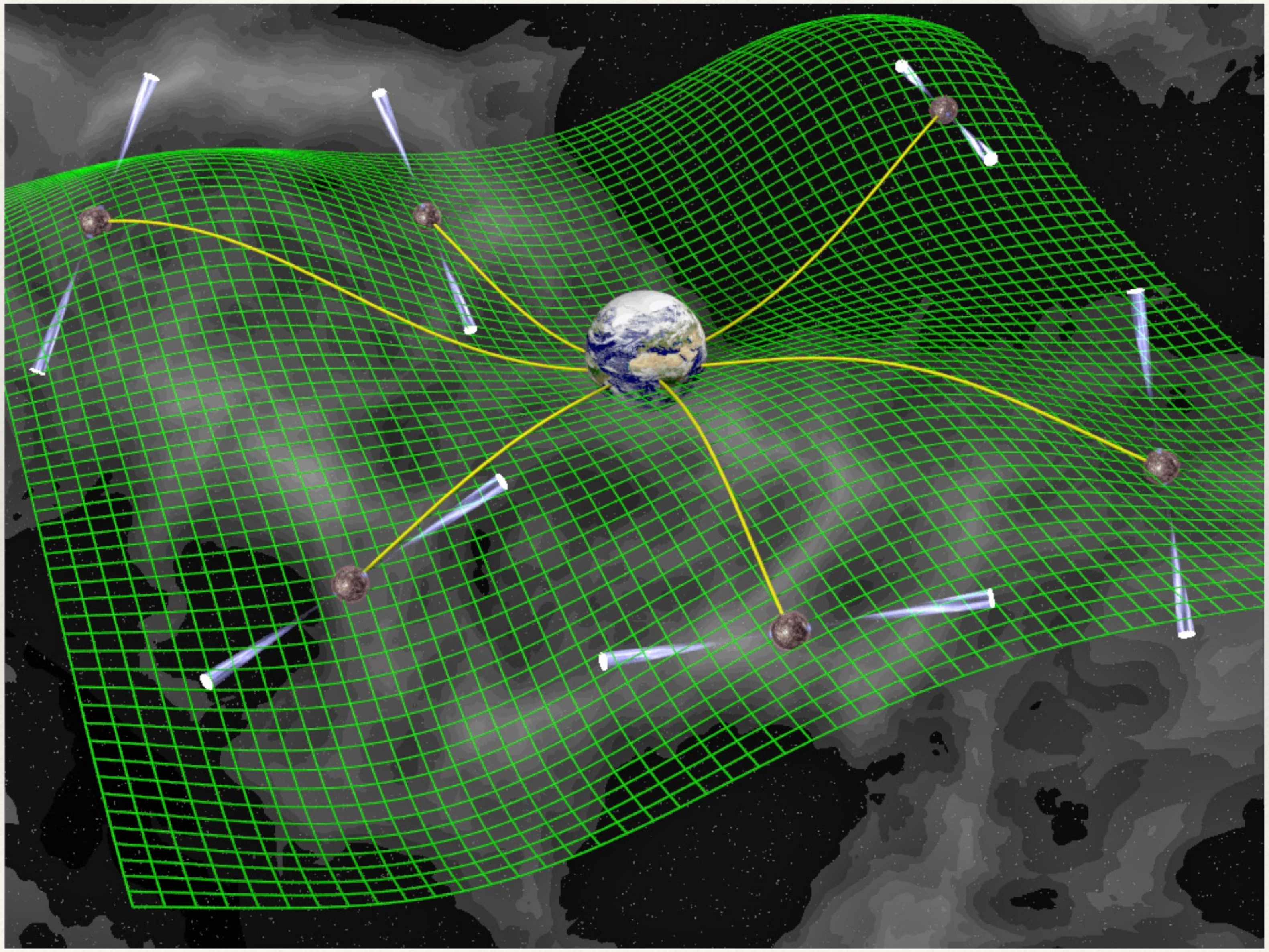

[Credits: D. Champion]

EPTA

Millisecond pulsars

- Pulsars - neutron stars (end product of evolution of stars with the mass > 7 solar) with rapid rotation and strong magnetic field
- Emit beamed e/m radiation from the magnetic poles. Powered by rotation: spinning down.
- Beamed radio emission swaps across the line of sight — seen as pulses in observations (similar to the lighthouse)

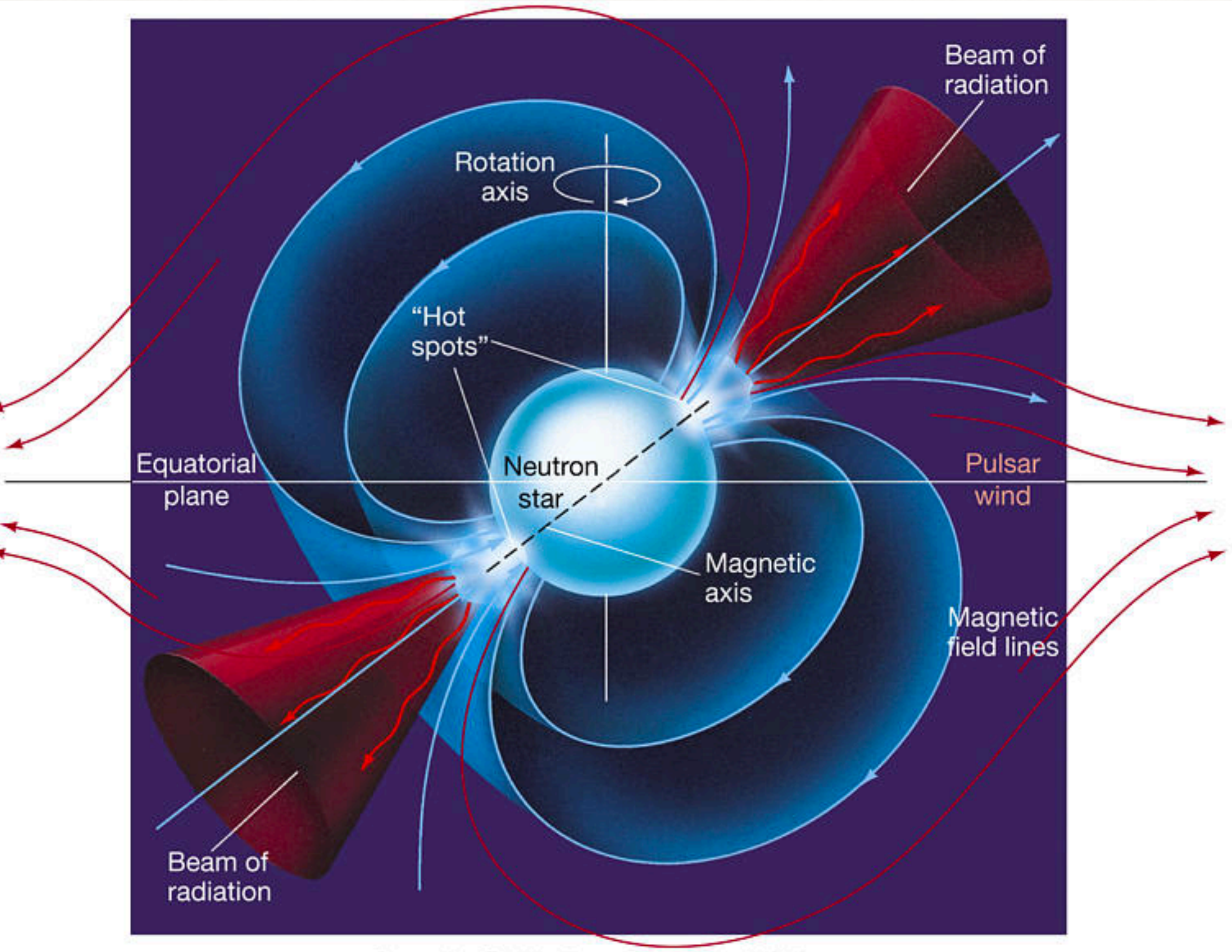

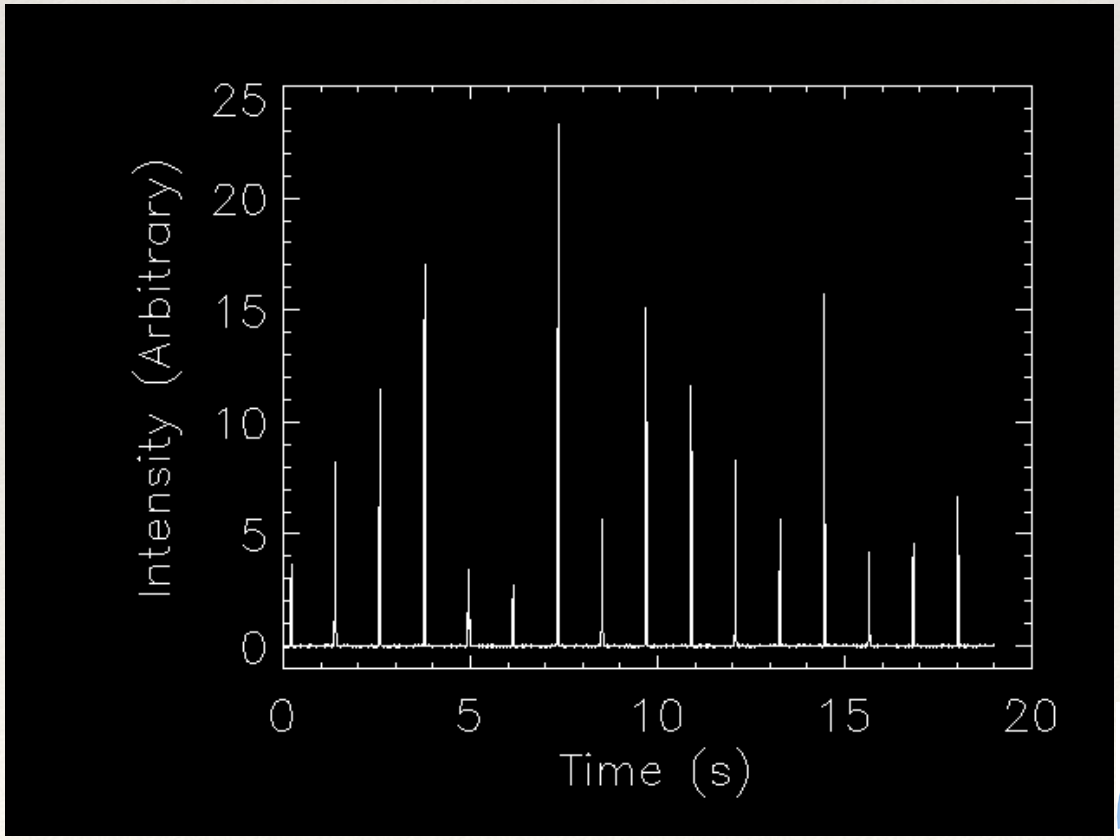

Millisecond pulsars

- Millisecond pulsars: period of rotation ~ millisec
- Often in binaries
- Very old NSs, very stable rotation
- The most accurate clock on the long time scale (decades)

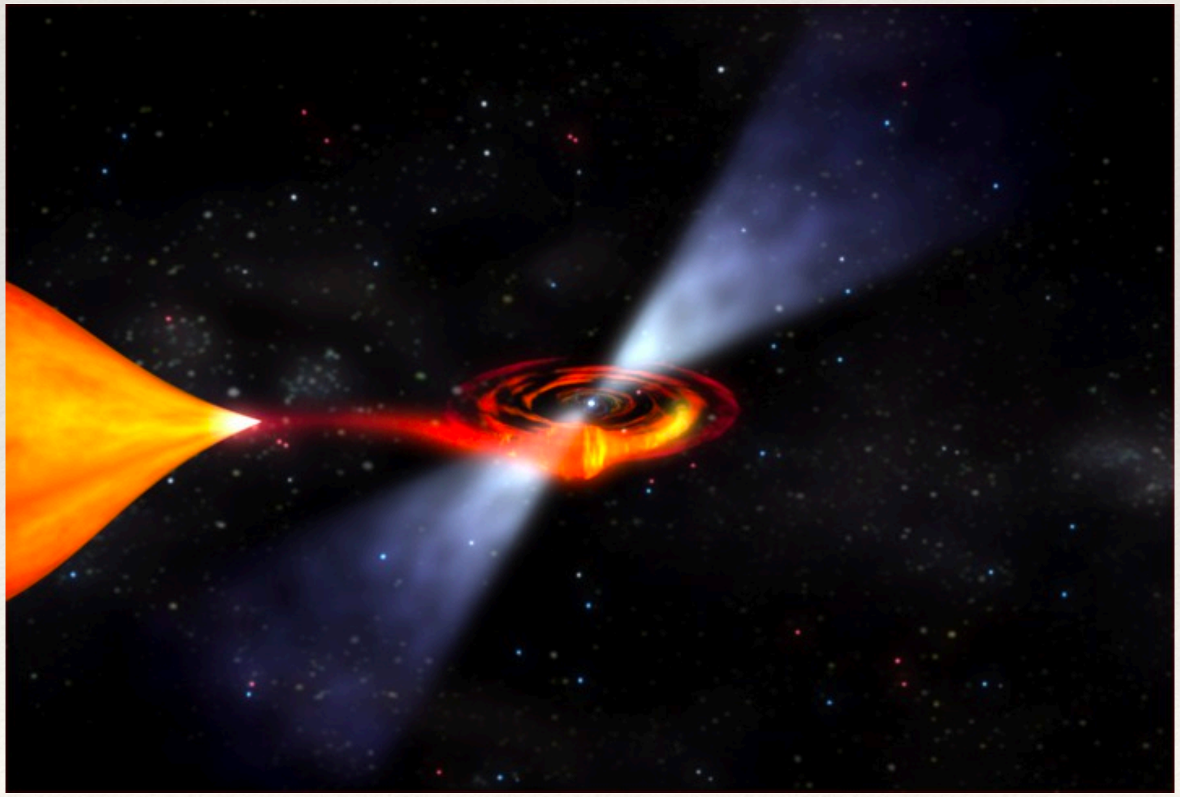

[Credits: NASA]

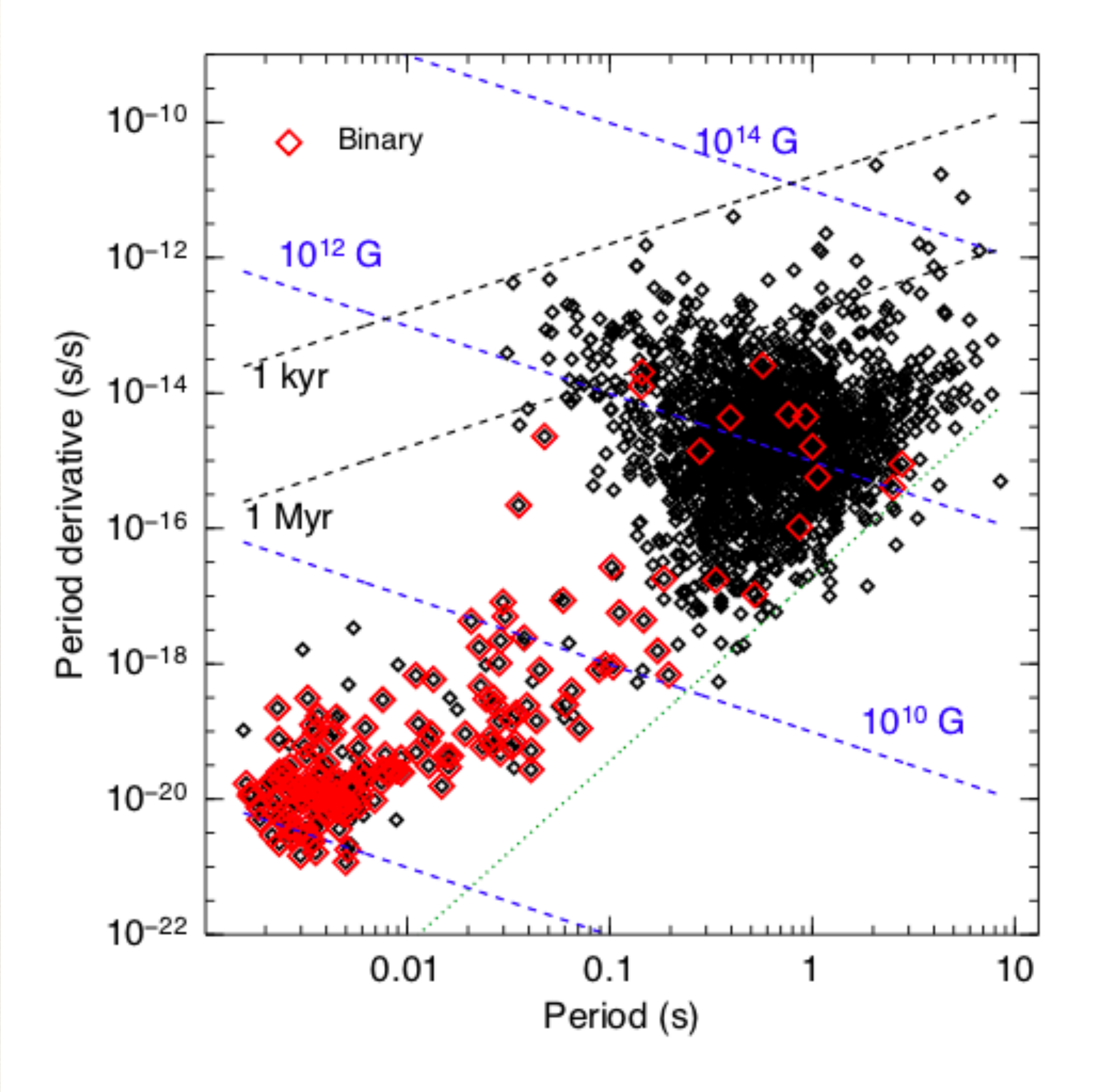

[Wikimedia]

Pulsar timing

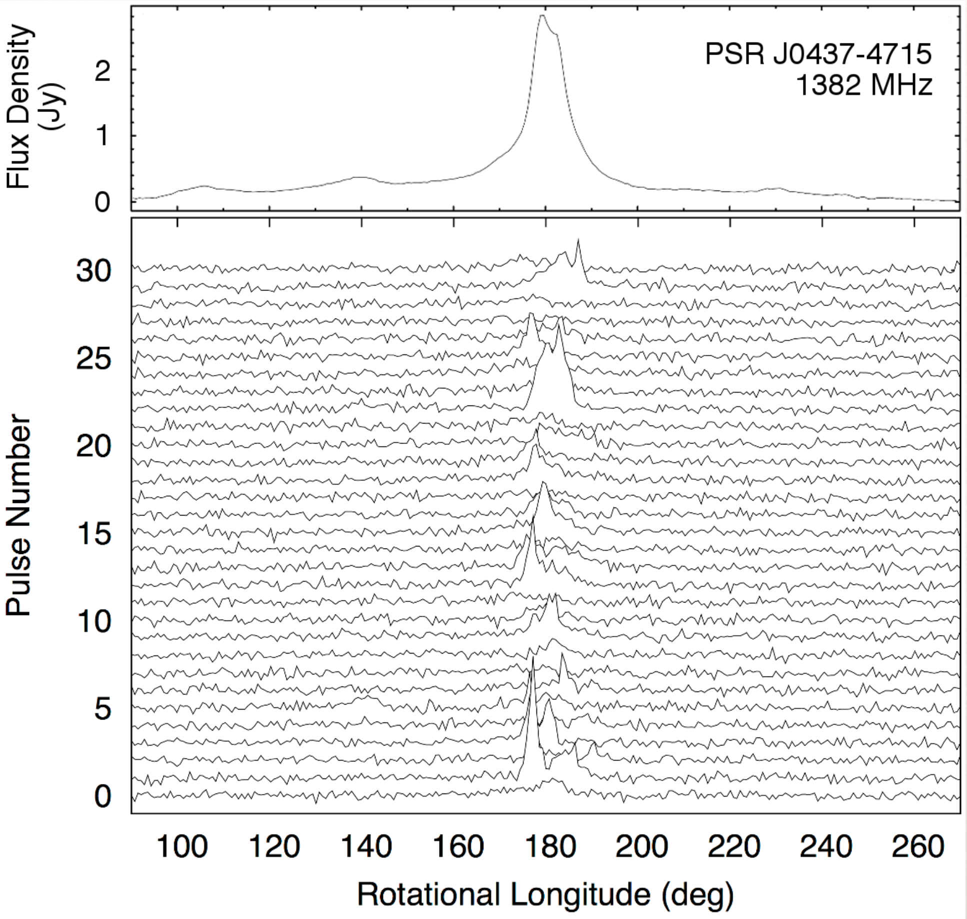

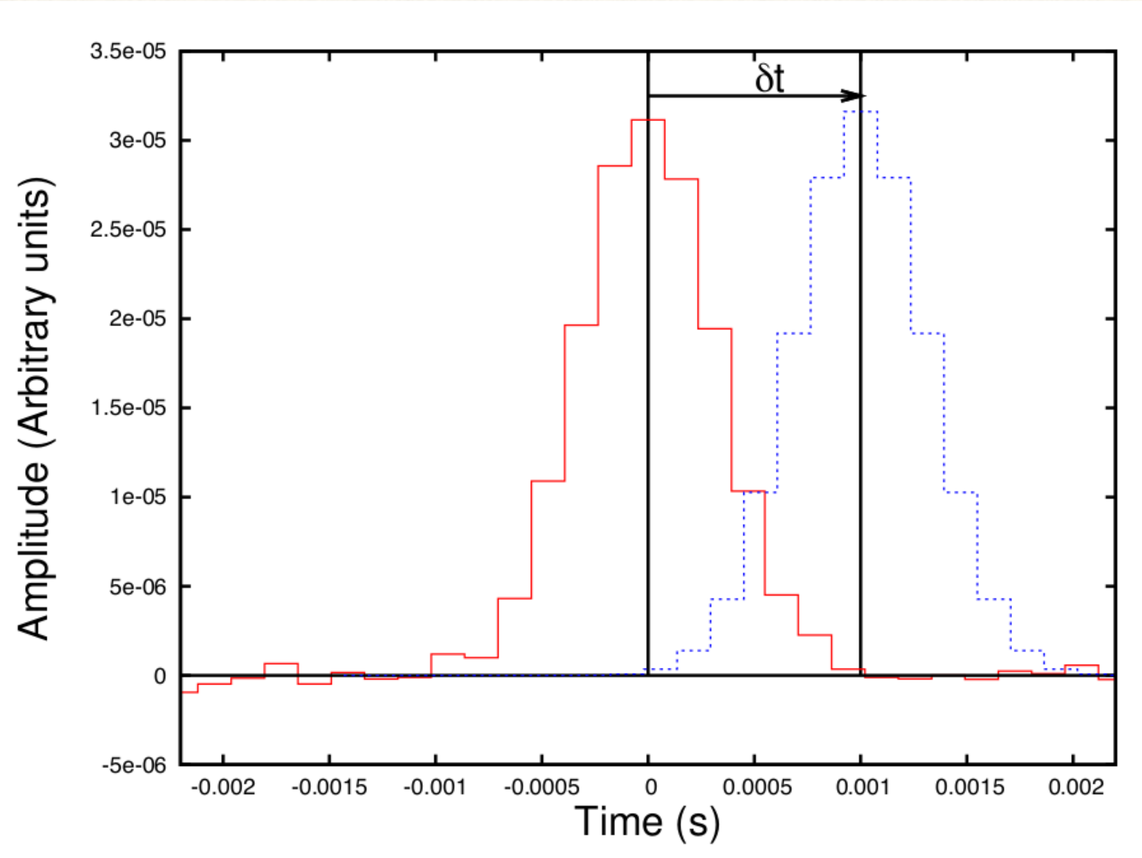

[Figs: credits
S. Burke-Spolar & L. Lentati]

- Each observed radio pulse profile has a lot micro-structure. If we average over ~hour the (average) profile is very stable
- We can use the average pulse profile to estimate the time-of-arrival (TOA) of the pulses.
- The idea is to measure the TOA, and compare to the expected TOA. We know the spin of the pulsars, so we can predict the TOA. The difference between measure and expected TOA: ***residuals***

Timing pulsars

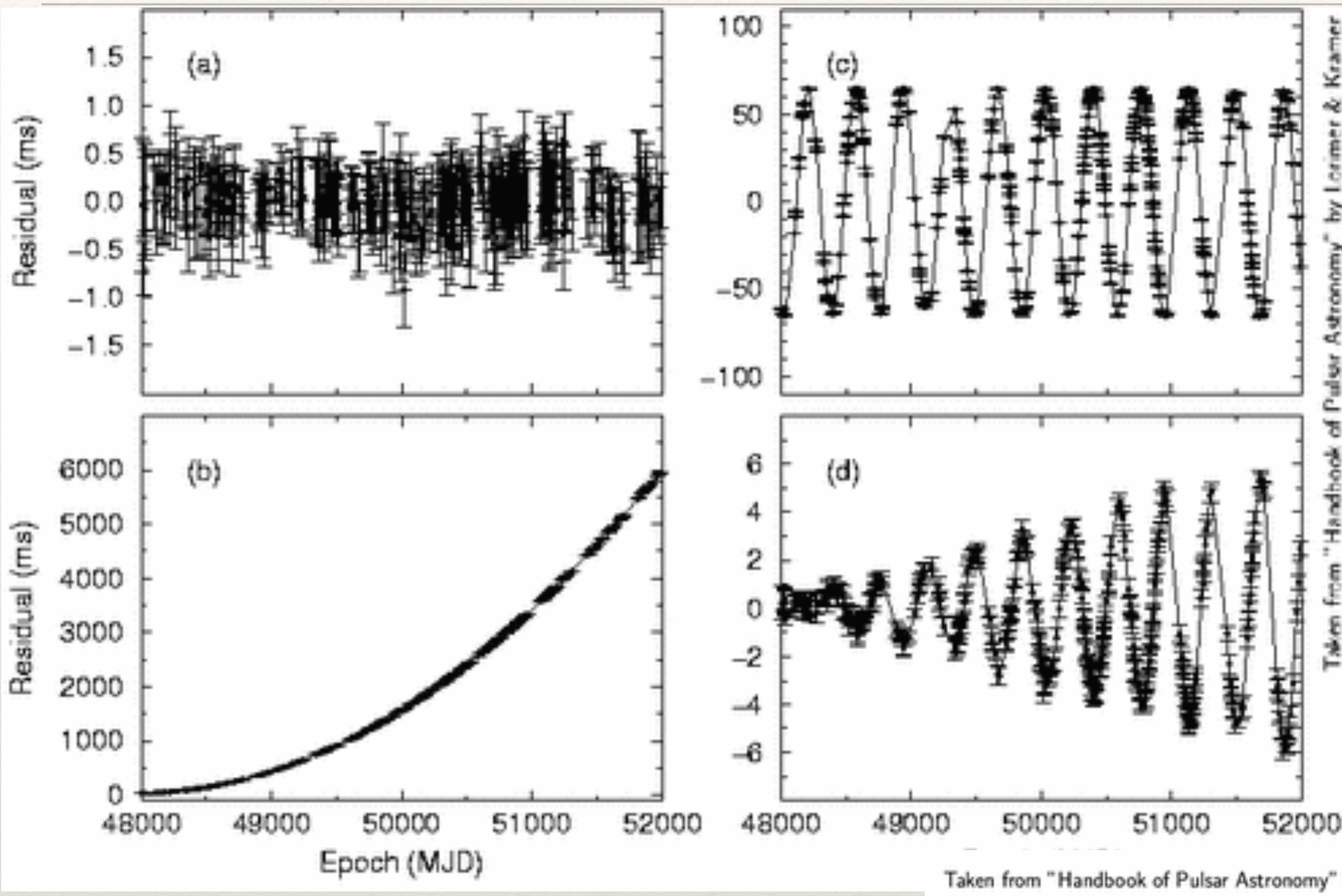

- We need to build a timing model to make accurate prediction for TOAs - take into account various physical effects
- Dispersion of e/m wave and its time dependence
- Rate of change of rotation (b)
- Sky position of the pulsar (c)
- Proper motion of a pulsar (d)

- Timing model could be quite complex if pulsar is in the binary

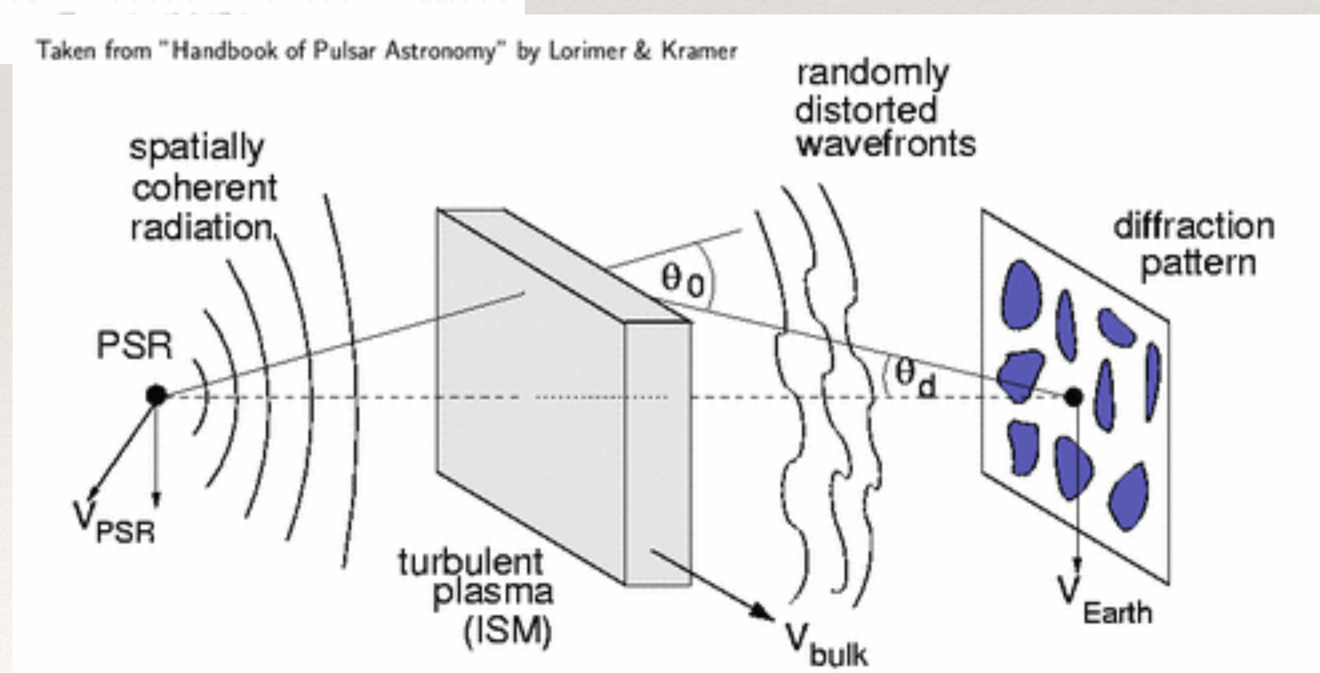

Residuals

- Building the timing model: depends on many parameters

$$t_{toa} = t_{toa}(P, \dot{P}, \ddot{P}, \Delta_{clock}, \Delta_{DM}(L), \Delta_{\odot-\oplus}, \Delta_E, \Delta_S)$$

$P, \dot{P}, \ddot{P}$ period of pulsar' rotation and its derivatives: spin-down

Δ_{clock} difference in the local clock and terrestrial standrad

$\Delta_{DM}(L)$ delays caused by propagation in the interstellar medium

$\Delta_{\odot-\oplus}$ Transformation from the local frame to the solar system barycentre

Δ_E Accounts for relative motion (Doppler) + gravitational redshift caused by the Sun, plantes or binary companion.

Δ_S Extra time required to trave in the curved spacetime containng Sun/companion (if in binary)

$$dt = t^p_{toa} - t^o_{toa} = dt_{errors} + \delta\tau_{GW} + noise$$

Errors in fitting the model

due to GWs

Timing Residuals

credits: Mikel Falxa

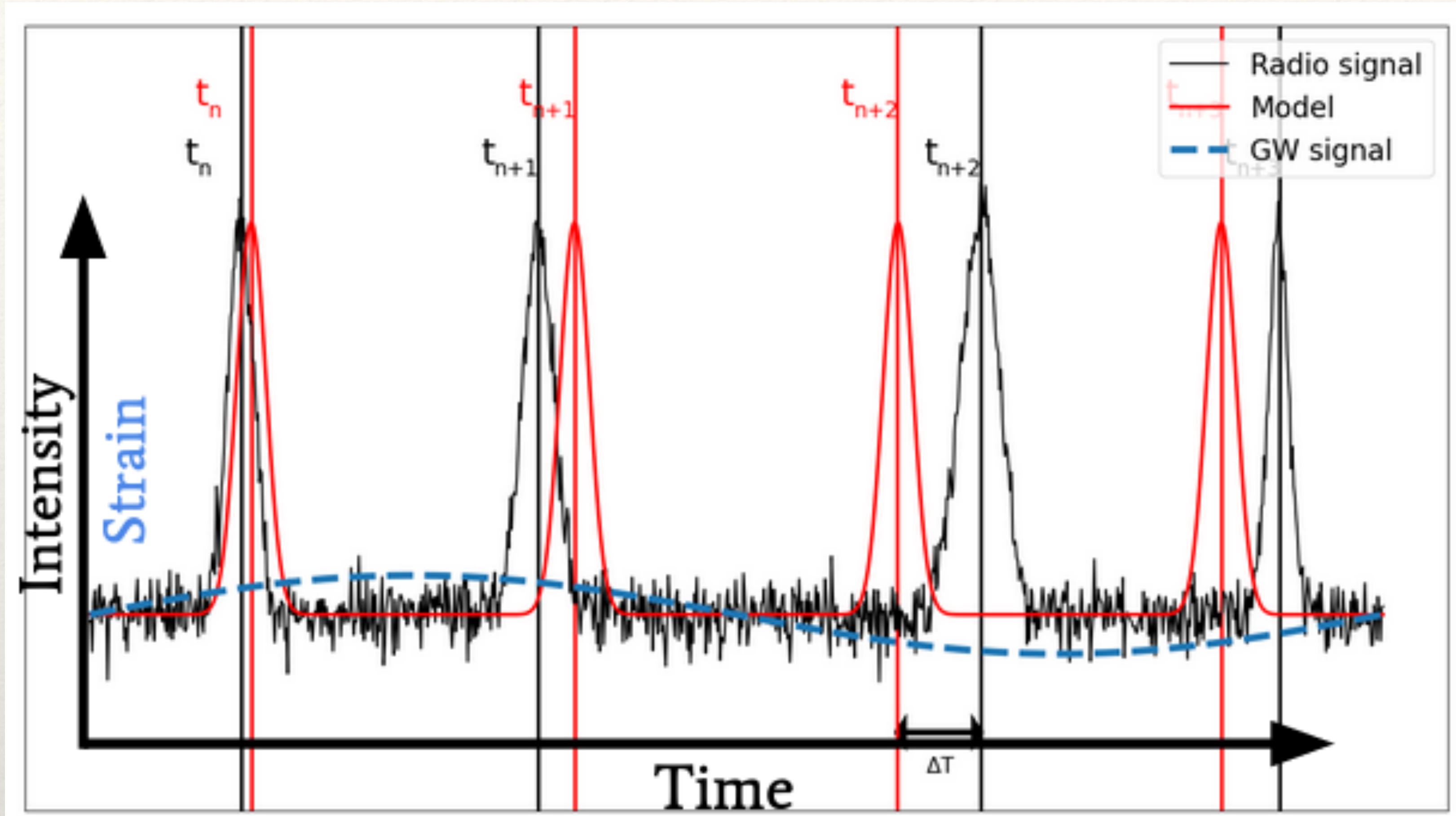

$$dt = t^{p}_{toa} - t^{o}_{toa} = dt_{errors} + \delta\tau_{GW} + noise$$

Errors in fitting the model

due to GWs

Response to GW signal

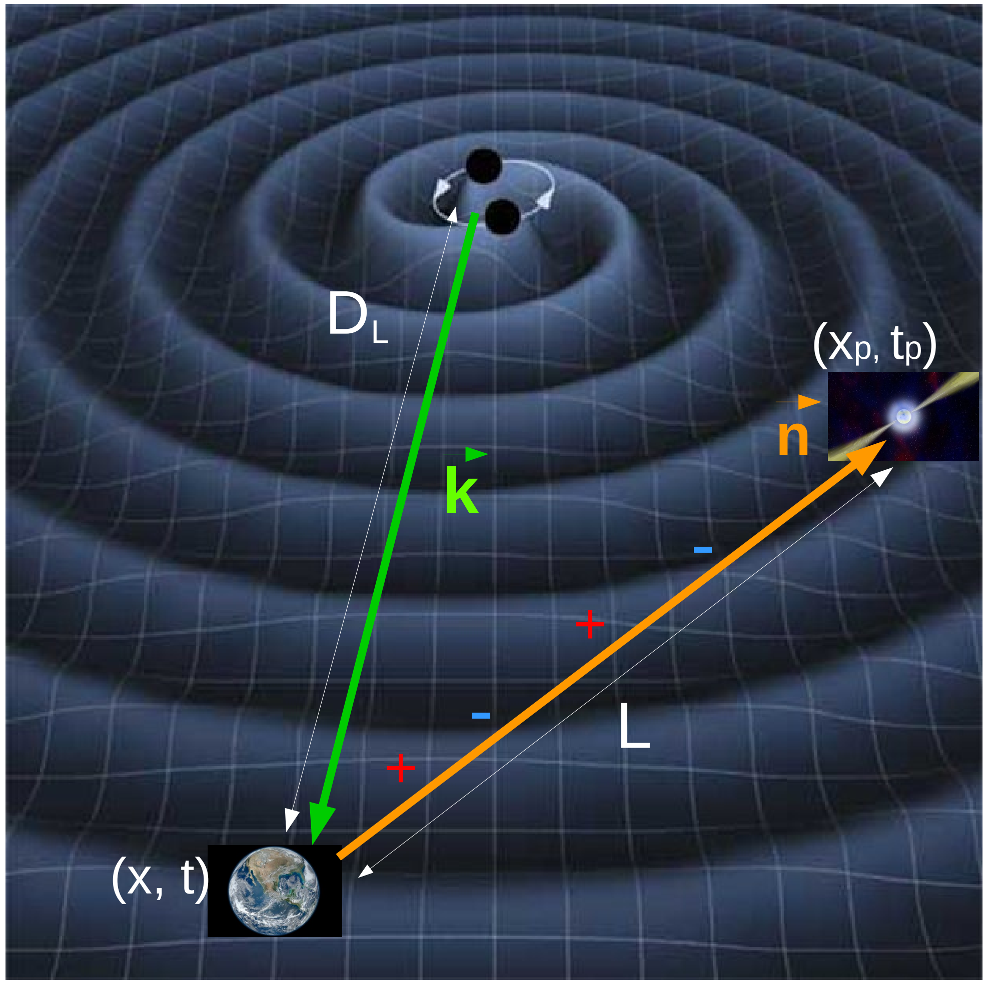

- PTA can be seen as a multi-arm detector where e/m signal travels only in onedirection (from a pulsar to the Earth). Pulsar plays role of an accurate clock, andwe measure change in phase (frequency) of arriving pulses (similar to thefrequency (phase) of the laser light)

- Important quantity which characterizes the response of any GW observatory is $\epsilon = (2\pi f_* L/c)$

size of GW detector

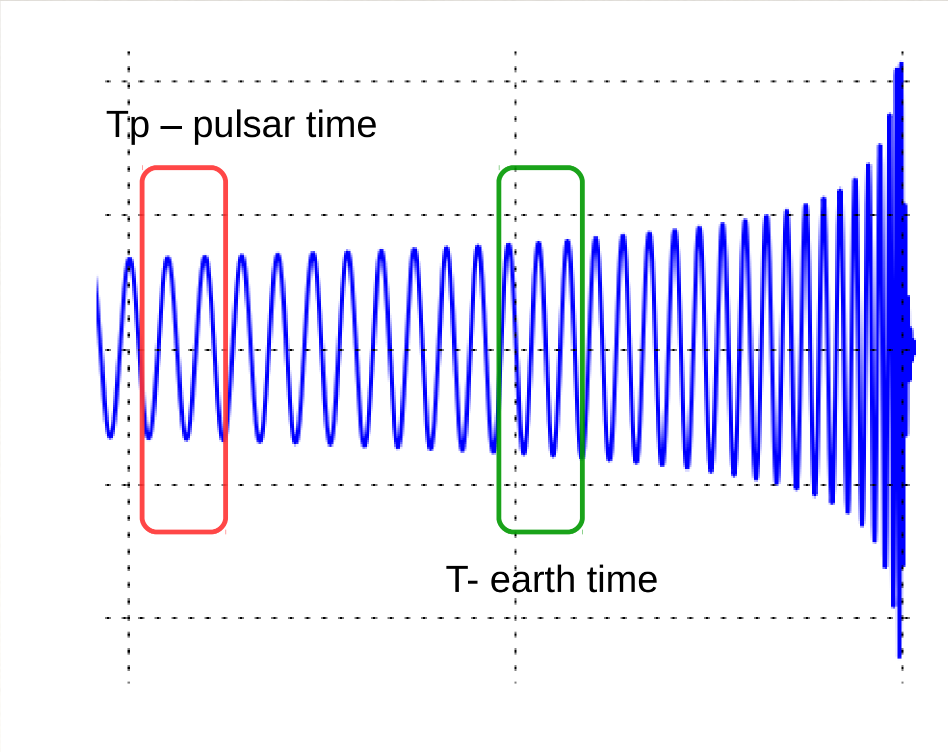

$\epsilon \ll 1 \rightarrow R \propto h_{ij} n^i n^j$ long wavelength approximation: LIGO/Virgo

$\epsilon = 1 \rightarrow$ LIGO: f* ~12 kHz, LISA: f*~ 0.05 Hz, PTA: f*~0.002 nHz

PTA: $\epsilon \gg 1$

Response to GW signal

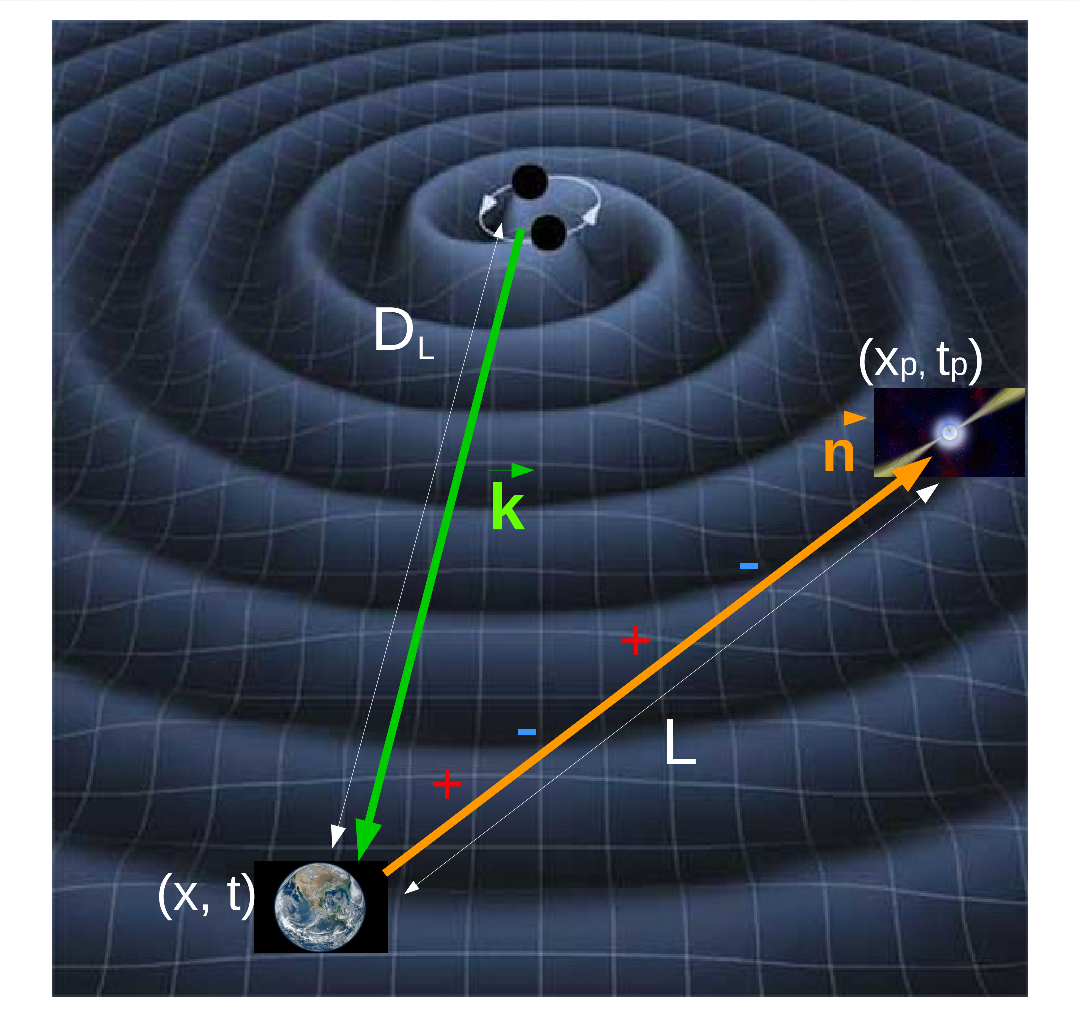

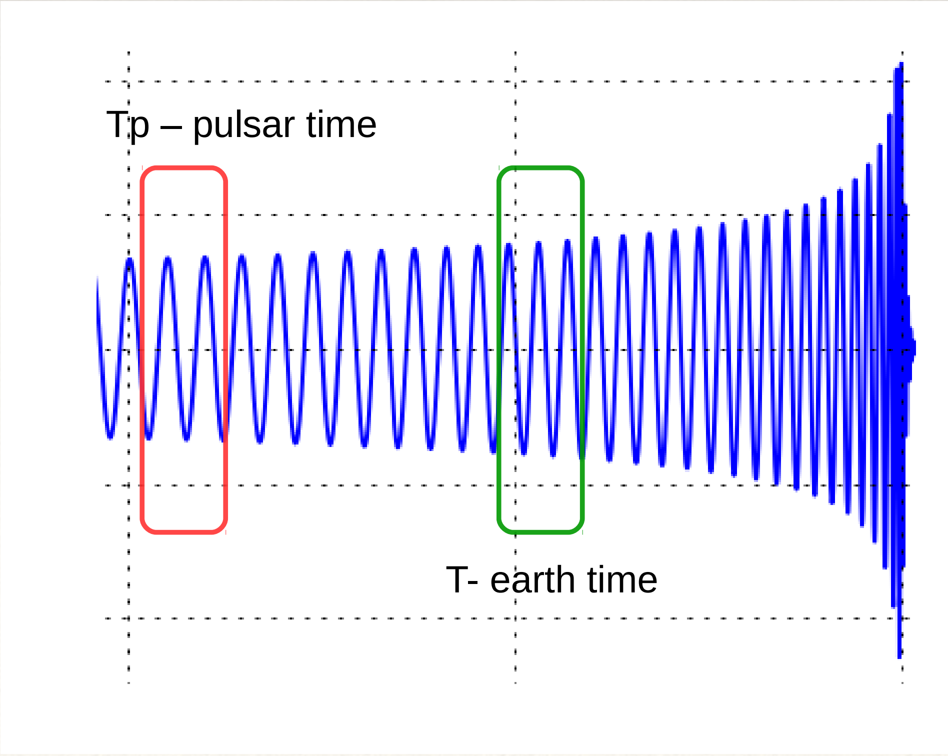

$$dt = t^p_{toa} - t^o_{toa} = dt_{errors} + \delta\tau_{GW} + noise$$

$$\delta\tau_{GW} = r(t) = \int_0^t \frac{\delta\nu}{\nu_0}(t')dt'; \quad \frac{\delta\nu}{\nu_0} = \frac{1}{2}\frac{\hat{n}^i\hat{n}^j\Delta h_{ij}}{1+\hat{n}.\hat{k}}$$

Familiar from LISA

$$\Delta h_{ij} = h_{ij}(t_p = t - L(1+\hat{n}.\hat{k})) - h_{ij}(t)$$

t_p — pulsar time, ~ time of emission of the radio pulse:

- depends on the relative position of a pulsar and GW source
- depends on the distance to the pulsar L
- L ~ few kpc ~10 000 years — "pulsar" term $h(t_p)$ contains info about the system 10^5 years in the past as compared to the "earth" term
- pulsar term depends on the pulsar.

Radiotelescops: EPTA

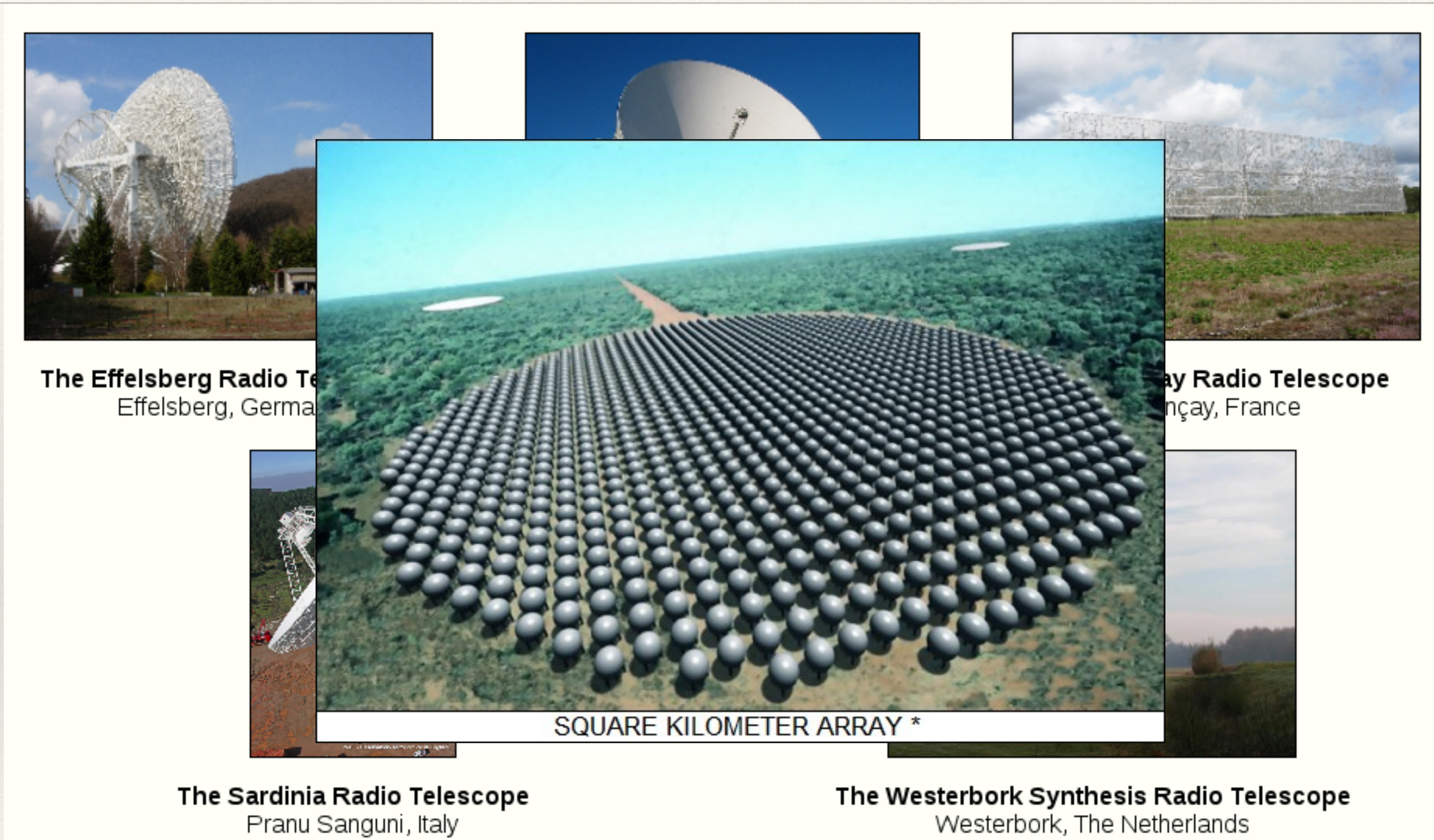

Super-massive black holes (SMBHs)

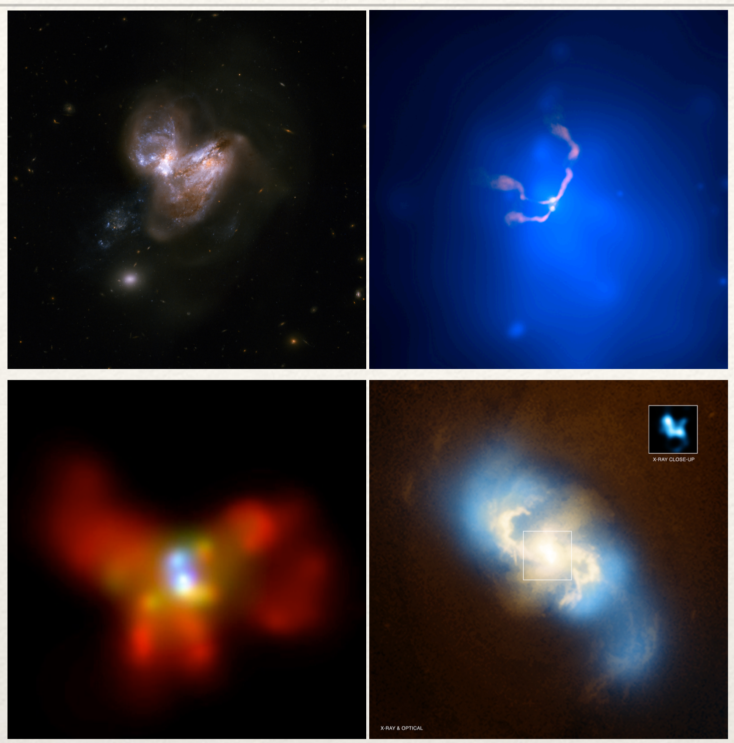

Massive black holes should reside in the nuclei of (we hope) every galaxy. (S)MBH are formed from relatively small seeds (remnants of popIII stars, direct collapse of giant protocloud) and acquire mass through accretion and major mergers (result of galactic encounter)

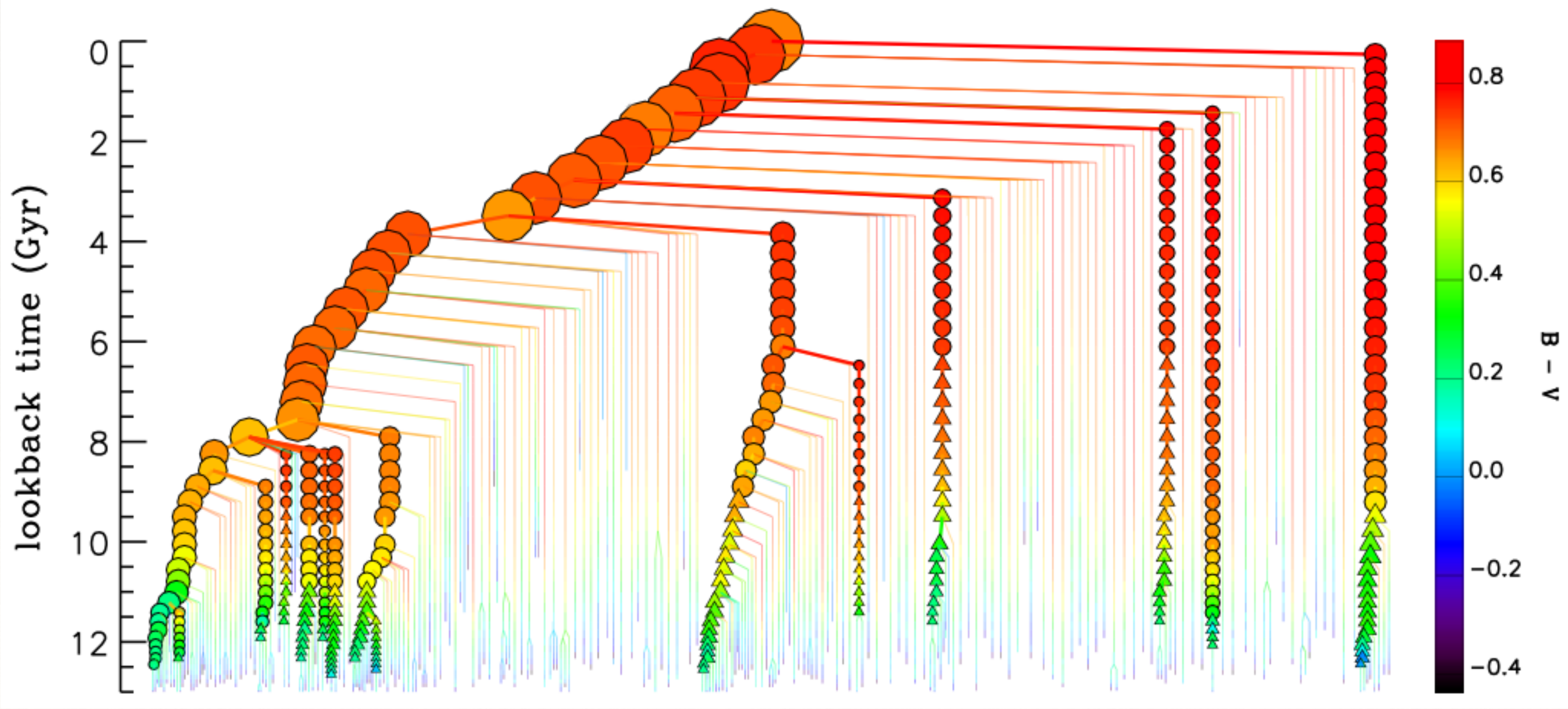

credits: G. De Lucia

Supermassive black hole binaries

- Main sources are supermassive black hole binaries (mass 10^7 — 10^{10} solar) on very broad orbit (period ~ year(s))
- The orbital evolution due to GW emission is very slow: $\frac{dE}{dt} \propto \eta (M/r)^5$ signal is (almost) monochromatic over period of observations

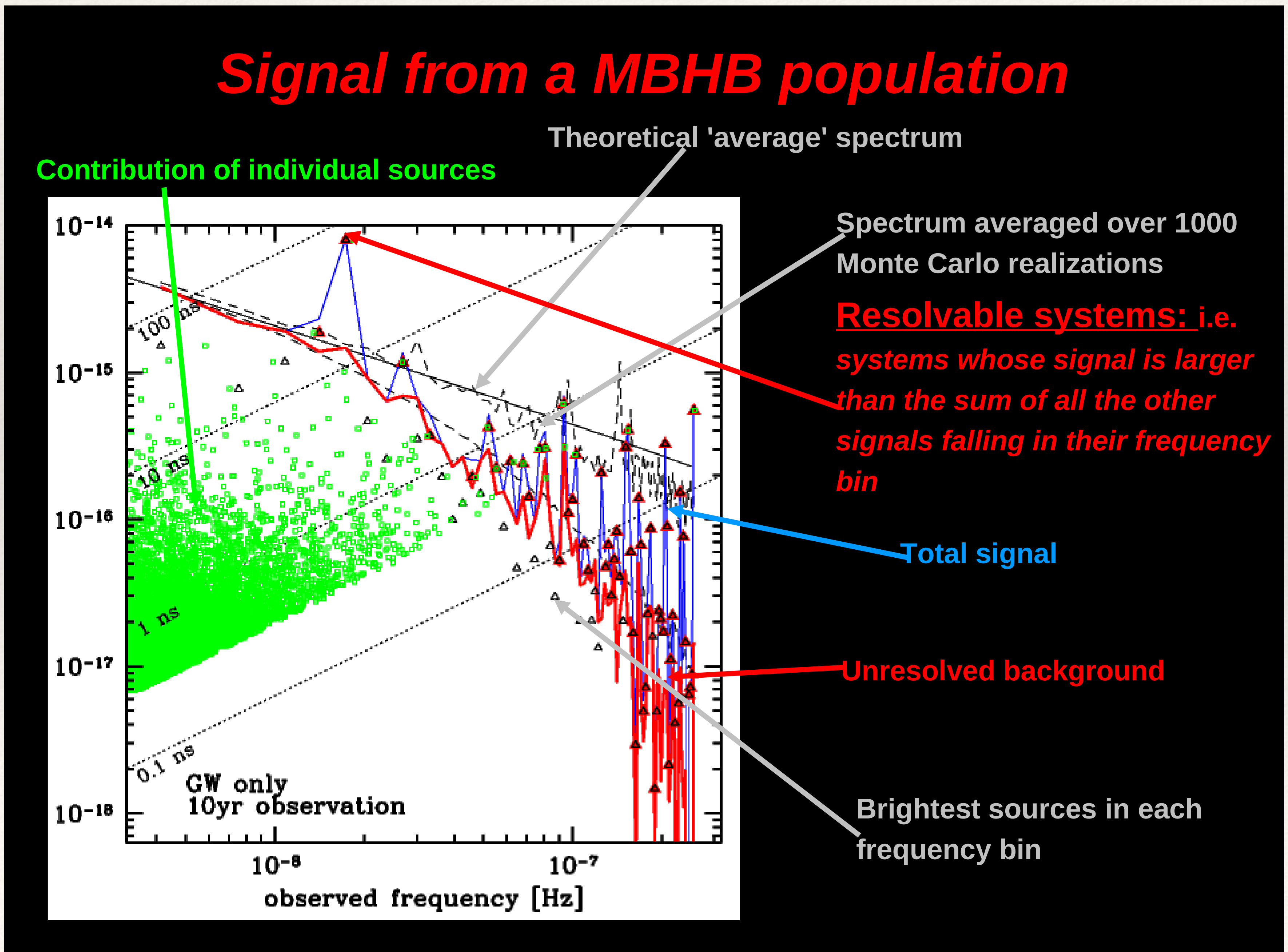

GW signal from the population of SMBH binaries: forms a stochastic signal at low freqs. (similar to Galactic binaries in LISA

[Credits: A. Sesana]

GW signal

Consider non-spinning SMBH binary in circular orbit

- pulsar and earth terms: each is monochromatic signal
- frequency. of pulsar term might or might not coincise with the erath term: $t_p = t - L(1 + \hat{n}\,.\,\hat{k})$
- amplitude of the pulsar term is larger: $\sim \omega^{-1/3}$

$$s_\alpha = F_\alpha^+(\hat{k}, \hat{n}_\alpha)\left[\frac{h_+(t_p^\alpha, \omega_\alpha)}{2\pi f_\alpha} - \frac{h_+(t, \omega)}{2\pi f}\right] +$$

α - pulsar index

$$\underbrace{F_\alpha^\times(\hat{k}, \hat{n}_\alpha)}_{\text{relative position pulsar and GW source}}\left[\underbrace{\frac{h_\times(t_p^\alpha, \omega_\alpha)}{2\pi f_\alpha}}_{\text{Pulsar term}} - \underbrace{\frac{h_\times(t, \omega)}{2\pi f}}_{\text{Earth term coherent across pulsars}}\right]$$

relative position
pulsar and GW source

Earth term coherent
across pulsars

Pulsar term
$\omega_\alpha = \omega(t - L_\alpha(1 + \hat{n}_\alpha\,.\,\hat{k}))$

GW signal in PTA

Response to GW signal of PTA in freq. domain

credits: A. Petiteau

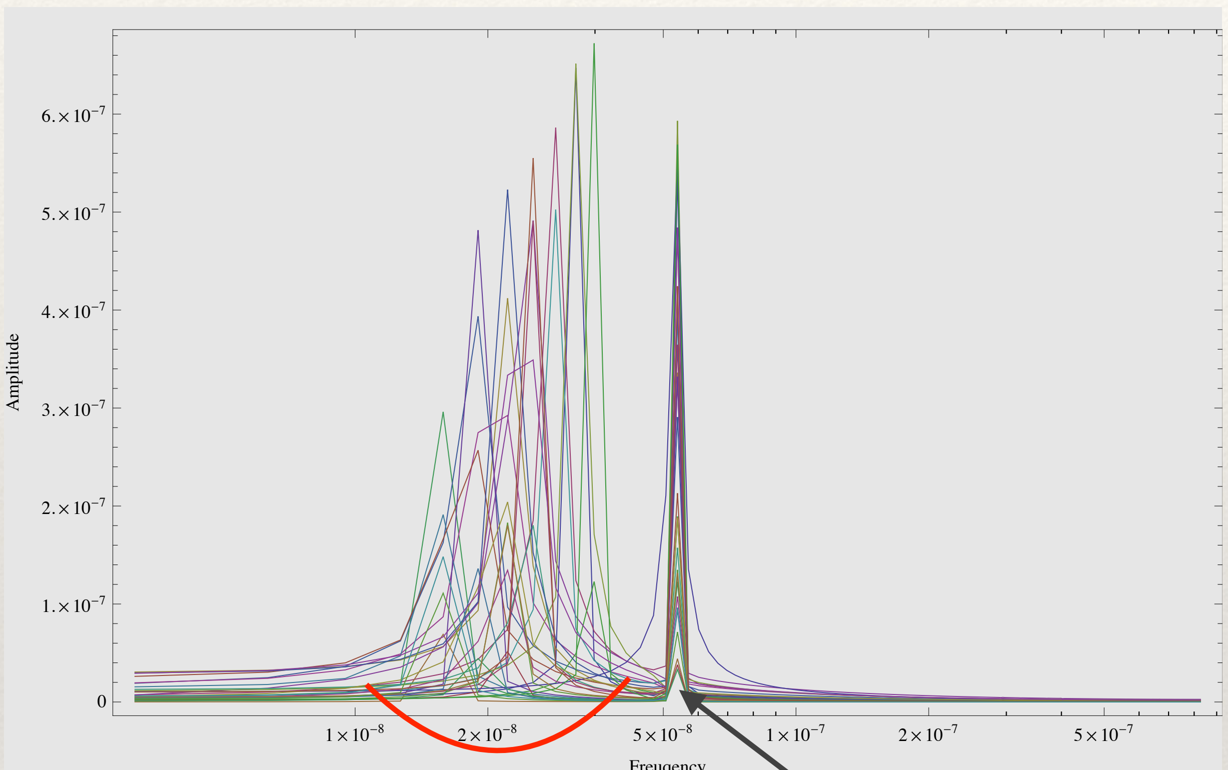

Pulsar term contribution

Earth term contribution

or

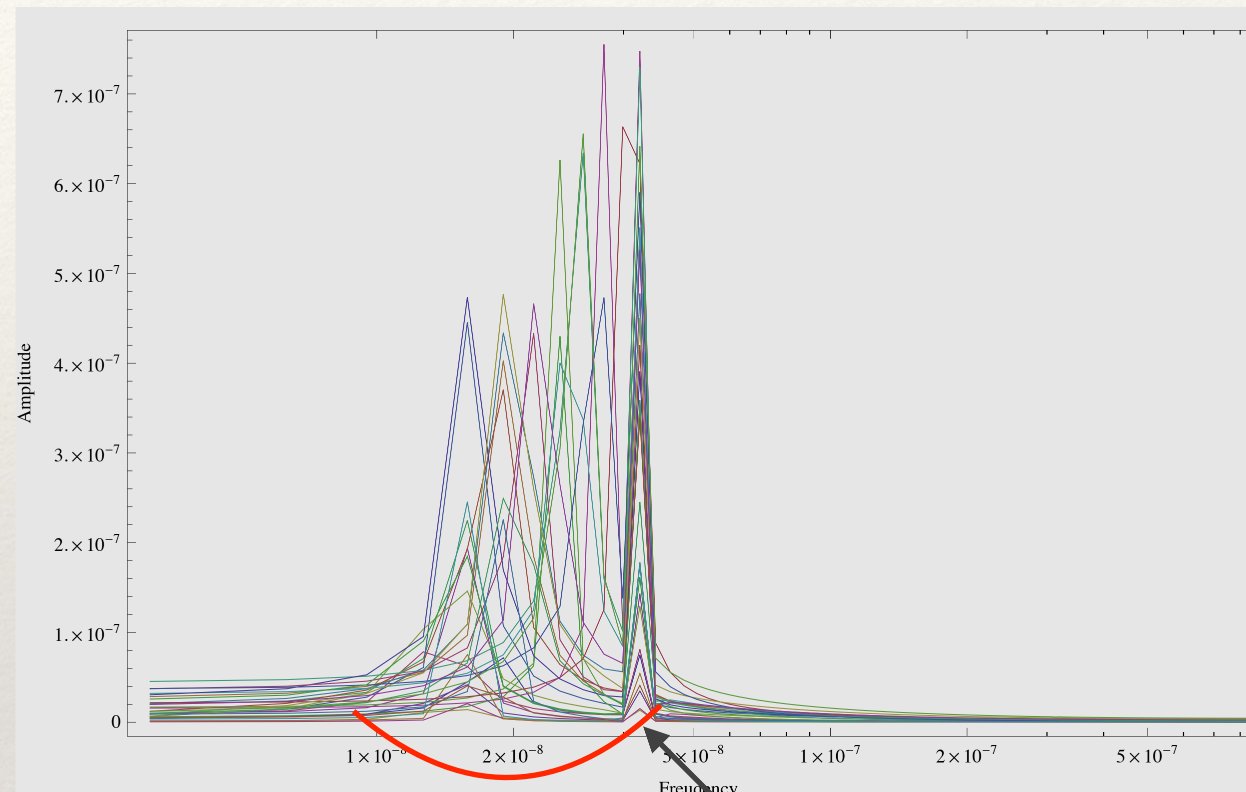

Pulsar term contribution

Earth term contribution

Detection statistic and search algorithm

- We assume that noise is Gaussian: he likelihood function (likelihood of the signal with given parameters is

$$P(\vec{\delta t}, \vec{\theta}) = \frac{1}{\sqrt{(2\pi)^n det(C)}} \exp\left(-\frac{1}{2}(\vec{\delta t} - \vec{s})^T C^{-1} (\vec{\delta t} - \vec{s})\right),$$

- $\overrightarrow{\delta t}$ - concatenated residuals from all pulsars in the array: total size n
- $\vec{s}$ - is a model of deterministic signals (for example GW signals from individually resolvable SMBHBs
- C is the noise variance-covariance matrix (size $n \times n$)

$$C_{\alpha i,\beta j} = \underbrace{C^{wn}\delta_{\alpha\beta}\delta_{ij}}_{\text{white measurement noise}} + \underbrace{C^{rn}_{ij}\delta_{\alpha\beta}}_{\text{red noise spin noise}} + \underbrace{C^{dm}_{ij}\delta_{\alpha\beta}}_{\text{dispersion variation noise}} + \underbrace{C^{GW}_{\alpha i,\beta j}}_{\text{stochastic GW signal}} + \ldots$$

Noise modelling in PTA

- White noise — not very interesting. two parameters per backend per pulsar: unaccounted noise.
- Red noise: very generic noise description in freq. domain

$$S(f) = A_{rn}^2 f^{-\gamma}$$

common, uncorrelated red noise

$$S_\alpha(f) = A_{rn,\alpha}^2 f^{-\gamma_\alpha}$$

red noise in each. pulsar

- DM (dispersion measurement variation) noise: depends on the radio-frequency of observation

$$S_{DM}(f) \propto \frac{A_{dm}^2}{\nu^2} f^{-\gamma_{dm}}$$

- Correlated red noise processes

$$S_{\alpha\beta} = \Gamma_{\alpha\beta} A_{cor}^2 f^{-\gamma_{cor}}$$

— includes also cross spectrum between each pair of pulsars: $\Gamma_{\alpha\beta}$ - spacial correlation coefficients

Correlated noise

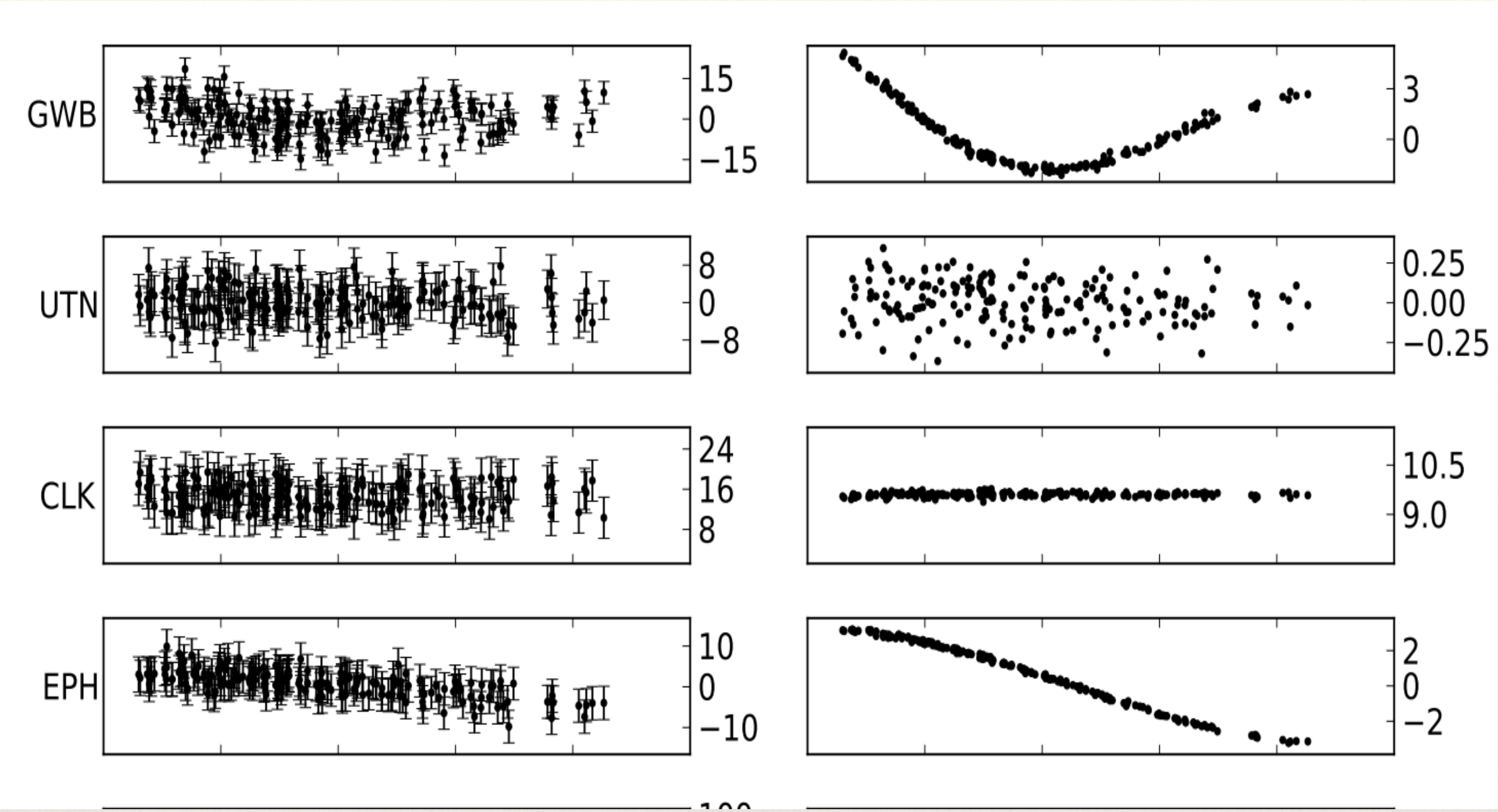

GWB (Quadrupole)

Uncorrelated RN

Clock error (monopole)

Ephemeris (dipole)

TOAs, time

Correlation, angular separation

stochastic GW from population of SMBHBs: $S_{\alpha\beta}^{SMBHB} = \Gamma_{\alpha\beta}^{H-D} A_{GW}^{2} f^{-13/3}$

Hellings-Downs curve: stochastic GW signal

- Stochastic GW signal — noise like signal which is correlated in observation of all pulsars. The correlation due to GW is very specific: Hellings-Downs curve.
- Correlation for the isotropic stochastic GW signal depends only on the angular separation between the pairs of pulsars.

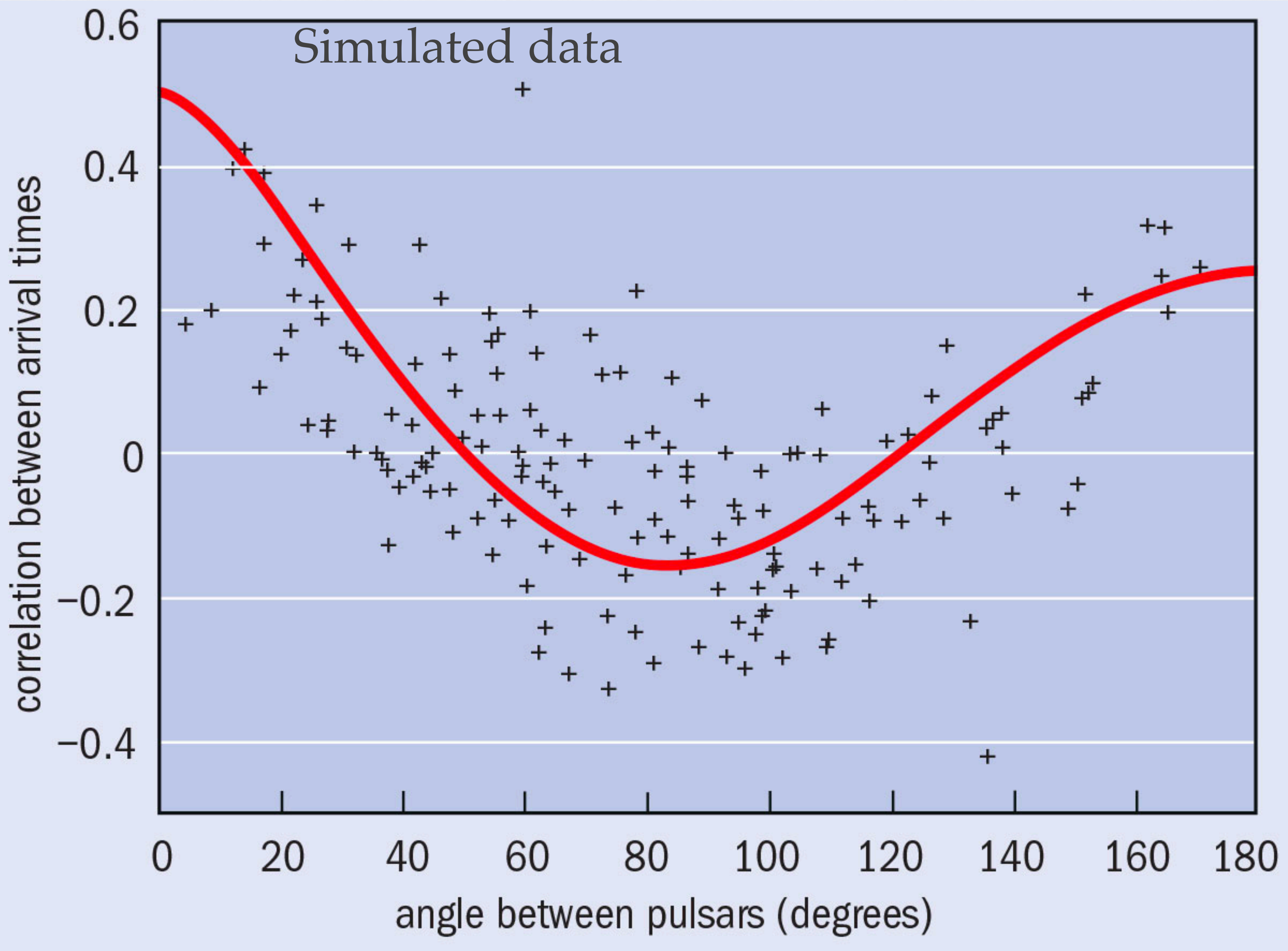

[Fig. from IOP, Physics World]

Gaussian-process approach to PTA: falling into a rabbit hole

Short intro into a Gaussian Process (GP)

- GP generalize the notion of Gaussian randiom variables to the case of infinite number of degrees of freedom
- GP can be specified in 2 equivalent ways:
  - as a sum of deterministic basis functions: $\sum_i \phi_i(x) w_i$ - where w_i are weights - Gaussian random variables $\mathcal{N}(w_i^0, \Sigma_{ij})$. weight-space view
  - as a continuous f-n $f(x)$ such that the ensemble average $\mathbb{E}[f(x)] = m(x)$ and the covariance: $\mathbb{E}[(f(x) - m(x))(f(x') - m(x'))] = k(x, x')$. function-space view
- Those two approaches are connected by

$$k(x, x') = \sum_{i,j} \phi_i(x) \Sigma_{ij} \phi_j(x')$$

Gaussian-process approach to PTA: falling into a rabbit hole

- Applying GP to the PTA likelihood function:

Gaussian prior on weights

GP

$$p(\delta t|w_i, GP) = \frac{e^{-\frac{1}{2}\cdot\sum_{ij}(\delta t_i - \sum_a \phi_a(t_i)w_a)(C^w_{ij})^{-1}(\delta t_j - \sum_a \phi_a(t_j)w_a)}}{\sqrt{(2\pi)^n \det(C^w)}} \times \frac{e^{-\frac{1}{2}\sum_{a,b} w_a(\Sigma_{ab})^{-1}w_b}}{\sqrt{(2\pi)^m \det(\Sigma)}}$$

weight-space approach

white noise

$$p(\delta t|w_i, GP) = \frac{e^{-\frac{1}{2}\cdot\sum_{ij}\delta t_i(C^w_{ij}+C^{rn}_{ij})^{-1}\delta t_j}}{\sqrt{(2\pi)^n \det(C^w + C^{rn})}} \qquad \text{with} \qquad C^{rn}_{ij} = k(t_i, t_j) = \sum_{a,b} \phi_a(t_i)\Sigma_{ab}\phi_b(t_j)$$

red noise variance-covariance matrix

In time domain, uncorrelated red noise:

$$C^{rn}_{ij} = A^2(f_L/\mathrm{yr}^{-1})\left\{\Gamma(1-\gamma)\sin\left(\frac{\pi\gamma}{2}\right)(f_L\tau_{ij})^{\gamma-1} - \sum_n \frac{(-1)^n(f_L\tau_{ij})^{2n}}{(2n)!(2n+1-\gamma)}\right\}$$

where $\tau_{ij} = |t_i - t_j|$ and f_L is low freq. cut-off

Gaussian-process approach to PTA: falling into a rabbit hole

- Alternatively we can use basis functions: based on the decomposition of residuals in the Fourier modes:

$$\delta t(t_i) \approx \sum_k a_k \sin 2\pi f t_i + b_k \cos 2\pi f t_i$$

weights

basis functions $\phi^F(f_a, t_i) = \phi_a^F(t_i)$

We use non-complete set of Fourier modes: covariance matrix can be approximated as

$$C_{ij}^{rn} \approx \sum_{a,b} \phi_a^F(t_i) \Sigma_{ab}^F \phi_b^F(t_j)$$ where

$$\Sigma_{ab}^F \propto \left(A_{rn}^2 f_a^{-\gamma}\right) \delta_{ab}/T$$ — red noise PSD

and for stochastic GW signal: $C_{i\alpha,j\beta}^{GW} = \sum_{i\alpha,j\beta} \phi_a^F(t_{i\alpha}) \Sigma_{i\alpha,j\beta}^{F,GW} \phi_a^F(t_{j\beta})$, where

$$\Sigma_{i\alpha,j\beta}^{F,GW} = \Gamma_{\alpha\beta}(A_{GW}^2 f_a^{-\gamma_{gw}})\delta_{ab}/T$$

Gaussian-process approach to PTA: falling into a rabbit hole

Advantage of this description: again likelihood

$$p(\delta t|w_i, GP) = \frac{e^{-\frac{1}{2}\cdot\sum_{ij}\delta t_i (C^w_{ij}+C^{rn}_{ij})^{-1}\delta t_j}}{\sqrt{(2\pi)^n \det(C^w + C^{rn})}}$$

Data size: n - large, need to invert very large (covariance) matrices - $n \times n$
Can use Woodbury f-la

$$(C_w + C_{rn})^{-1} = (C_w + \Phi\Sigma\Phi^T)^{-1} = C_w^{-1} - C_w^{-1}\Phi \underbrace{\left(\Sigma^{-1} + \Phi^T C_w^{-1}\Phi\right)^{-1}}_{\text{inversion of } m\times m \text{ matrix}} \Phi^T C_w^{-1}$$

Number of modes: $m \ll n$

Residuals of 6 best EPTA pulsars

From top to bottom these are PSRs: J0613-0200, J1012+5307, J1600-3053,J1713+0747, J1744-1134, and J1909-3744

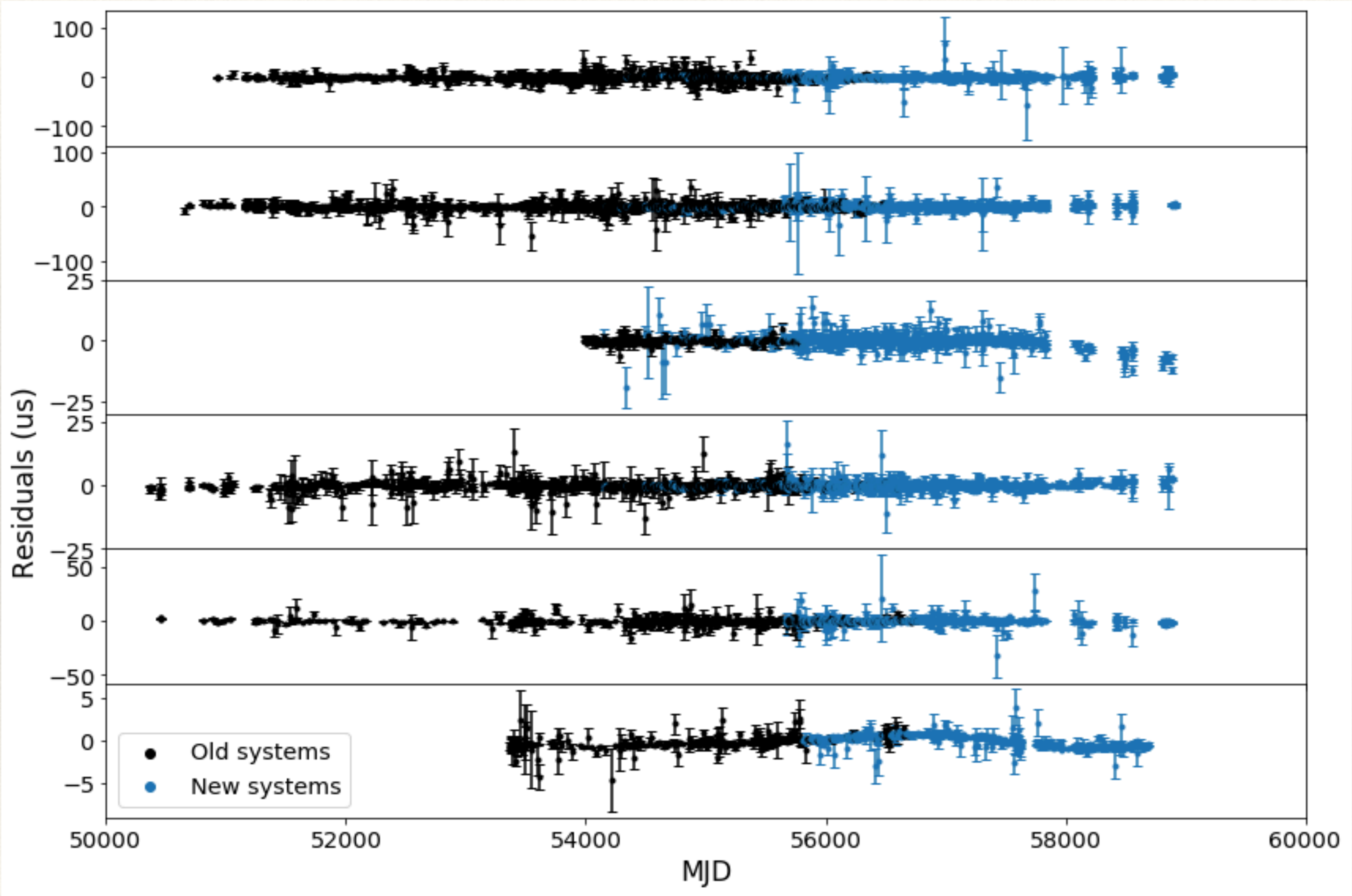

Up to 25 years of monitoring: black - DR1, blue - DR2 (data release)

Common red noise in EPTA data

preliminary

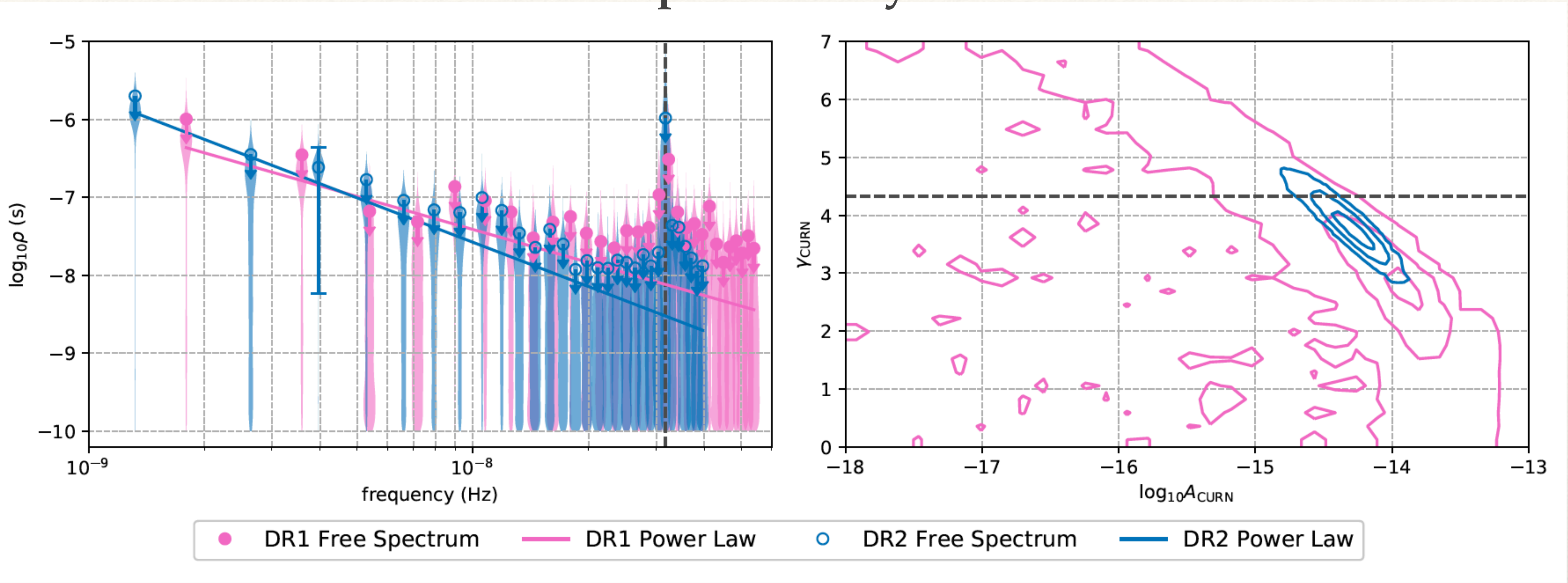

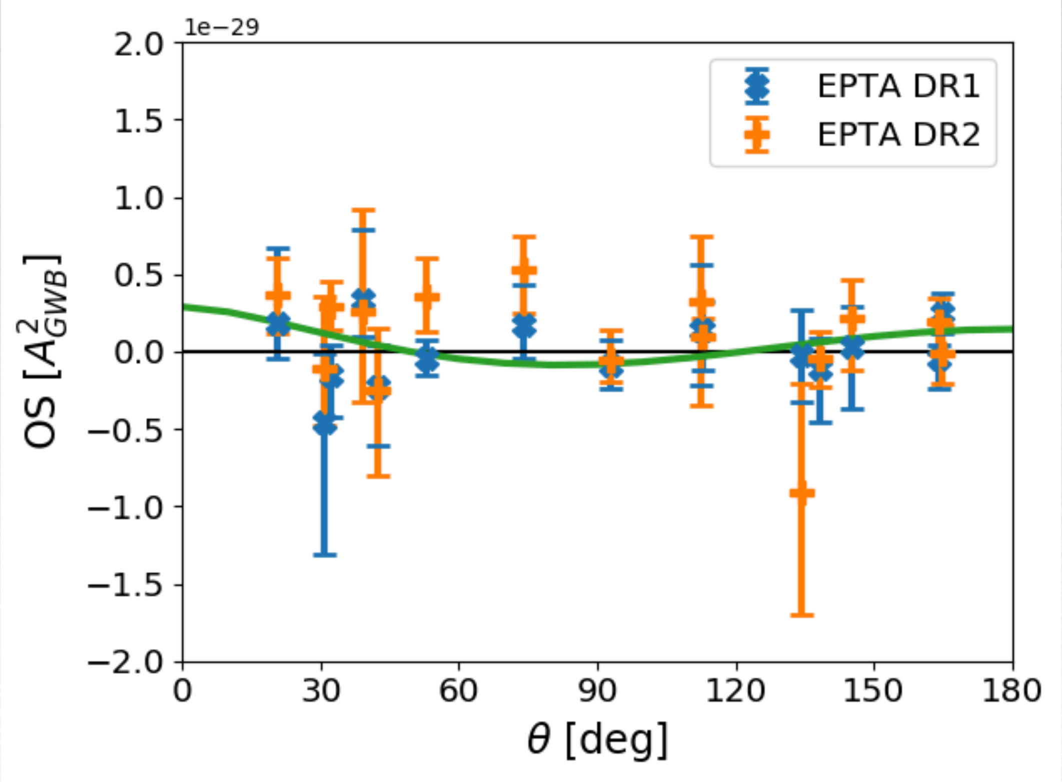

There is a strong statistical support for presence of common red noise

$$S(f) = A_{rn} f^{-\gamma}$$

common, uncorrelated red noise

NanoGrav 12.5 yrs data result

[Arzoumanian+ 2020]

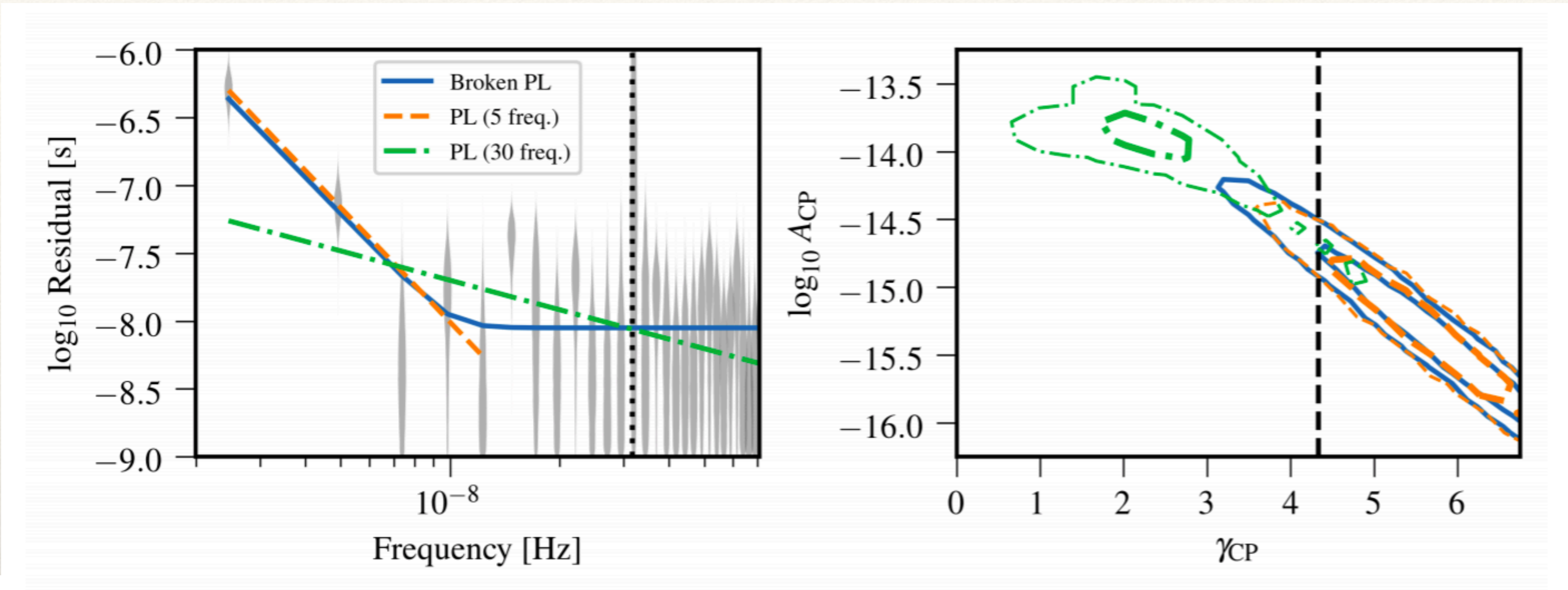

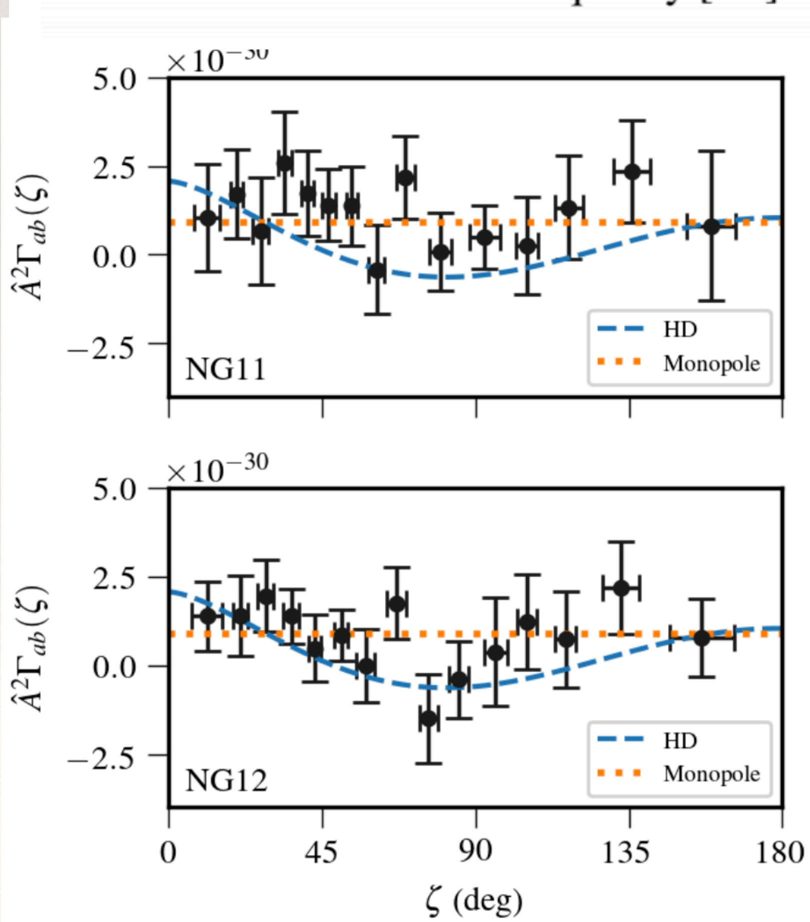

There is a strong statistical support for presence of common red noise

$$S(f) = A_{rn} f^{-\gamma}$$

common, uncorrelated red noise

Common uncorrelated red noise

NanoGrav , EPTA and PPTA support presence of a common red noise

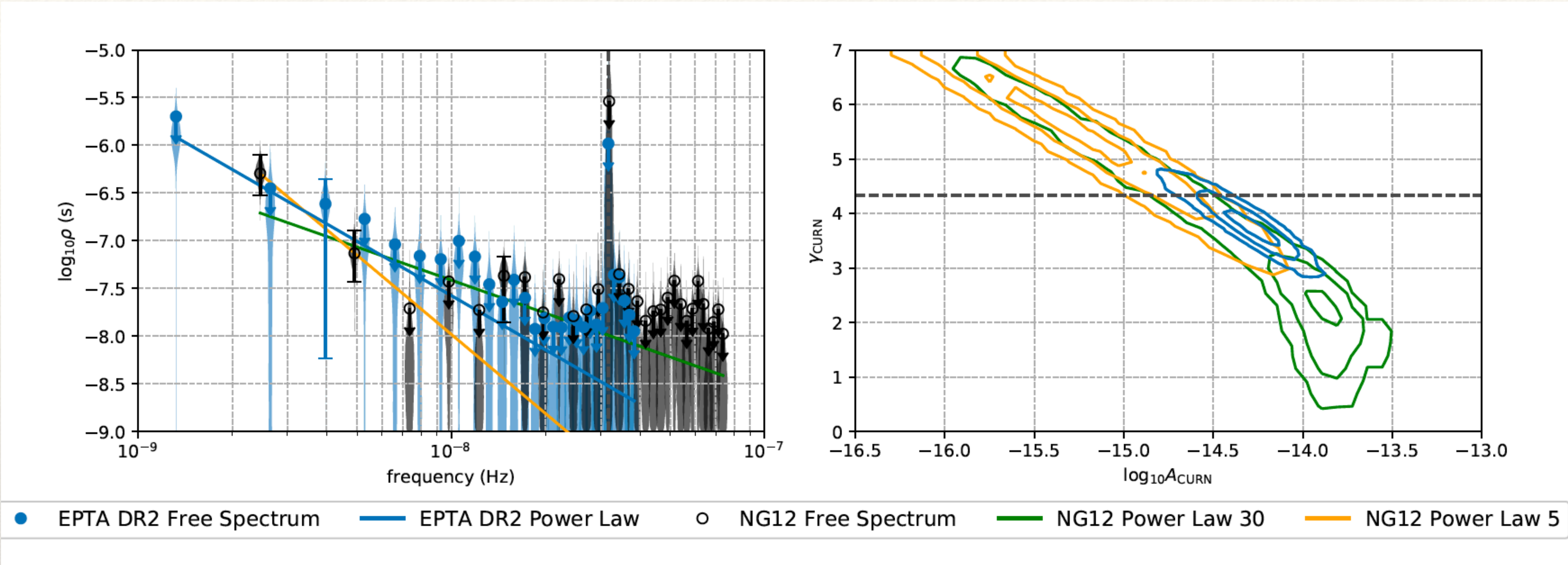

Stochastic GW signal?

[Arzoumanian+ 2020]

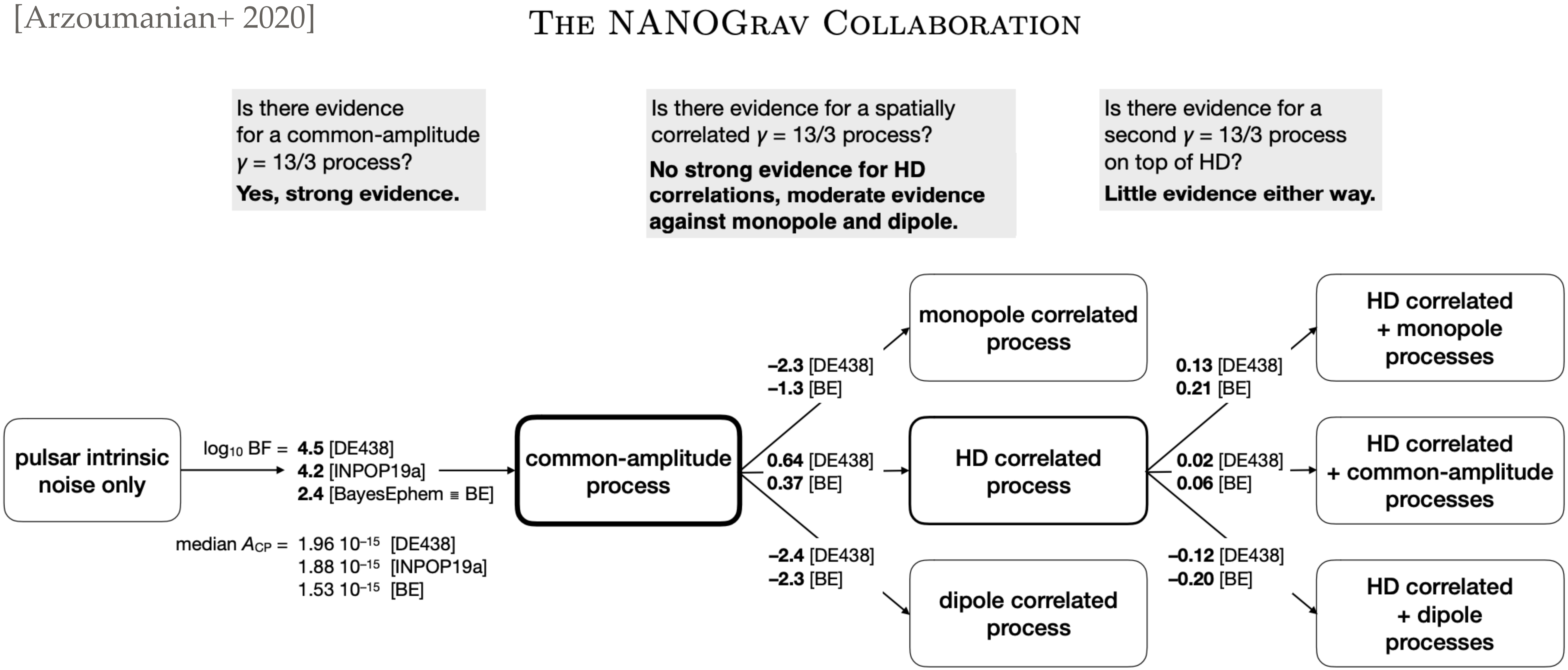

- No statistical significance to support Hellings-Downs spacial correlation:
  - Need more pulsars to compute more pair-wise correlations (EPTA->20)
  - Need longer data set to uncover more of the red signal (Nanograv-> 15 yrs)

Can it be GW from SMBHs?

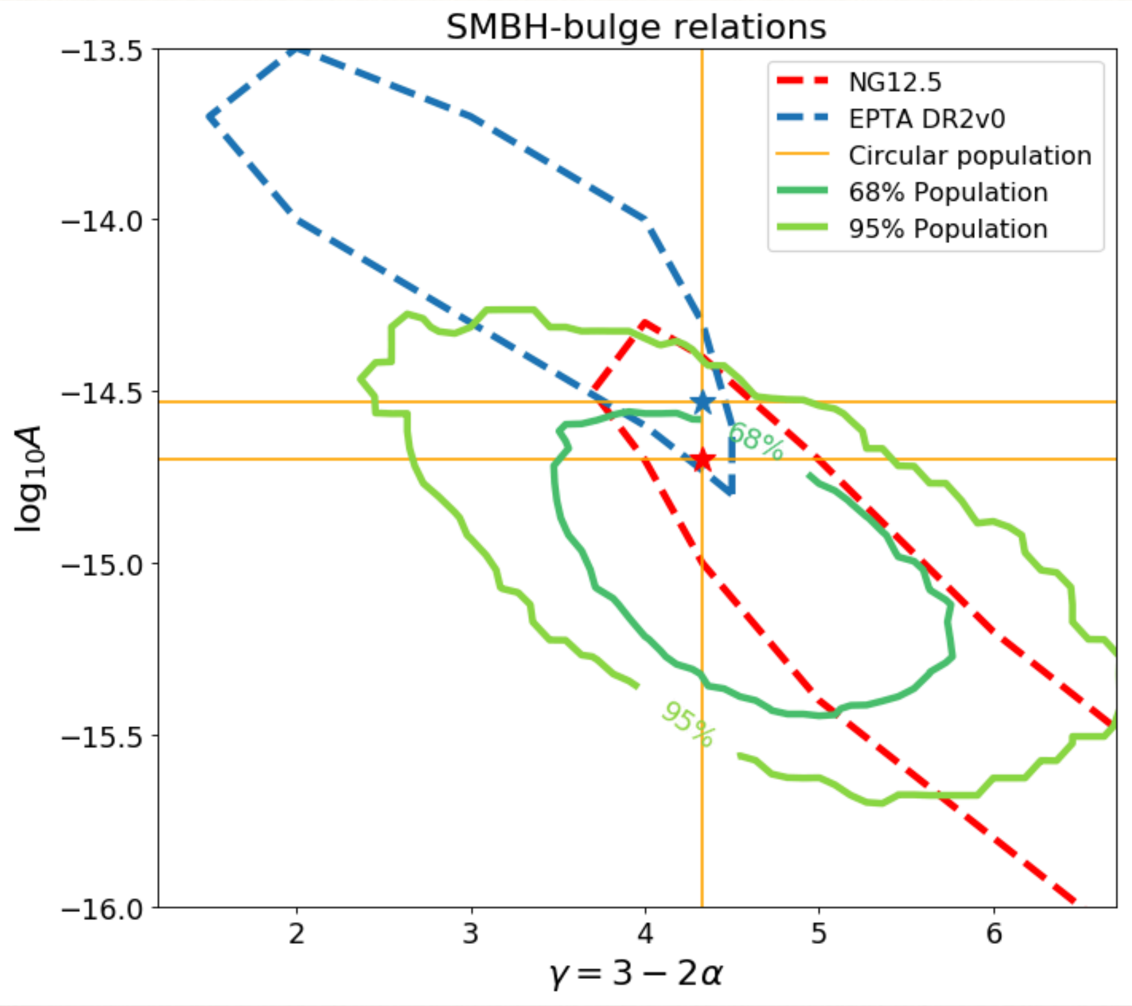

- Analytic prediction: spectral index
- Simulation of SMBHB populations is shown as green contours: wide range spectral indices
- Results of NanoGrav and EPTA are consistent with spectral index from the population of SMBHBs

Solar system ephemeris

- We use Solar system barycenter (SSB) as a reference system to reduce all observations
- The systematic error in SSB (from ephemeris) could create residual (dipolar cos-like spacial correlation) common signal with red-noise like spectrum
- Poorly determined position of SSB
- Use phenomenological model (vary orbital elements of Jupyter and Saturn) to mimick possible systematics (BayesEphem)

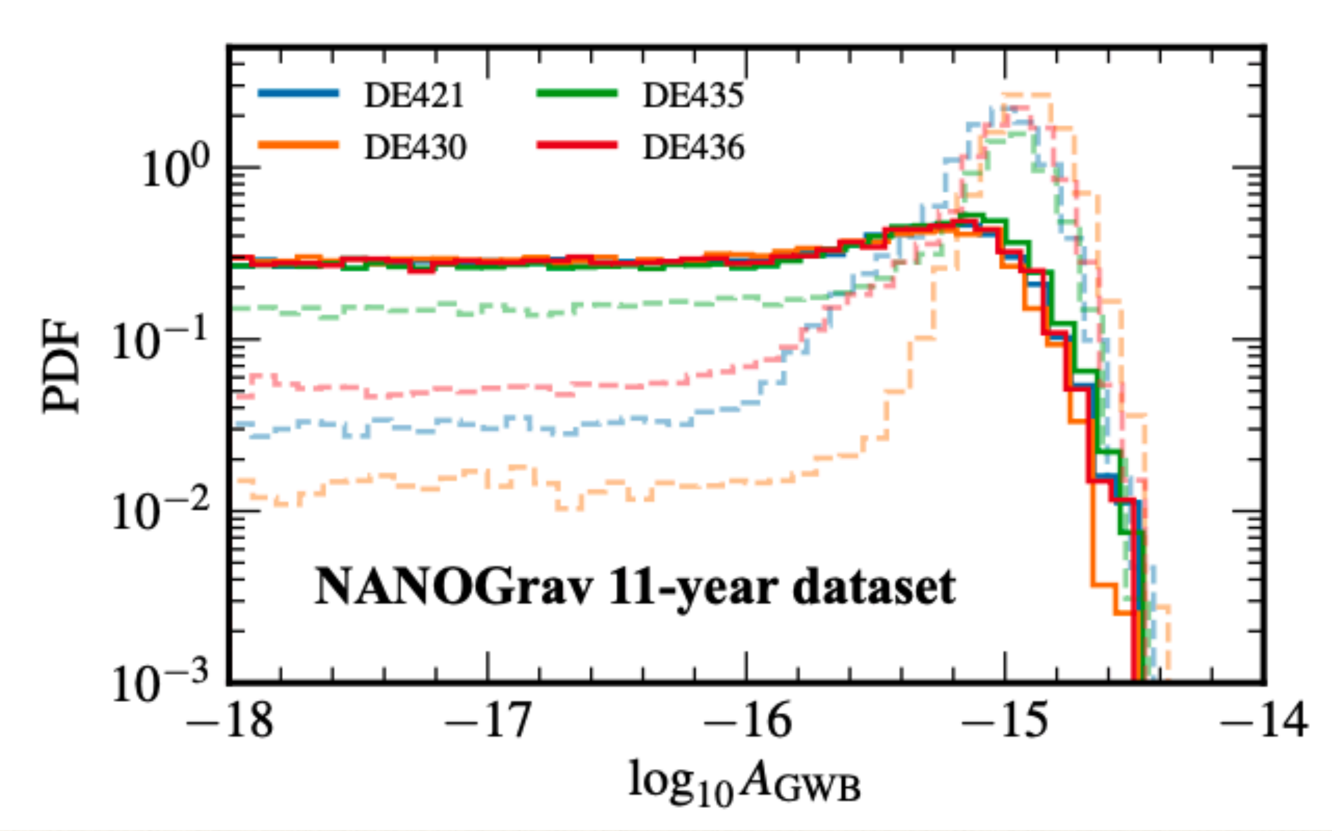

[Arzoumanian+ 2018]

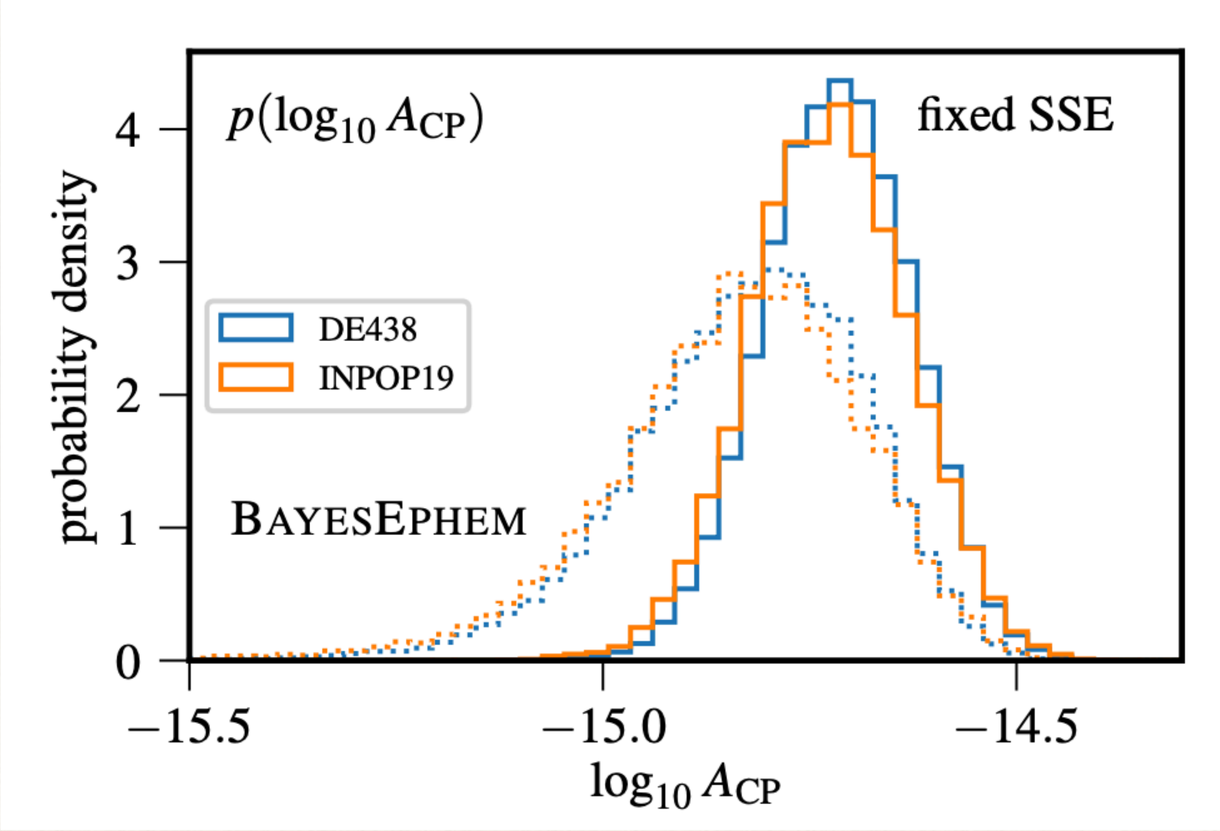

[Arzoumanian+ 2020]

Search for indivdual SMBHBs

Reminder: GW signal(s) from a population of SMBHBs:

- We are now after "loud" individual systems (hot spots) sticking above the stochastic component

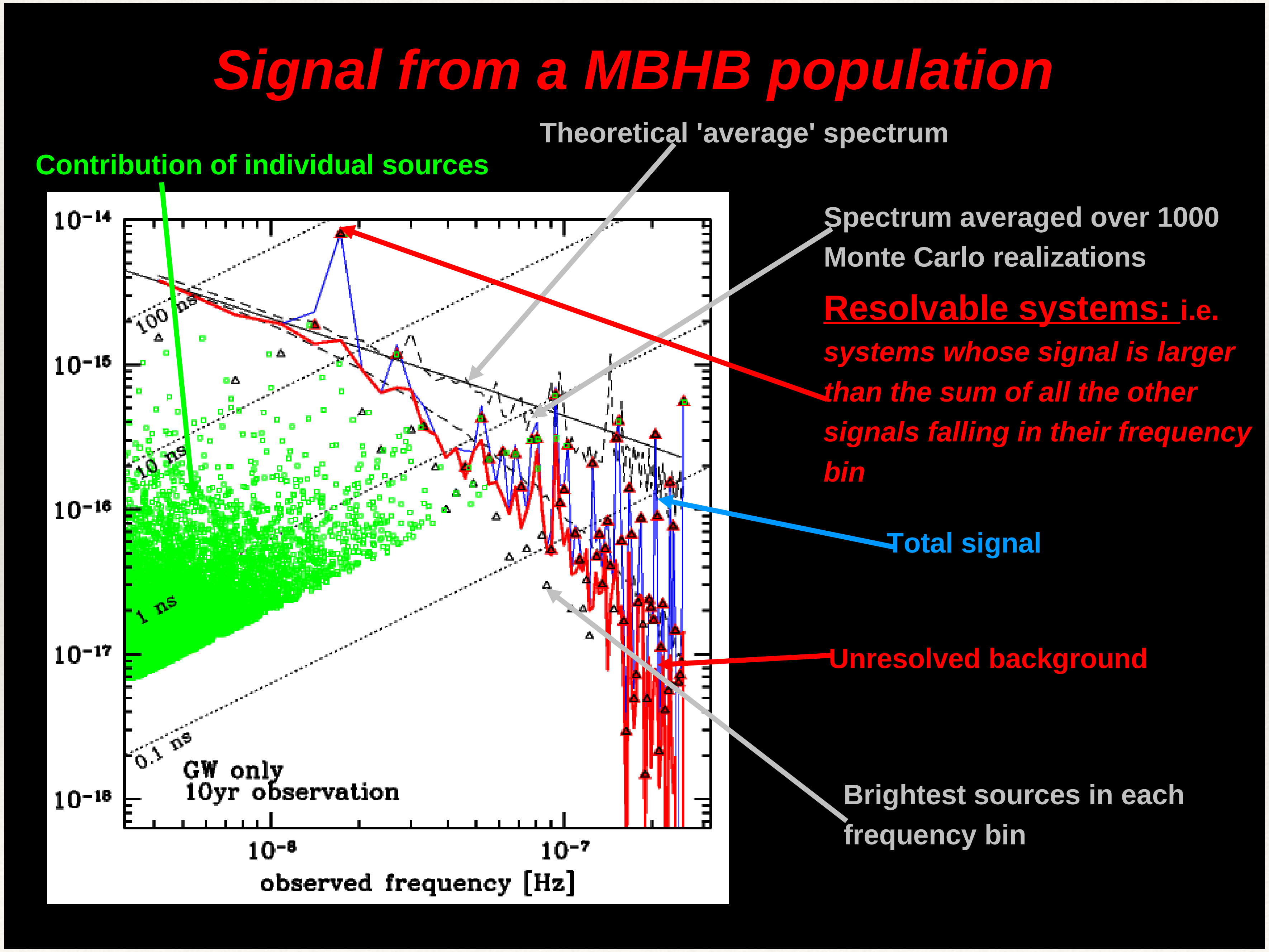

Continuous GW signal

- Each GW signal from SMBHB is characterized by:
  - Earth term: $A, \iota, \psi, \phi_0, f, \theta_{sky}, \phi_{sky}$
  - Pulsar term: L_α, M_c — distance to the pulsar (poorly known), chirp mass
  - In total $8 + N_p$ parameters
- Each pulsar gives 2 measurements: (real and imaginary at each freq.)
- Earth term depends on 6 params (for a given freq.)
  - We need at least 3 pulsars per GW source for parameter estimation

SIMULATED DATA

Sky map: 3 pulsars and 1 GW source

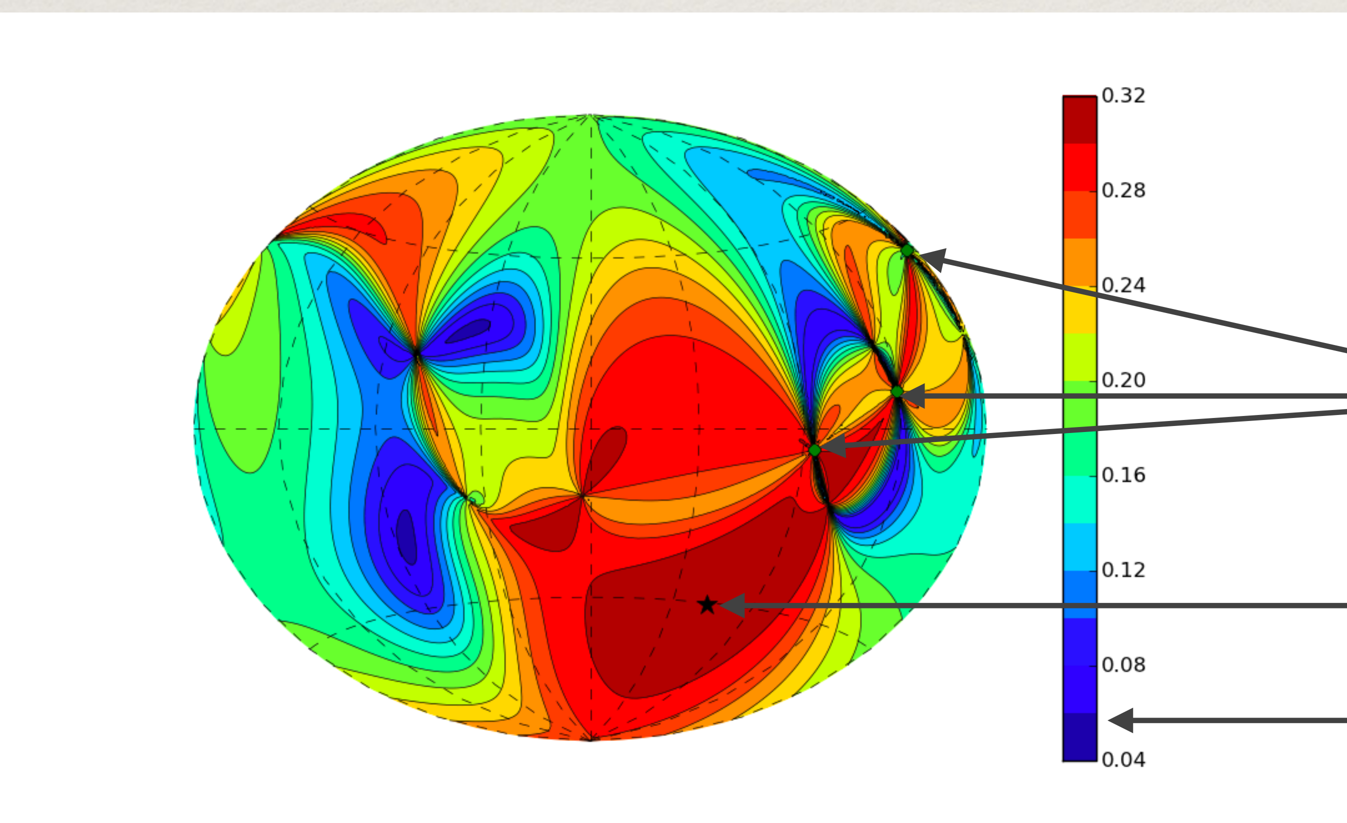

Pulsars

Source

scaled likelihood

Continuous GW signal

Another example: 5 GW sources, and 50 pulsars.
Assume that there is only 1 GW source.

SIMULATED DATA

The likelihood sky map

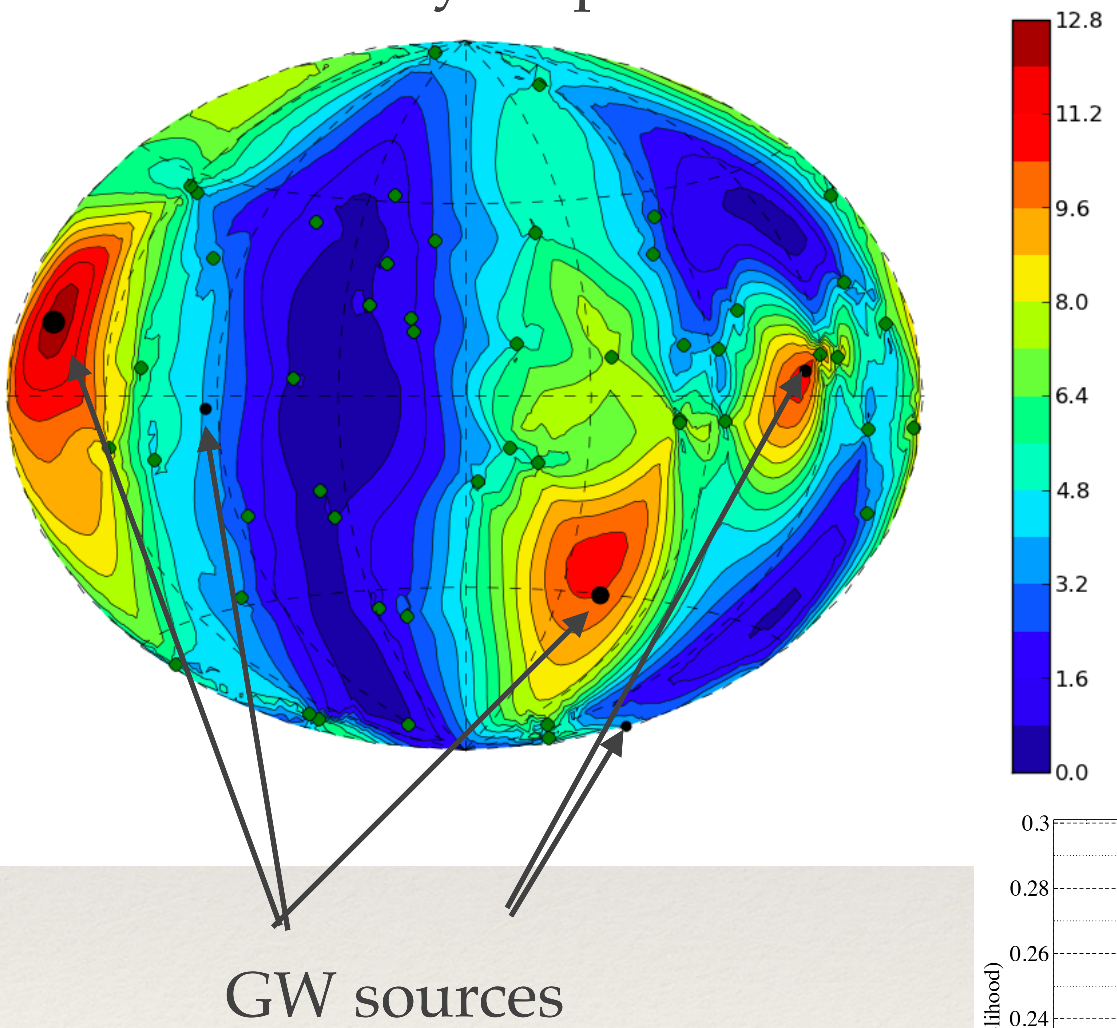

With 1-source model we resolve three strongest sources: size of black circle is proportional to GW strain

Likelihood for 2,3,4,5,6,7-source model

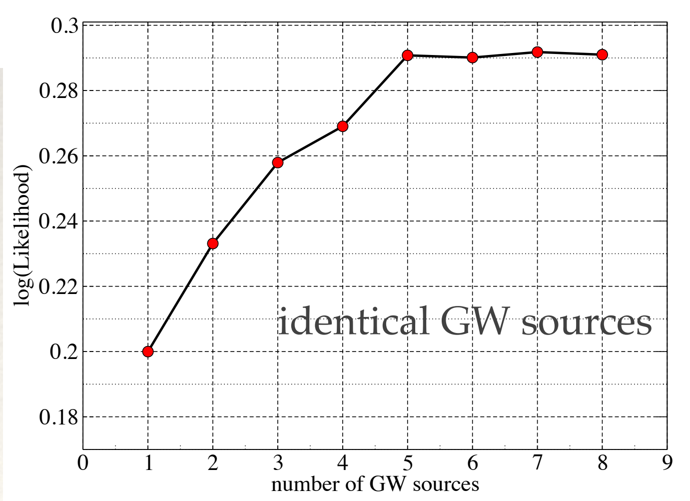

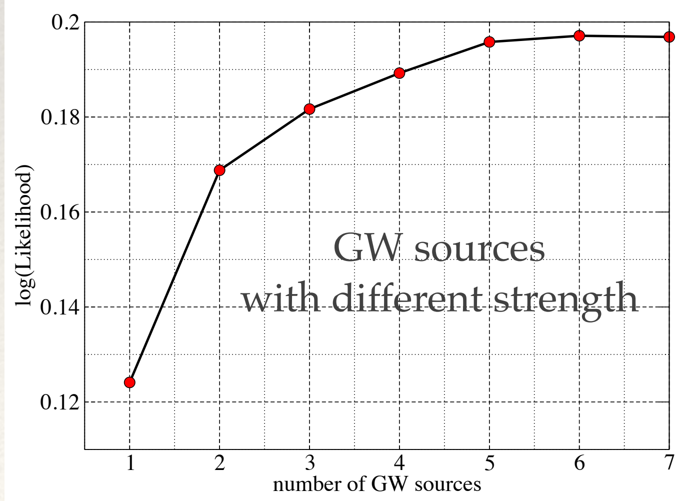

Continuous GW signal (EPTA)

- Search for continuous GW signal using frequentist and Bayesian techniques
  - analytic maximization (marginalization) over some parameters
- Search for continuous GW signal using earth-term only (coherent) or using earth+pulsar term (more expensive)
- Pulsar ranking: 41 pulsar in EPTA data, search is expensive - rank pulsars by “goodness” - how much they contribute to the total signal-to-noise ratio. Monte-Carlo simulation

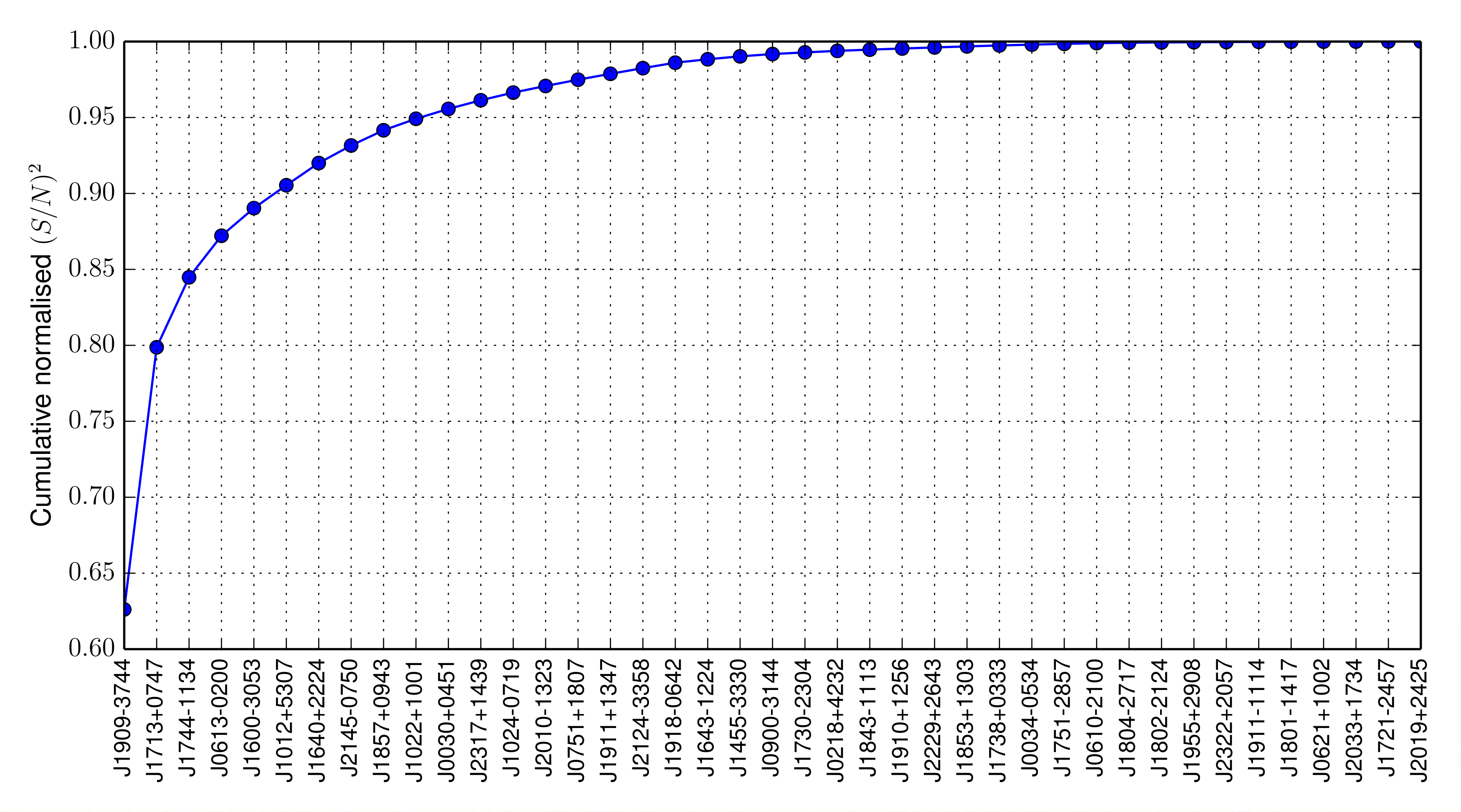

Upper limit on continuous GW signal in EPTA data

upper limit of GW strain using different statistics, methods, frameworks

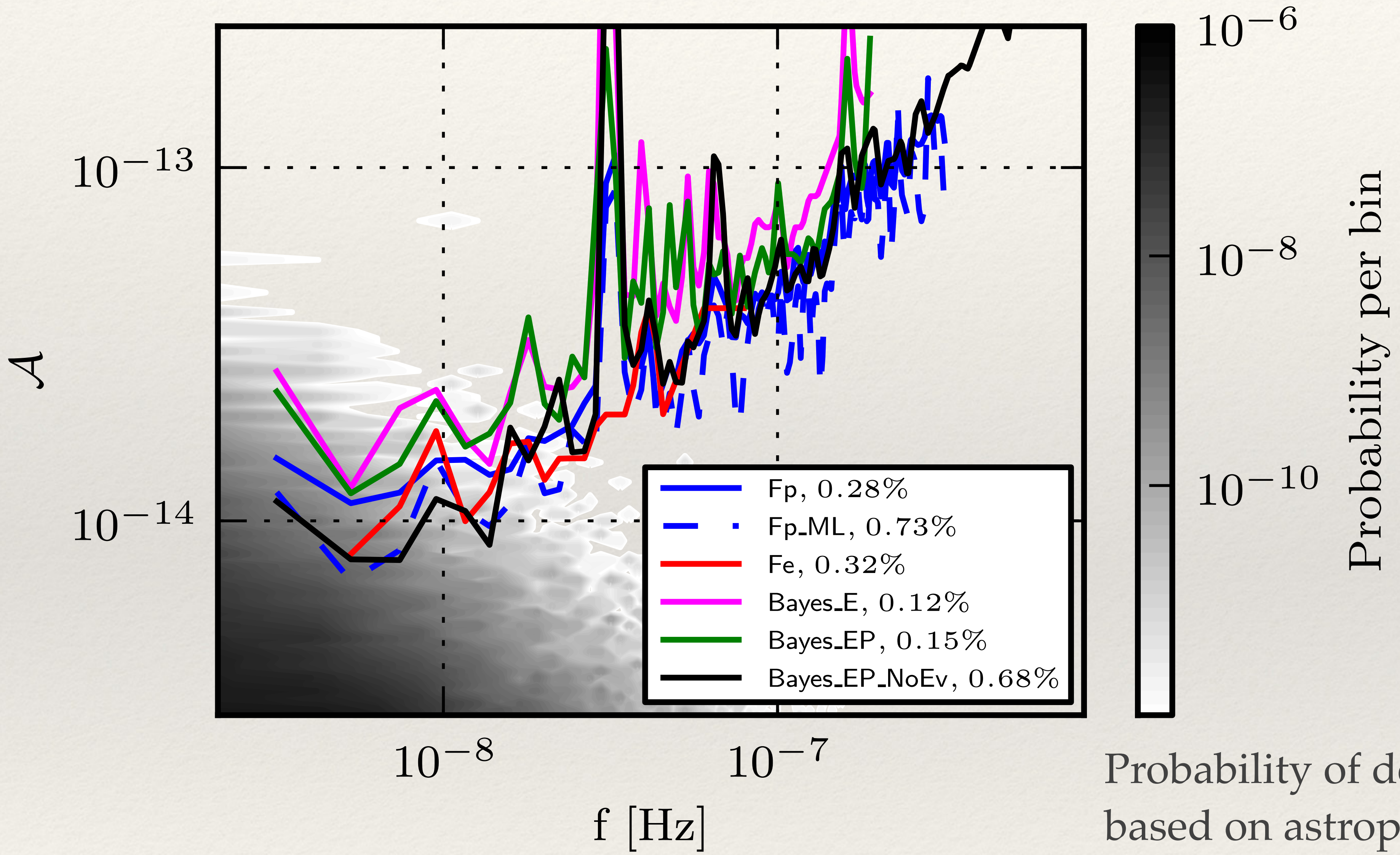

Probability of detecting GW source based on astrophysical simulation of SMBHB population

Upper limit on continuous GW signal in EPTA data

Directional upper limit (sky map) at 7nHz (best EPTA DR1 frequency)

- white circles: pulsars used to set upper limit, size proportional to "goodness"
- two nearest supeclusters: Coma and Virgo

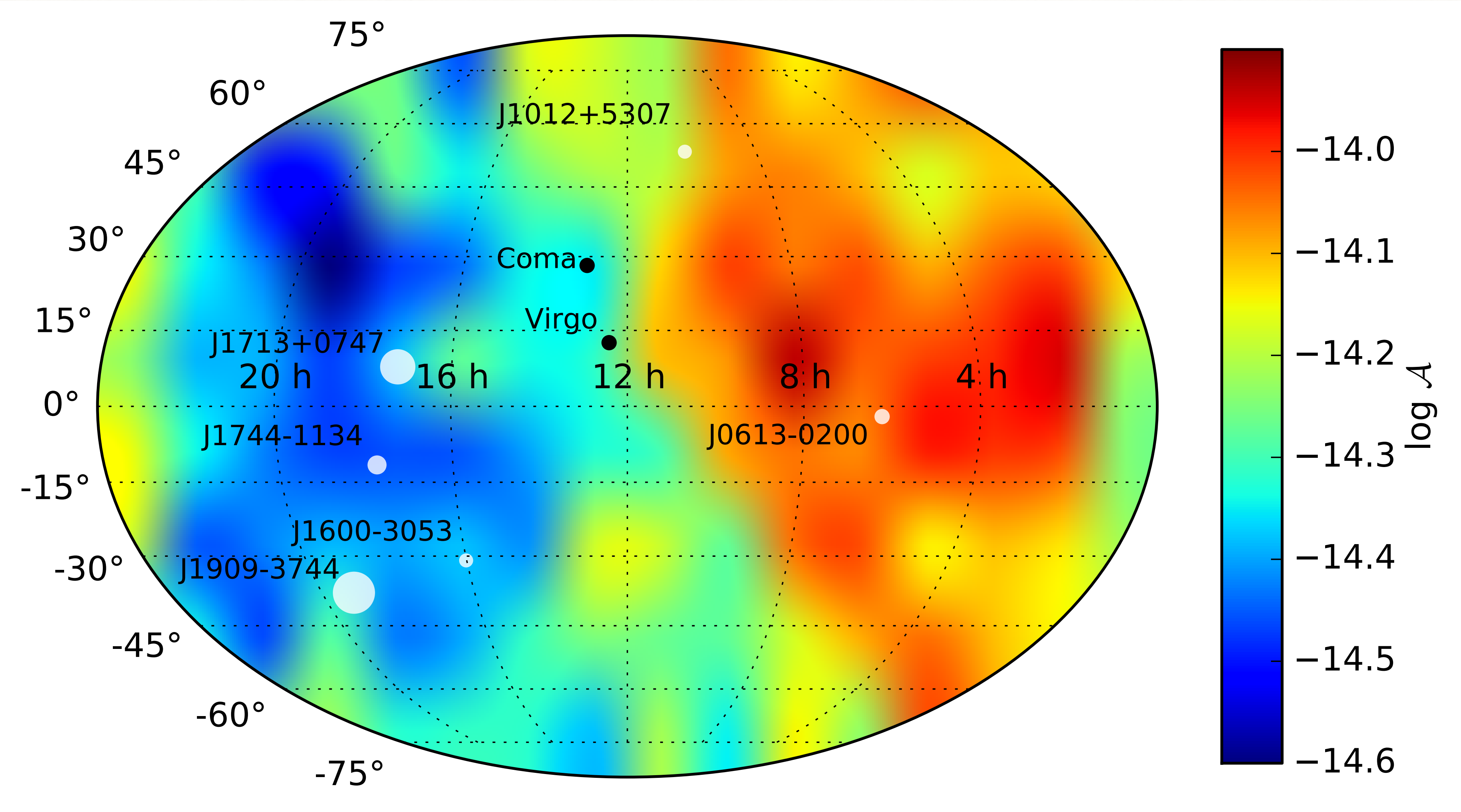

[Babak+ 2015, EPTA]

What is next?

- NanoGrav: require longer observations (combining 15 yrs of data)
- EPTA: (i) need to finish analysis of 6 best pulsars, (ii) need to include more pulsars (20) to confirm H-D correlations
- PPTA: have very long observations and few very good MSP (south): another confirmation of common red process
- IPTA: combine all data together to see if significance grows as expected.
- Need to confirm GW (if it is GW signal) using methods [Cornish+ 2016, Taylor+ 2017] to destroy correlations and test statistical significance of our findings (preserving the noise properties)
- Wait longer:
  - new high quality data SKA (MeerKAT), Fast, …
  - Check SNR as a function of time

$< SNR > \propto T^{\gamma} \to \propto T^{1/2}, \gamma > 1$ — RN spectral index (e.g. 13/3 for stochastic GW signal from SMBHBs)

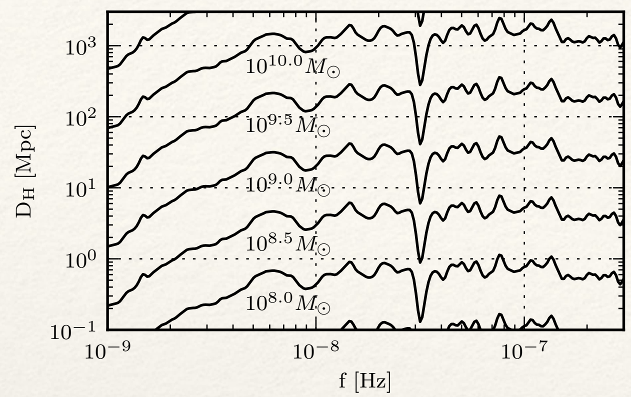
D$_H$ [Mpc]
$10^{10.0} M_\odot$
$10^{9.5} M_\odot$
$10^{9.0} M_\odot$
$10^{8.5} M_\odot$
$10^{8.0} M_\odot$
f [Hz]

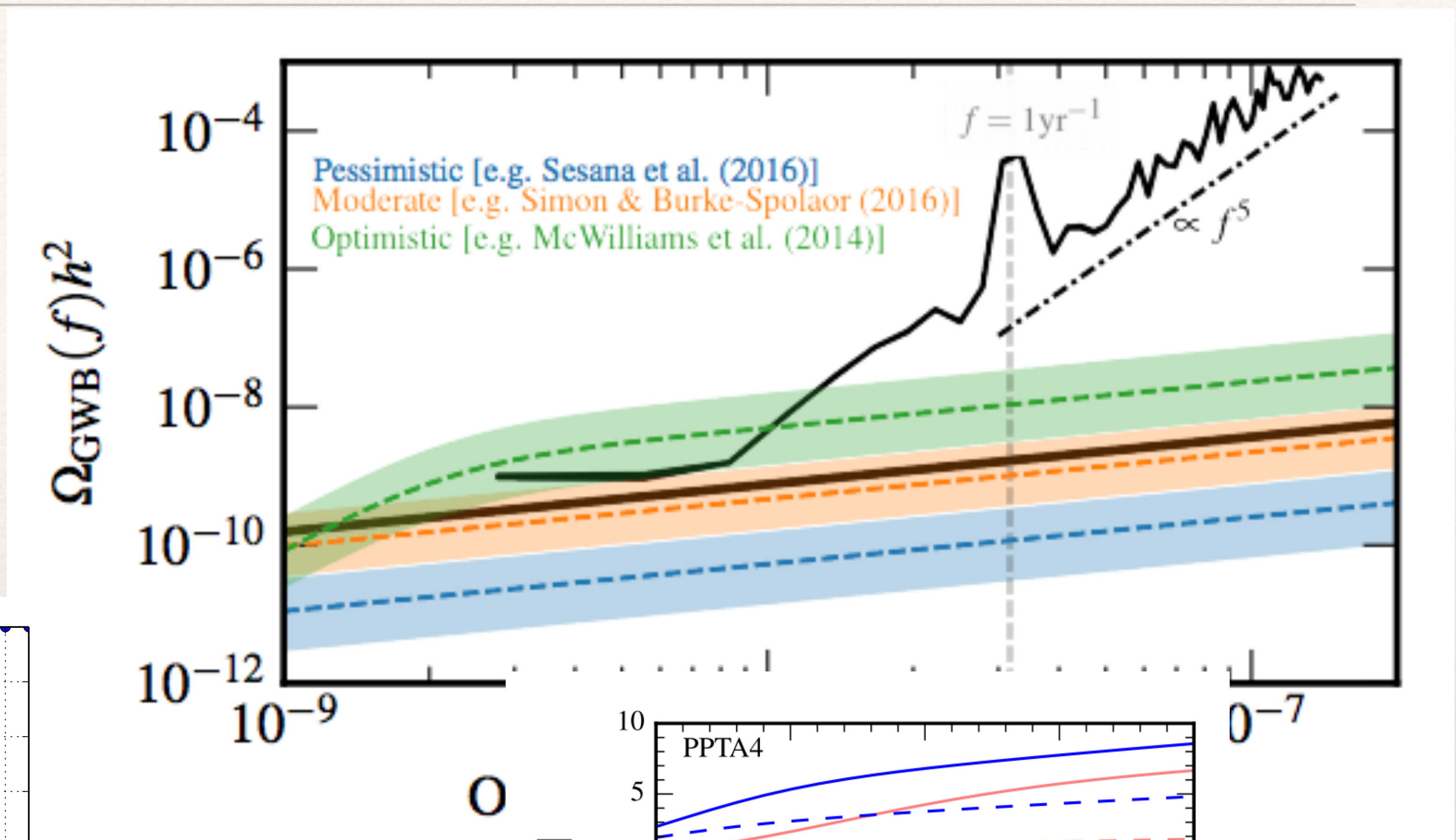
$\Omega_{\rm GWB}(f)h^2$
$f = 1\mathrm{yr}^{-1}$
Pessimistic [e.g. Sesana et al. (2016)]
Moderate [e.g. Simon & Burke-Spolaor (2016)]
Optimistic [e.g. McWilliams et al. (2014)]
$\propto f^5$

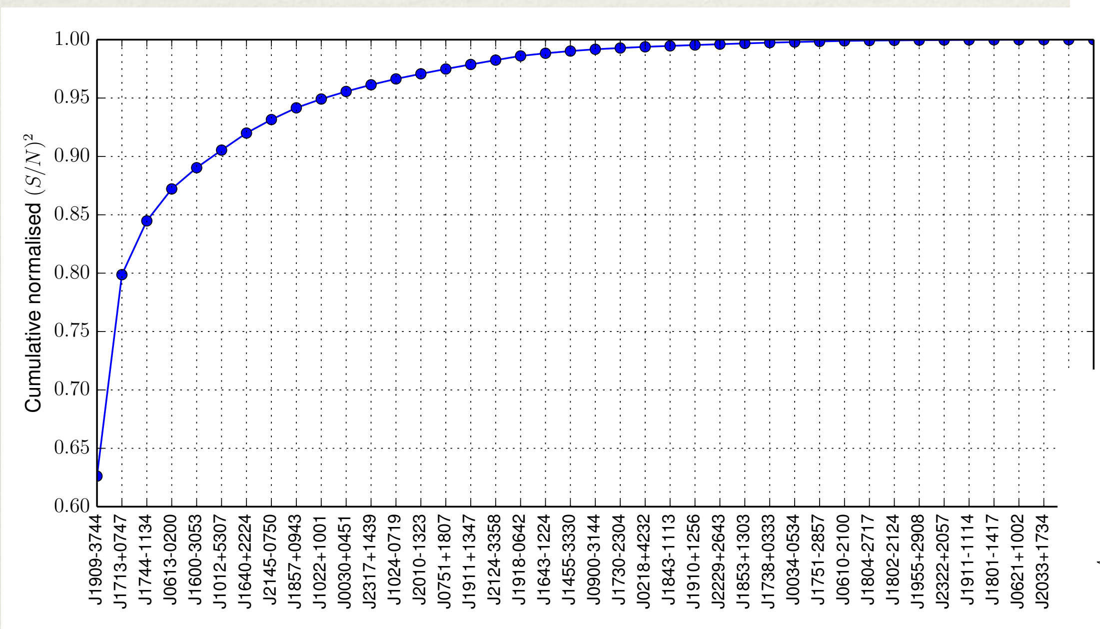
Cumulative normalised $(S/N)^2$
J1909-3744
J1713+0747
J1744-1134
J0613-0200
J1012+5307
J1640+2224
J2145-0750
J1857+0943
J1022+1001
J0030+0451
J2317+1439
J1024-0719
J2010-1323
J0751+1807
J1911+1347
J2124-3358
J1918-0642
J1643-1224
J1455-3330
J0900-3144
J1730-2304
J0218+4232
J1843-1113
J1910+1256
J2229+2643
J1853+1303
J1738+0333
J0034-0534
J1751-2857
J0610-2100
J1804-2717
J1802-2124
J1955+2908
J2322+2057
J1911-1114
J1801-1417
J0621+1002
J2033+1734

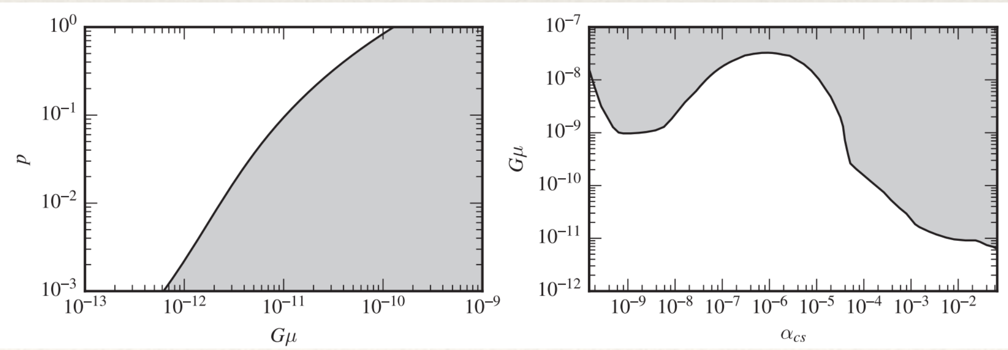
p
$G\mu$
α_{cs}

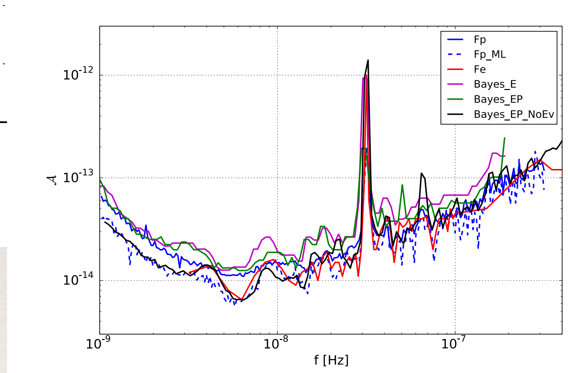
Fp
Fp_ML
Fe
Bayes_E
Bayes_EP
Bayes_EP_NoEv
f [Hz]

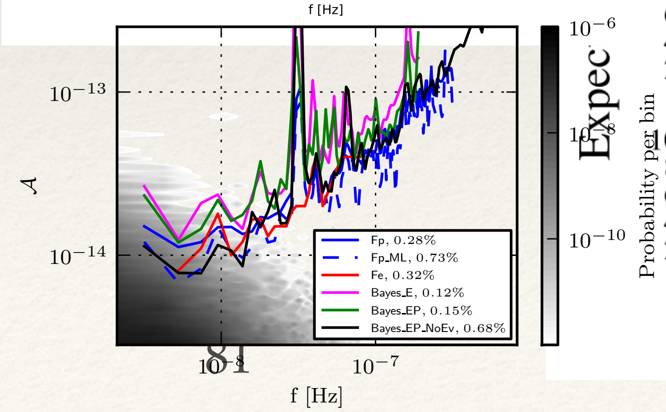
Fp, 0.28%
Fp_ML, 0.73%
Fe, 0.32%
Bayes_E, 0.12%
Bayes_EP, 0.15%
Bayes_EP_NoEv, 0.68%
f [Hz]

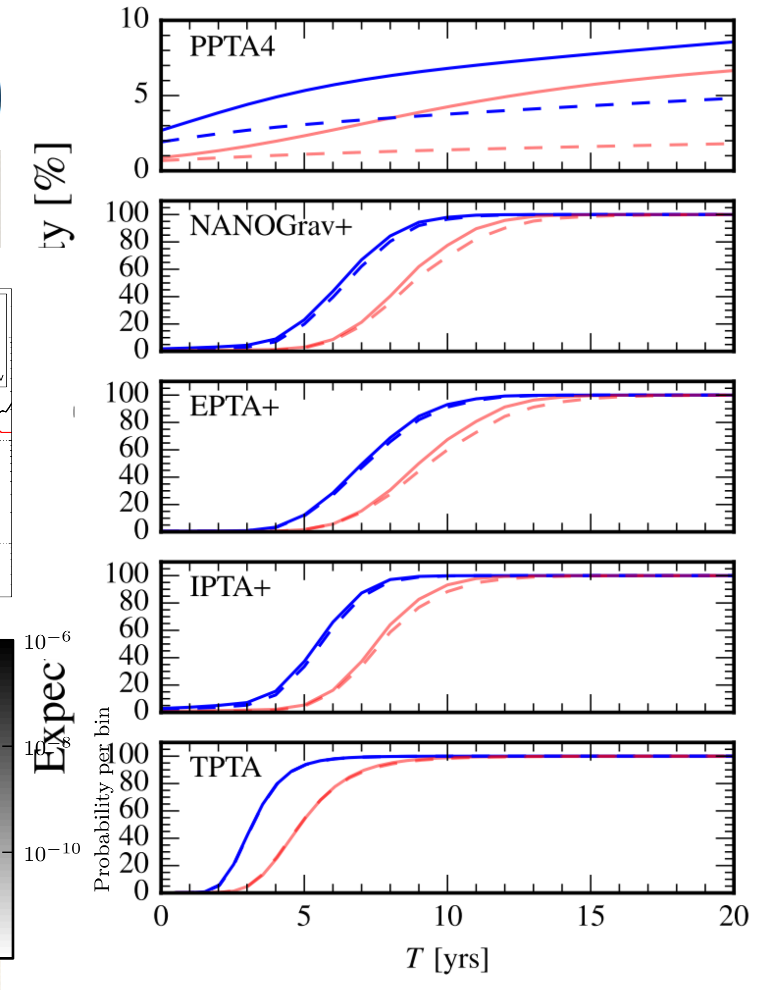
PPTA4
NANOGrav+
EPTA+
IPTA+
TPTA
Probability per bin
T [yrs]

Stanislav (Stas) Babak.

AstroParticule et Cosmologie, CNRS (Paris)

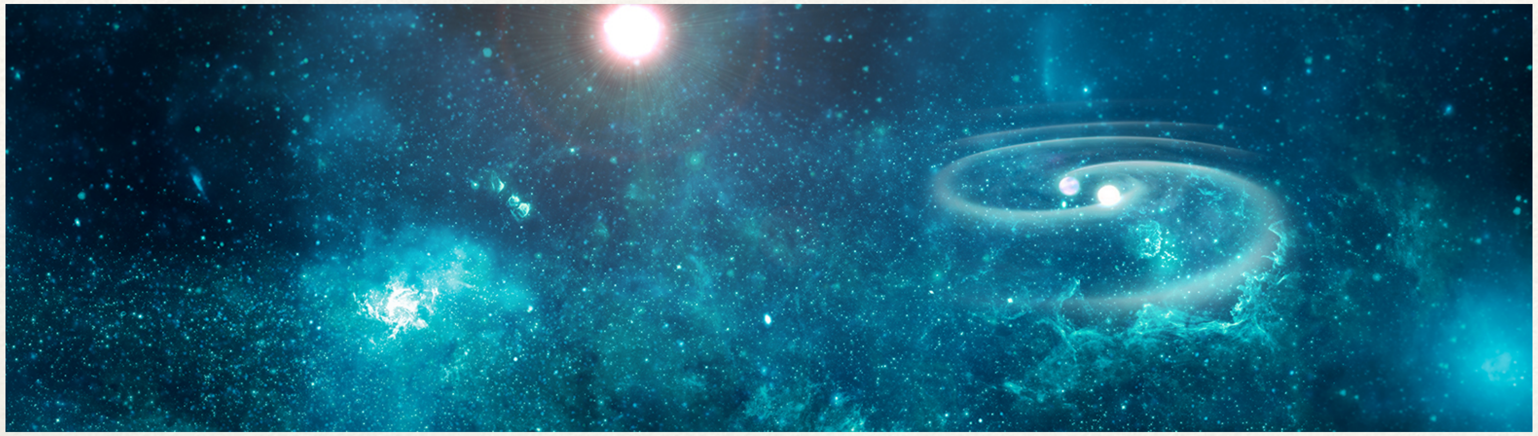

LISA: detecting ravitational waves from space.

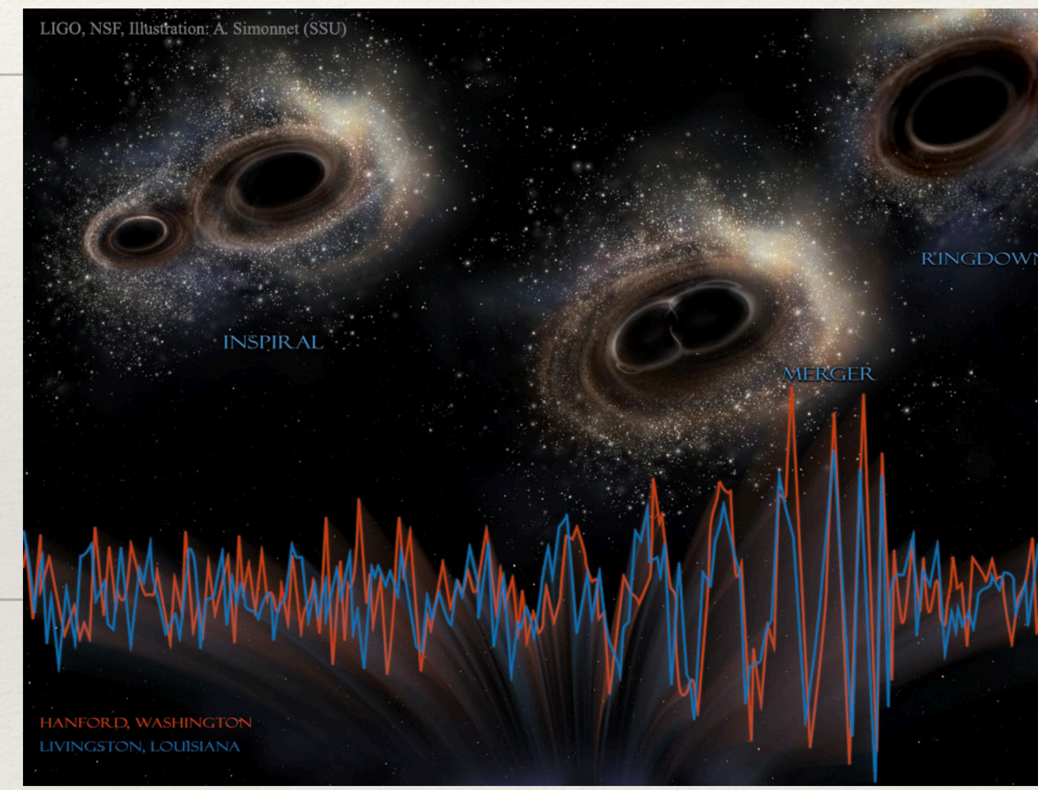

ISAPP, 7-17 June 2021